The role and regulation of class IIa HDACs in neuronal antioxidant responses

Laura Alice Keiko Neat

Master of Science (by Research)

University of York

Biology

March 2021

Abstract

Reactive oxygen species (ROS) are highly reactive signalling molecules, produced naturally as by-products of oxidative metabolism, which can lead to a state of oxidative stress when in excess. ROS can be cytotoxic to neurons and high levels are linked to many neurodegenerative diseases. Neurons counter excessive ROS in part through transcriptional upregulation of antioxidant enzymes. Class IIa histone deacetylases (HDACs) are transcriptional co-regulators that can either repress or activate gene transcription. They repress MADS box (MEF2) transcription factor mediated gene expression by promoting chromatin compaction and activate forkhead (FOXO) transcription factors through deacetylation. Class IIa HDACs are regulated by signal-dependent nucleocytoplasmic shuttling whereby increased neuronal firing triggers their nuclear export. Whilst these HDACs are linked to both neuroprotection and neurodegeneration, little is known about their activity and regulation under oxidative stress.

This thesis aimed to investigate class IIa HDAC regulation under oxidative stress conditions. Oxidative stress was imposed using either diethyl maleate (DEM) to deplete cellular glutathione levels or paraquat which affects the mitochondrial electron transport chain. Work here shows that both HDAC4 and 5 translocate to the nucleus of rat cortical neurons under DEM-induced oxidative stress, whereas paraquat has different effects on HDAC4/5 localisation. Furthermore, HDAC5 showed a dephosphorylation, essential for its nuclear import. Putative FOXO target genes Tpm2 and Spp1 were induced in neurons during moderate oxidative stress, suggesting that ROS-induced nuclear imports of HDAC4/5 promote deacetylation and activation of FOXOs. Transgenic flies expressing human HDAC5 or a constitutively nuclear HDAC5 mutant, raised on DEM food, displayed strong increases in *Drosophila* Gadd45 gene mRNA levels, and *in silico* approaches revealed Gadd45 as a putative FOXO target. Moreover, transgenic flies showed a possible translocation of expressed HDAC5-GFP to the nucleus of *Drosophila* neuronal cells. Therefore, the proposed mechanism occurring during low oxidative stress may be conserved and exploited therapeutically.

List of Contents

List of Figures

List of Tables

Acknowledgments

I would like to express my immense gratitude to my supervisors; Dr. Sangeeta Chawla, for her invaluable expertise, guidance and continuous support throughout my project and Dr. Gareth Evans, for his insightful advice and technical support. I would also like to thank my Thesis Advisory Panel member Betsy Pownall, and all members of the Chawla, Evans, Elliott and Sweeney labs for their help throughout my time in the lab.

I wish to extend my special thanks to Chris Ugbode, especially for his help in culturing primary rat neurons which were essential for this project, as well as his consistent help and kind feedback.

Author's Declaration

I declare that this thesis is a presentation of original work and I am the sole author. This work has not previously been presented for an award at this, or any other, University. All sources are acknowledged as references. All collection and analysis of data for this thesis was performed de novo.

Fly brain dissections were performed by Dr. Chris Elliott. Due to Covid-19 restrictions, one person only was allowed to culture neurons in the lab at one time. Due to this and reductions in overall lab time, it was not possible for me to learn to culture cells successfully in the time frame. Therefore, the culturing of neuronal cells used in this project was performed by a lab colleague Chris Ugbode.

1. Introduction

Reactive oxygen species (ROS) are unstable, highly reactive chemical species produced as natural by-products of oxidative metabolism in all eukaryotic cells. Neurons are shown to be particularly vulnerable to ROS, partly due to their postmitotic nature and high metabolic activity. At low levels, ROS play essential roles in neuronal homeostasis and signalling including in the regulation of synaptic plasticity (Oswald et al., 2018). However, ROS can accumulate when cellular antioxidant capacity is impaired or overwhelmed, leading to a state of oxidative stress (Liu et al., 2018). Neurons can counter ROS in part through transcriptional regulation of antioxidant enzymes (Qiu et al., 2020). This introduction summarises our current understanding of some of these antioxidant mechanisms in neurons.

1.1. Reactive oxygen species and the oxidative stress phenomenon

Reactive oxygen species can oxidise many cellular molecules due to their highly reactive and cytotoxic nature. Examples of ROS include hydrogen peroxide (H_2O_2), superoxide (O_2^-) and hydroxyl radicals (OH^-). Neuronal ROS are generated endogenously by neurons during mitochondrial ATP generation (Figure 1) and subsequent 'leakage' of the electron transport chain (Oka et al., 2009). Energy created through redox reactions using enzymes of the electron transport chain generates an electrochemical proton gradient across the inner mitochondrial membrane, which provides the energy required for ATP synthesis (Zhao et al., 2019).

Electrons are passed through complexes I to IV on the inner mitochondrial membrane (IMM), and a series of redox reactions provide energy for proton pumping which sets up the electrochemical proton gradient (Figure 1). Complex IV normally reduces oxygen to water, but occasionally electrons passing through complexes I and III react with oxygen to generate superoxide. These ROS 'leak' out of the electron transport chain and contribute to cellular ROS levels. Elevated levels of ROS themselves can also cause more ROS release from mitochondria (Zorov et al., 2014), a phenomenon known as ROS induced ROS release (RIRR) (Figure 1).

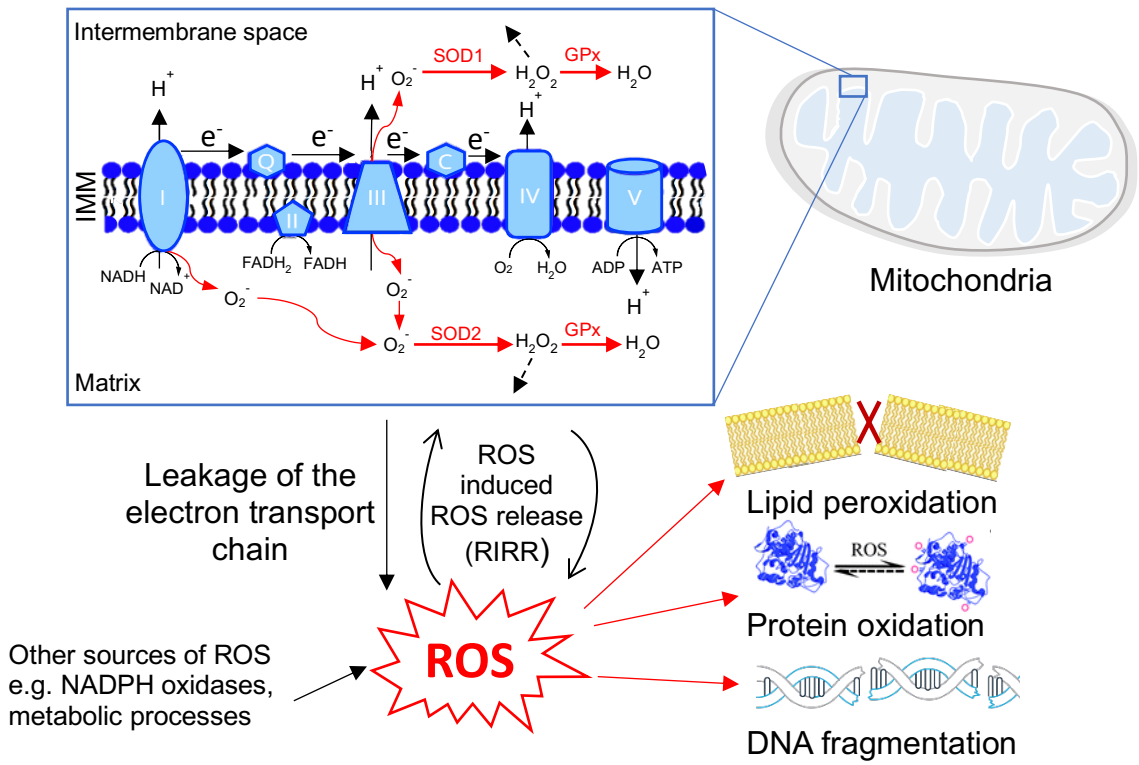

Figure 1: Representation of ROS sources including leakage of the electron transport chain in mitochondria and subsequent damage caused by oxidative stress. Other sources of ROS include metabolic processes, NADPH oxidases and ROS induced ROS release (RIRR) from the mitochondria. Oxidations to cellular components can lead to damages such as lipid peroxidation leading to membrane degradation, protein oxidation causing enzyme inactivation and changes in protein function, folding and interactions as well as DNA fragmentation.

The unpaired electrons which classify these ROS species can result in oxidation (Figure 1) and significant damage to DNA, lipids and proteins (Wiseman & Halliwell, 1996). This process has been implicated in aging, cancer and many neurodegenerative diseases, where it can contribute to functional decline in Alzheimer's Disease (AD) and Parkinson's Disease (PD) amongst others (Gandhi & Abramov, 2012). Specifically, oxidative stress can become deleterious to normal brain functioning. The human brain is said to make up around 20% of the body's total basal oxygen consumption (Magistretti & Allaman, 2015) requiring high rates of mitochondrial ATP synthesis, oxidative metabolic activity, and ROS production (Lee et al., 2020). The brain also contains a high concentration of polyunsaturated fatty acids which can become targets of free radical induced lipid peroxidation (Burnside & Hardingham, 2017). Additionally, DNA fragmentation as a result of oxidative stress can lead to aberrant gene expression and even cell death (Choi, 1993), and the disruption of protein functioning via oxidation can inhibit the action of receptors, neurotransmitters and enzymes key to healthy brain functioning and activity. Moreover, neurons have comparatively low antioxidant levels in comparison to other

organs, making the brain particularly sensitive to oxidative stress and its effects (Dringen, 1999). Finally, the non-regenerative nature of neurons ensures the brain is vulnerable to oxidative stress induced insults. Thus, maintenance of redox homeostasis in the brain is especially important.

1.2. Antioxidant defence mechanisms

Redox control has emerged as one of the most fundamental amongst the biological control mechanisms (Lincoln et al., 2003). The human body has natural defences to maintain redox homeostasis, partly through balancing the delicate equilibrium of ROS generation with antioxidative processes. Under normal conditions, several antioxidant systems work to scavenge and detoxify ROS and their precursors, repairing the normal redox state and mitigating oxidative stress. These antioxidant mechanisms work to bind catalytic metal ions required for ROS formation, as well as generate and upregulate more endogenous antioxidant defences (Poon et al., 2004).

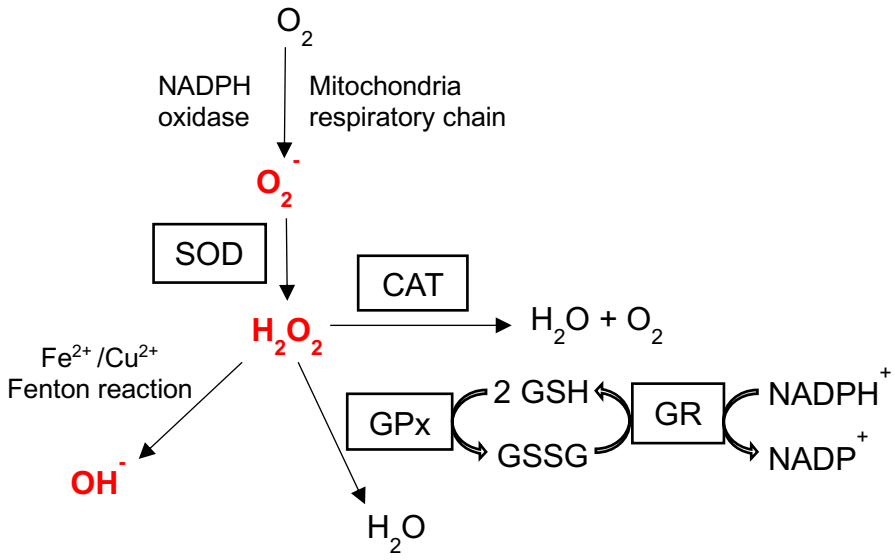

Figure 2: Schematic of antioxidant defences including SOD, CAT and GPx enzymes. Coloured in red are examples of cell generated ROS species and contributors to oxidative stress. Superoxide species are produced largely by mitochondria and NADPH oxidases. Resulting H_2O_2 can be reduced to H_2O and oxygen by CAT enzymes, or to H_2O by GPx enzymes, using glutathione (GSH) as a co-factor. Lastly, hydroxyl radicals are produced from H_2O_2 through the Fe^{2+}/Cu^{2+} Fenton reaction.

The first line of defence consists of a robust enzymatic antioxidant system which includes superoxide dismutase (SOD), catalase (CAT), and glutathione peroxidase (GPx) (Nandi et al., 2019). NADPH oxidases and the mitochondrial respiratory chain are major sources of superoxide, which can then be converted into hydrogen peroxide by SOD enzymes. SOD enzymes function in converting superoxide anions (O_2^-) to hydrogen peroxide

(H_2O_2) in mitochondria. The resulting highly reactive H_2O_2 species can be reduced to stable H_2O by CAT enzymes (Figure 2) (Birben et al., 2012), shown to be crucial in building cell tolerance to oxidative stress (Usui et al., 2009). The H_2O_2 species can also be converted to hydroxyl radicals through the $Fe^{2+/}Cu^{2+}$ Fenton reaction (Figure 2). The conversion of H_2O_2 to H_2O can also be catalysed by glutathione peroxidases (GPx), enzymes which are also shown to act on other organic hydroperoxides.

Reduced glutathione (GSH) acts as a co-factor for the breakdown of H_2O_2 by GPx enzymes and is converted to oxidised glutathione (GSSG) in the process. After being oxidised, glutathione reductase (GR) can reduce the GSSG back, using nicotinamide adenine dinucleotide phosphate (NADPH) as an electron donor (Figure 2). This glutathione redox cycle is shown to be most active during low levels of stress conditions, whilst CAT enzymes take over in protecting against severe oxidative stress (Lee et al., 2020). Specifically, neurons are shown to have lower catalase levels than astrocytes (Baxter & Hardingham, 2016), as well as lower GSH levels (Dringen, 1999). As part of their glutathione metabolism pathway, astrocytes release glutamine, a GSH precursor (Hertz et al.,1999) which is taken up and used by neurons to feed into their own biosynthetic pathways required for neuronal GSH synthesis. Thus, neuronal GSH levels rely heavily on the speed and efficacy of this concurrent mechanism in astrocytes.

1.3. Neuronal transcriptional regulation

A further response to oxidative stress and constantly changing ROS levels is for neurons to change their gene expression. ROS, in modest doses, have long been established to function as intracellular signalling molecules despite their toxic nature. ROS species are considered essential as secondary messengers in a range of physiological functions including cell cycle progression, differentiation, immune responses and even cell death (Redza-Dutordoir & Averill-Bates, 2016). Redox regulated signal transduction has most often been found to be achieved through the reversible oxidation of protein cysteine residues. The cellular transcriptional response to ROS is mediated mainly by activation of kinase signalling cascades, such as the MAP protein kinase cascade, that in turn activate transcription factors such as AP-1 and ATF-1 (Zhang et al., 2016; Turpaev et al., 2002). In neurons, activation of c-Jun N-terminal kinase (JNK) signalling via ROS (Matsukawa et al., 2004) is shown to regulate neuronal plasticity and growth (Collins et al., 2006). The exact mechanism of ROS-mediated JNK activation is not known, however JNK is found to positively regulate neuronal antioxidant defense (Ugbode et al., 2020).

The expression of several antioxidant genes, including those involved in glutathione biosynthesis and recycling, are induced by neuronal firing. Neuronal activity regulates an array of transcription factors (see section 1.5) that control plasticity-associated genes as

well as antioxidant genes. How neuronal transcription factors are regulated by increased synaptic firing is well studied, but their regulation under conditions of oxidative stress is poorly understood.

Neuronal activity induced signalling pathways regulate both transcription factors and their co-activators and co-repressors, including the family of histone modifying enzymes. Such enzymes, which modify the epigenetic status of cells, provide attractive targets for therapy in disease (Jayathilaka et al., 2012). In this report, they are of special interest to us in the context of neurodegeneration, specifically within the oxidative stress state.

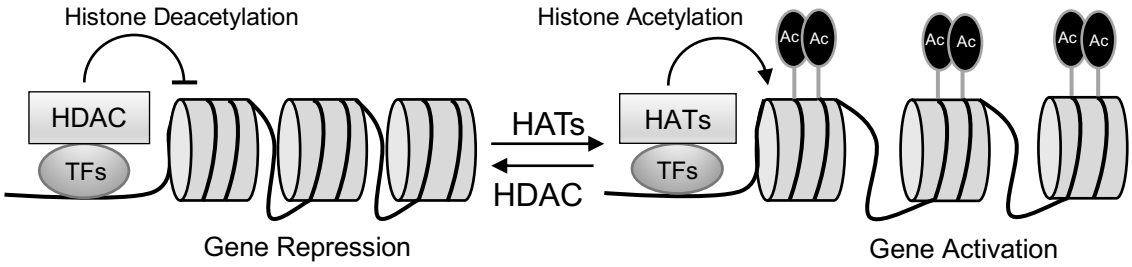

Figure 3: Histone acetylation and deacetylation. Histone deacetylation via histone deacetylases (HDACs) causes tight chromatin compaction which inhibits access to DNA, causing gene repression. Histone acetylation via histone acetyltransferases (HATs) leads to relaxed chromatin, allowing greater access to DNA and target gene activation.

The reversible modifications of histone acetylation and deacetylation have long been established as fundamental parts of gene regulation (Konsoula & Barile, 2012). The acetylation of the ε-amino group of lysine residues on the N-terminus of histones, via histone acetyltransferases (HATs), neutralises their positive charge and subsequently decreases their affinity for negatively charged DNA (Figure 3). This inhibits the generation of higher order chromatin structures, and so condensed chromatin becomes more relaxed, allowing for increased gene transcription. Conversely, the removal of the acetyl group through the action of histone deacetylase (HDAC) enzymes causes improved association with DNA, tighter chromatin compaction and significant decreases in gene transcription.

1.4. Class IIa HDACs

Histone deacetylases (HDACs) are zinc-dependent enzymes which function as epigenetic repressors, working to block transcription of many neuronal genes through this deacetylation process (Thomas & D'Mello, 2018). All HDACs are found to have a conserved set of active site residues used in a common mechanism for the hydrolysis of acetylated substrates (Seto & Yoshida, 2014). The removal of acetyl groups occurs

through a charge relay system, requiring a Zn^{2+} ion. Generally, co-repressors are found to be required for HDAC activity (De Ruijter et al., 2003).

The known mammalian HDACs are classified based on their homology to yeast HDACs (Blander & Guarente, 2004) and are divided into two groups based on structure, expression patterns and the specificity of their catalytic mechanism (Martin et al., 2007). Group I HDACs can be further divided into class I and class II enzymes based on sequence similarities, and additional domains allow even further subdivisions of class II HDACs into class IIa (HDAC4, -5, -7 and -9) and IIb (HDAC6 and -10).

The IIa subclass of HDAC enzymes are characterised by the presence of a 450-600 amino acid N-terminal extension of residues with distinct regulatory and functional properties, including cleavage and phosphorylation sites (Figure 4). The phosphorylation sites on conserved serine residues interact with the chaperone protein 14-3-3, which escort phospho-HDACs to the cytoplasm and sequester them there. Their N-terminal extensions also include a general/MEF2 transcription factor binding domain (MEF2) which allows interactions with transcription factors and enables their repressive activity. These N-terminal residues of HDAC4 and 5 play key roles in regulating their localisation, with the inclusion of a unique and strong nuclear localisation signal (NLS), and are necessary, but not sufficient, for their characteristic transcriptional repression activity. Conversely, the C-terminal end contains a highly conserved large deacetylase domain (DAC) and a hydrophobic nuclear export signal (NES) which is required for their cytoplasmic retention (Figure 4).

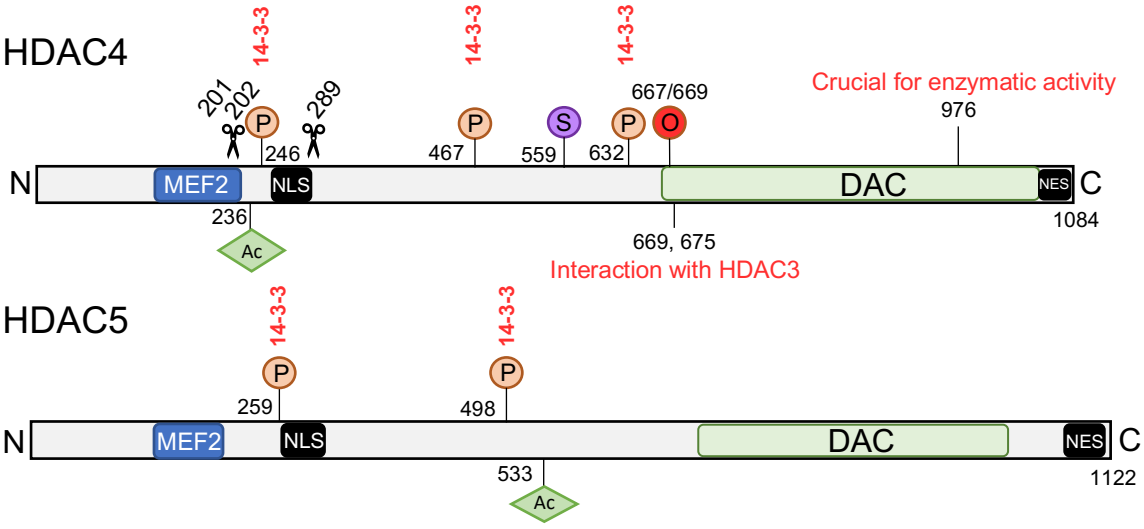

Figure 4: Structural domains of class IIa HDACs 4 and 5. Summary of significant post translational modifications including phosphorylation (P), SUMOylation (S) and oxidation (O). Domains include a MEF2/transcription factor binding domain (MEF2), nuclear localisation signal (NLS), nuclear export signal (NES) and deacetylase domain (DAC).

This IIa subclass of HDACs are distinctly unique in a few ways. Firstly, whilst they can bind acetylated lysine, critical amino acid substitutions in their catalytic site are thought to cause catalytically inactive deacetylase domains (Haberland et al., 2009). Therefore, they require associations with the ubiquitously expressed and catalytically active HDAC3 (a class I HDAC) in order to have any sort of deacetylase activity (Fischle et al., 2002). A H976Y histidine to tyrosine HDAC4 mutant was shown to have a 1000-fold increase in deacetylase activity compared to wildtype HDAC4 (Park and Kim, 2020). This tyrosine residue in the catalytic site is conserved in class I HDACs indicating a large difference between class I and class II HDAC deacetylase activities.

Secondly, separate to other members of the family, class IIa HDACs are unique in their ability to shuttle between the nucleus and cytoplasm of neurons (Figure 5) in response to a number of diverse stimuli, including synaptic activity (Chawla et al., 2003). This nucleocytoplasmic shuttling mechanism is controlled through calcium dependent phosphorylation and cAMP dependent dephosphorylation of specific serine residues on the class IIa HDACs (Mielcarek et al., 2015).

An increase in neuronal activity (such as with stimulus B) triggers Ca^{2+} influx into the cell through ligand and voltage gated Ca^{2+} channels leading to an activation of the Ca^{2+}/calmodulin dependent protein kinases (CaMKII and CamKIV). These kinases phosphorylate two conserved serine residues on the class IIa HDACs, where these phosphorylation events mask the NLS and create a docking site for 14-3-3 chaperone proteins (Figure 5). Interactions with 14-3-3 proteins sequester class IIa HDACs in the cytoplasm through unmasking of the NES and preventing their interactions with importin-α (Wang et al., 2001). This nuclear export means the class IIa HDACs can no longer work to repress their target gene transcription through binding transcription factors in association with HDAC3 (Liu et al., 2012).

In contrast to the nuclear export triggered by Ca^{2+}, cAMP signals (such as with stimulus A) induce a nuclear translocation of class IIa HDACs. The cAMP induced nuclear shuttling mechanism is thought to involve dephosphorylation of specific serine residues, triggering a dissociation of the 14-3-3 proteins (Figure 5). This dephosphorylation can be mediated by protein phosphatase A (PP2A) in the case of HDAC4 (Paroni et al., 2008), which associates with the N terminus of the HDACs, where PP2A activity is regulated by the cAMP dependent kinase PKA (Ahn et al., 2007).

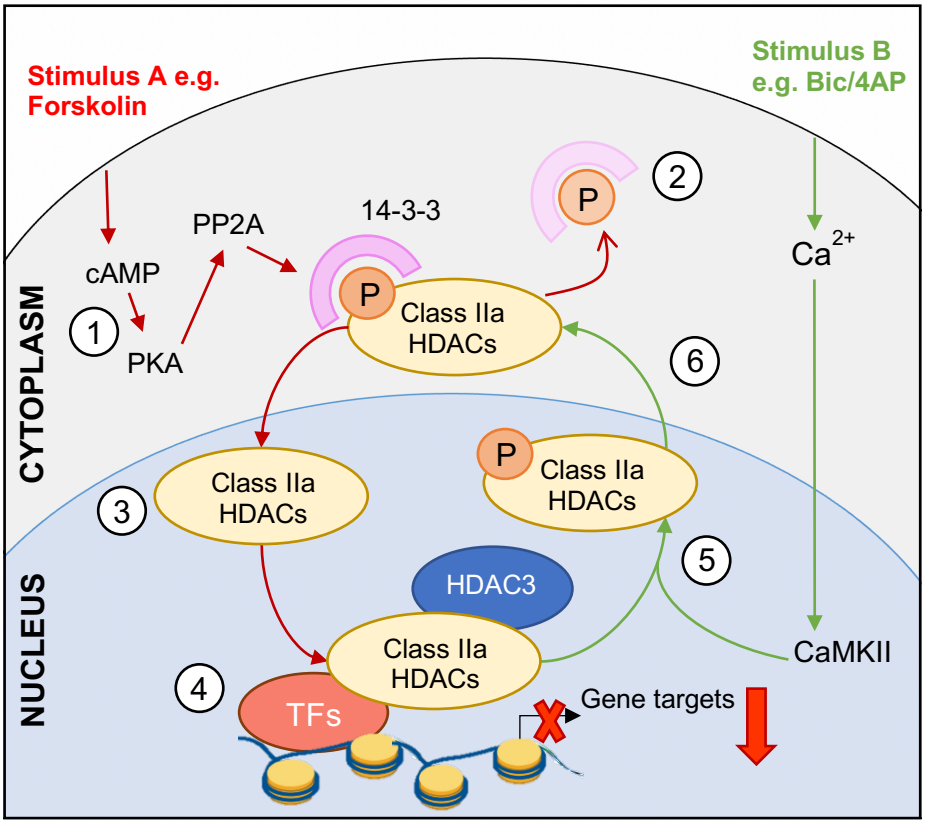

Figure 5: Schematic of nucleocytoplasmic shuttling of class IIa HDACs. Intracellular signals such as stimulus A/B induce reversible pathways of class IIa HDAC shuttling between the nucleus and the cytoplasm via their phosphorylation status, enabling or disabling the repression of specific gene targets in the nucleus. (1) elevated cAMP levels activates PKA and PP2A (2) PP2A associates with the N terminus of class IIa HDACs and causes a dephosphorylation on serine residues, triggering 14-3-3 to dissociate (3) The class IIa HDACs shuttle into the nucleus (4) In association with HDAC3, the IIa HDACs can bind to transcription factors (TFs) and repress their gene targets (5) Influxes of Ca^{2+} into the cell allow CaMKII to phosphorylate the HDACs (6) The HDACs move to the cytoplasm and binding by 14-3-3 on their phosphorylation sites sequesters them in the cytoplasm.

Bic/4AP (stimulus B) and Forskolin (stimulus A) are experimental ways to increase Ca^{2+} and cAMP respectively. Forskolin activates the enzyme adenylyl cyclase, increasing intracellular levels of cAMP. Bic/4AP treatment includes the GABA receptor antagonist bicuculline along with the K+ channel blocker 4-aminopyridine, which together increase neuronal activity and intracellular Ca^{2+}.

1.5. The role of transcription factors

In recent years, HDACs have been shown to deacetylate both histone and non-histone proteins, including transcription factors (Bottomley et al., 2008). Many non-histone proteins have been shown to be deacetylated by HDACs, including cytoplasmic proteins (Parra, 2014). Specifically, the class IIb HDAC6 can deacetylate the cytoskeletal protein α-tubulin to regulate microtubule dependent cell motility (Hubbert et al., 2002). This demonstrates the ability of HDACs to not only regulate gene transcription but also important biological processes.

Like other HDACs, the class IIa subfamily of HDACs do not themselves bind DNA but instead depend on interactions with sequence specific DNA binding proteins for their recruitment to promoter sites and genomic targeting (Jayathilaka et al., 2012). Once recruited by transcription factors, class IIa HDACs can influence the acetylation status of histones and the transcription factors themselves through association with HDAC3/SMRT/N-CoR co-repressor complexes (Figure 5). Two key neuronal transcription factor families targeted by class IIa HDACs are the MADS-box (MEF2) and the forkhead (FOXO) family of transcription factors.

The MEF2 family of transcription factors are important regulators of neuronal development and differentiation and are heavily implicated in the adaptive stress responses of diverse tissues and organs (Potthoff & Olson, 2007). In the brain, they are actively involved in excitatory synapse number regulation (Flavell et al., 2006). Evidence of HDAC4-MEF2 interactions have been associated with HDAC4 nuclear import, MEF2 inhibition (and resulting repression of MEF2 dependent genes) and ultimately neuronal cell death (Bolger & Yao, 2005).

The function of transcription factors can be both positively and negatively affected by the binding of class IIa HDACs. Whilst MEF2-mediated gene transcription is repressed by the binding of these HDACs, the FOXO subfamily of transcription factors have been shown to be activated by class IIa HDACs during maintenance of glucose homeostasis (Mihaylova et al., 2011). FOXO transcription factors are implicated in the regulation of many cellular processes and are involved in critical cellular responses such as during oxidative stress (Accili & Arden, 2004). Separate to other transcription factor families, these FOXO factors are inactivated through lysine acetylation, reducing their DNA binding ability and altering their subcellular localisation. Increased cAMP levels cause a nuclear translocation of class IIa HDACs (as described in Figure 5) which, in association with HDAC3/N-CoR co-repressor complexes, interact with FOXO transcription factors in the nucleus. This interaction triggers a deacetylation and activation of the FOXO factors, allowing increased transcription of their gluconeogenic gene targets (Figure 6A). Conversely, phosphorylation of both the class IIa HDACs and FOXO factors through

serine/threonine kinase Akt dependent activation of AMP activated protein kinases (AMPK) causes their cytoplasmic retention and subsequent repression of their gluconeogenic gene targets (Figure 6B).

For example, in the liver, class IIa HDACs deacetylate and activate FOXO1 in response to the fasting hormone glucagon to induce expression of gluconeogenic genes (Figure 6A). Furthermore, during fasting in *Drosophila melanogaster*, AMPK kinases are inactivated causing dephosphorylation and a nuclear translocation of HDAC4 followed by FOXO deacetylation (Mihaylova et al., 2011; Wang et al., 2011). FOXO transcription factors appear to have a role in protecting against oxidative stress through their function in transactivating a series of genes with critical roles in the cellular response to stress stimuli, including repair of damaged DNA (Gadd45) and ROS detoxification (MnSOD) (Brunet et al., 2004). Therefore, they present themselves as major players in neuroprotection during oxidative stress, and especially are of interest in relation to the class IIa HDACs.

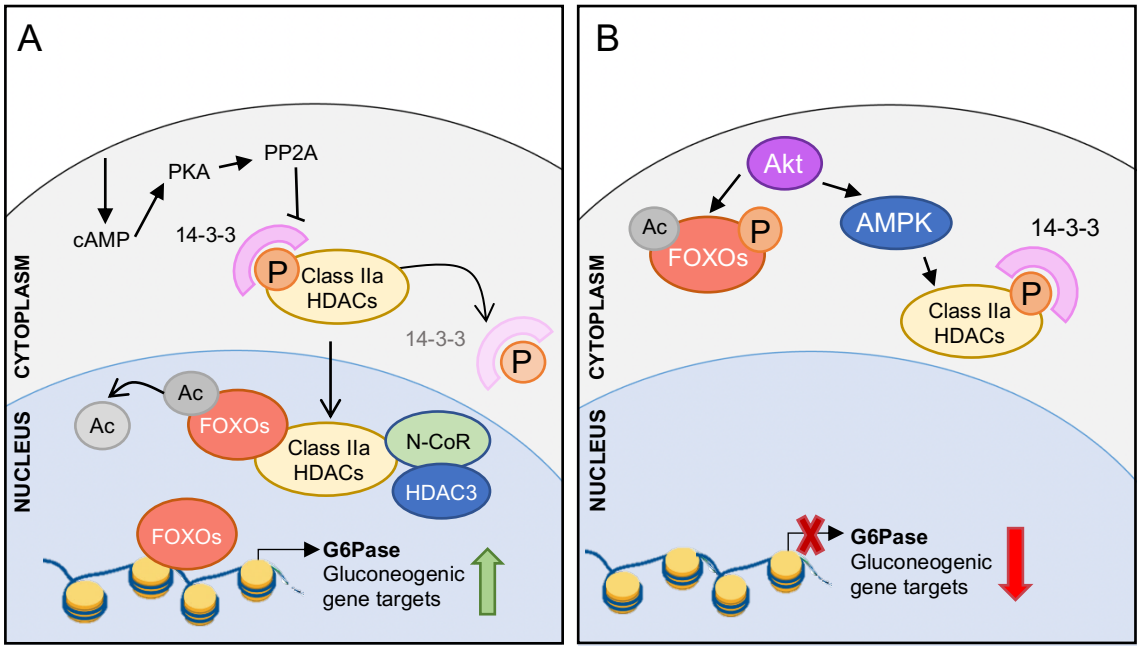

Figure 6: Schematic of FOXO transcription factor regulation via class IIa HDACs. (A) Class IIa HDACs bind, deacetylate and active FOXO transcription factors in the nucleus allowing increased transcription of their gluconeogenic gene targets (B) Phosphorylation of FOXO factors and class IIa HDACs through AMPK kinases allows their cytoplasmic retention and repression of gene targets.

1.6. The neuroprotective nature of synaptic activity

Another cog in the protective redox machinery in the brain appears to be neuronal activity itself. The idea that synaptic activity is neuroprotective has been of much interest in recent years, inspired by studies in which activity blockades cause death in disconnected target neurons (Mennerick & Zorumski, 2000). Whilst much of this research has focused on neuronal health during development, this work is also relevant in mature neurons. One key factor in neuronal health modulation, often dependent on synaptic activity and Ca^{2+} influxes, is changing and adapting vulnerability to oxidative stress (Bell & Hardingham, 2011), facilitated by anti-apoptotic genes being induced and pro-apoptotic genes being suppressed in response to synaptic activity. This is thought to be linked to the inactivation of transcription factors (such as FOXOs) controlling their expression. An example of these apoptotic genes includes the thioredoxin inhibitor Txnip, a FOXO target gene and a key antioxidant system component. The thioredoxin protective redox control system is a major player in the brain's protection against oxidative stress. Txnip acts as an oxidative stress sensor by interacting with the reduced form of thioredoxin and inhibiting its activity. This can help sensitise cells (including neurons) to H_2O_2 induced death.

There has also been much investigation into the induction of antioxidant genes during normal neuronal activity and therefore at physiological levels of ROS. This includes neuronal activity dependent changes in Ca^{2+} signalling and subsequent induction of antioxidant genes, including the glutathione (GSH) system. As discussed previously, neurons express comparatively low levels of GSH, but elevate GSH biosynthesis during bouts of increased synaptic activity. They can do this through transcriptional induction of genes encoding enzymes involved in the rate limiting step of the GSH biosynthesis process (Baxter et al., 2015). Synaptic activity also induces the expression of the antioxidant gene sulfiredoxin (SRNX1) as neurons recruit transcriptional induction of antioxidant proteins in order to adapt to synaptic inputs. Thus, numerous antioxidant defences are boosted when synaptic activity occurs, meeting the requirements for the subsequent increase in ROS production, through carefully balanced redox homeostasis in the brain (Qiu et al., 2020). Whilst this strategy is effective under normal conditions, the excessive level of ROS common in many neurodegenerative diseases appears to override it.

1.7. Oxidative stress and disease

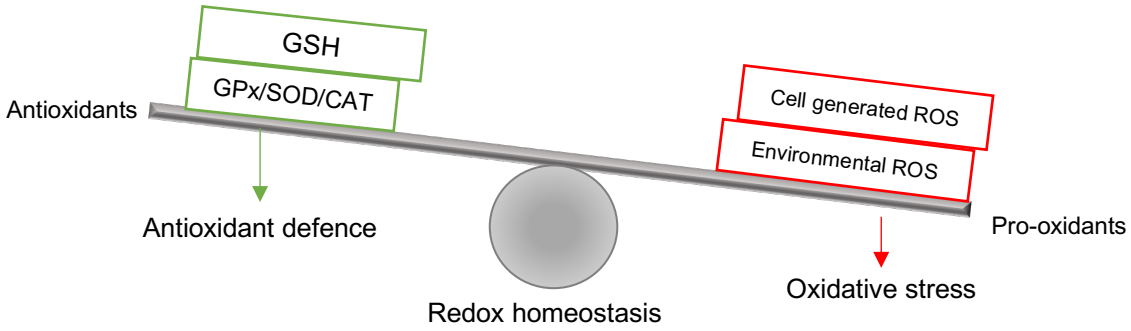

Figure 7: Representation of the balance of pro-oxidants to antioxidants that allows redox homeostasis. Both cell generated and environmental factors contribute to excessive ROS and oxidative stress where antioxidants such as glutathione (GSH) and scavenging enzymes such as GPx, SOD and CAT all work to detoxify and counteract ROS in excess.

Disruption of the careful ROS production and detoxification cycle, and the pro-oxidant to antioxidant balance (Figure 7) has been shown to contribute to the development of a number of human pathologies (Candas & Li, 2014). Strong links between the pathogenesis of many neurodegenerative diseases and the oxidative stress phenomenon has been found (Kim et al., 2015) where ROS increase susceptibility to neuronal damage. Evidence suggests that high levels of ROS are linked to neuronal death in various disorders (Popa-Wagner et al., 2013) and therefore delineating the mechanisms behind neuronal antioxidant defence mechanisms would be invaluable. Additionally, investigations of how these defences are regulated in both physiological and non-physiological contexts may contribute to the understanding of how they could be impaired in disease. Precise knowledge of the pathways involved is essential to find targets for treatment that would be both therapeutically beneficial and non-toxic to the brain.

Whilst it is well established how synaptic activity regulates class IIa HDAC localisation, little is known about the effects of ROS on them. Despite this, these class IIa HDACs have been linked to both neuroprotection and neurodegeneration.

1.8. HDAC4 and neurodegeneration

HDAC4 specifically has been implicated in neuroprotection, where loss of HDAC4 has been shown to lead to neurodegeneration in the retina and cerebellum (Majdzadeh et al., 2008). Whilst cytoplasmic HDAC4 is shown to promote the survival of interneurons, translocation to the nucleus and the deacetylation of nuclear proteins (including transcription factors and histones) is thought to expedite death in cerebellar granule and purkinje neurons (Sando et al., 2012). This raises the possibility that the loss of synaptic excitation, or other signals which cause this nuclear translocation, may lead to neurodegeneration, partially through the depletion of cytoplasmic HDAC4.

A recent study found that aspects of the neurodegenerative phenotype caused in PI3 kinase deficient mice were rescued through either inhibition of HDAC4 activity or blockage of HDAC4 nuclear accumulation in cerebellar neurons (Li et al., 2012). However, alternate findings show that HDAC4 activity inhibition may exert detrimental effects on learning, memory and synaptic processes (Kim et al., 2012). Furthermore, nuclear HDAC4 is shown to repress genes known to be essential in synaptic function, including those encoding for constituents of central synapses. Therefore, any alterations in expression or activity of these genes may influence not only synaptic structure and functioning, but also information processing in the brain (Sando et al., 2012).

Based on these findings, focusing on the alteration of the nucleocytoplasmic shuttling of HDAC4 instead of its complete inhibition may help in the consideration of future therapeutic approaches. Shifting the focus onto this dynamic shuttling pathway therefore requires understanding of the mechanism, interactions and pathways involved.

1.9. HDAC inhibitors

Histone deacetylases have been shown to play dynamic and key roles in regulating a wide range of normal cellular activities. Studies have shown that alterations in HDAC expression or activity as well as imbalances in histone and non-histone acetylation are common in the development of many human cancers (Gallinari et al., 2007) and other syndromes (Reddy et al., 2018). As a result, multiple HDAC inhibitors (HDACi) have been developed and tested in clinical studies, and some approved as treatments. Inhibiting different HDACs in the brain has been reported to be neuroprotective and beneficial in many neurological conditions including Alzheimer's (Lee et al., 2018) and Huntington's disease (Bassi et al., 2017).

Developed and currently used HDACi drugs fit into the active site pocket of Zn^{2+} dependent deacetylases. Such HDACis have been generally considered as pan inhibitors (Delcuve et al., 2012) but recent evidence has shown that most of these inhibitors do not specifically target class IIa HDACs (Bradner et al., 2010). Many of the available HDAC inhibitors are also associated with adverse effects. One of the major problems is the lack of specificity. Most inhibitors of the zinc dependent enzymes broadly target all class I and class II HDACs due to sequence similarities in their zinc containing catalytic sites. The level of specificity required to inhibit only the class IIa HDACs would be difficult to achieve as many of these deacetylases play important roles in cellular functions. Whilst general inhibition of HDAC expression or activity has been shown to be neuroprotective in some diseases, this approach in the brain could have detrimental effects without more thorough understanding of the neuronal specific function and mechanisms of HDACs enzymes.

1.10. Induced antioxidant expression rescues neurodegeneration

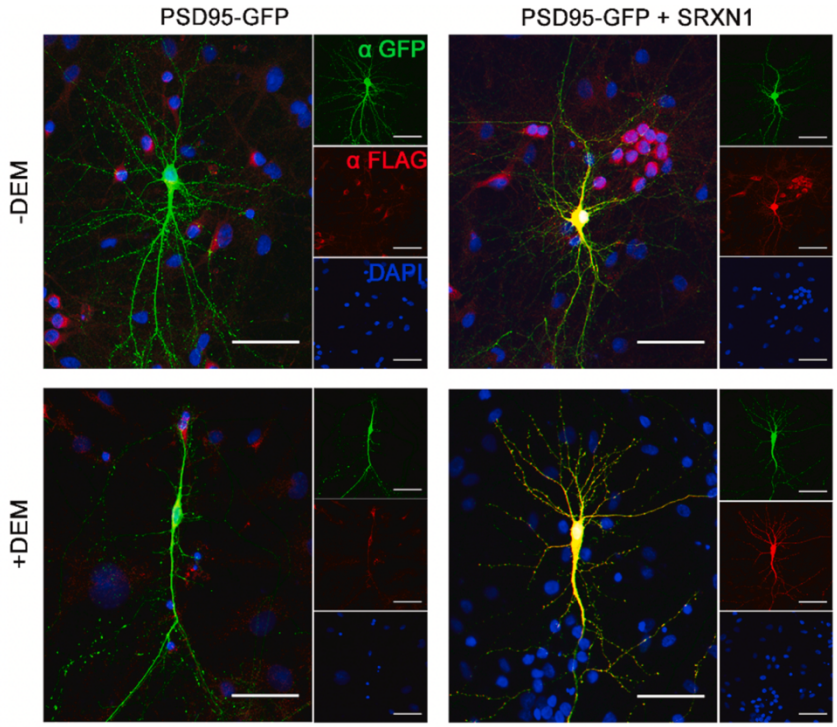

Figure 8: SRXN-1 overexpression rescues DEM-induced dendritic retraction (Figure from Ugbode et al, 2020). "Representative micrographs of mature neurons transfected with PSD95-GFP constructs alone (left panels) or in combination with Flag-tagged human SRXN-1 (right panels) ± 100 µM DEM (48hr). Cells stained with anti-GFP (green), anti SRXN-1 (Flag antibody, red) and nuclear staining with DAPI (blue). Scale bar = 100 µm" (Ugbode et al., 2020).

Whilst HDACi drugs may not be a plausible therapeutic outlook in the context of neurodegenerative conditions, recently published studies have shown how the manipulation of antioxidant gene expression could be a more promising approach. Recent studies demonstrate the possibilities of exploiting known antioxidant pathways in the brain to help prevent or even reverse neuronal ROS damages. Ugbode *et al.* (2020) found that overexpression of the antioxidant sulfiredoxin (SRXN-1) in rat neurons prevented dendritic loss (Figure 8) induced by long term glutathione depletion with diethyl maleate (DEM) in cultured rat neurons.

1.11. Aims

As class IIa HDACs have been linked with neuroprotection and neurodegeneration, this thesis aims to compare the regulation of class IIa HDACs under conditions of increased neuronal firing with conditions of oxidative stress generated by glutathione (GSH) depletion. Work described here investigates the subcellular localisation and phosphorylation status of class IIa HDACs in cultured primary rat cortical neurons during increased levels of synaptic activity and oxidative stress.

Established experimental paradigms are used to increase neuronal firing in cortical neurons through bath applications of bicuculline, a GABA receptor antagonist, along with 4-aminopyridine, a K+ channel blocker. Oxidative stress is induced by glutathione depletion (Figure 9) and increased mitochondrial H_2O_2 secretion (Figure 10).

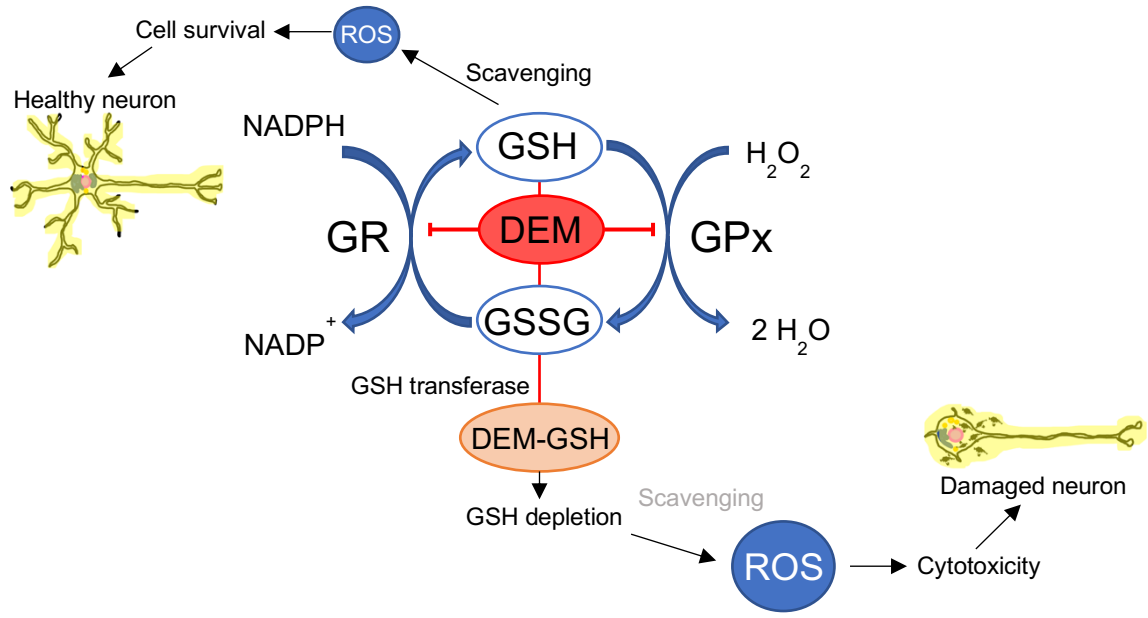

Figure 9: Schematic of diethyl maleate (DEM) action to deplete levels of neuronal glutathione (GSH), a key cellular antioxidant. Catalysed by glutathione-S-transferase, the formation of DEM-GSH conjugates alters the GSH to GSSG ratio, decreasing GSH concentrations and inducing a state of oxidative stress.

GSH homeostasis is found to be altered in many neurodegenerative diseases (Aoyama & Nakaki, 2015; Gu et al., 2015) and in the hippocampus of Alzheimer's disease patients and mouse models of AD, GSH levels are notably decreased (Mandal et al., 2015; Resende et al., 2008). Glutathione depletion was achieved through treatments with diethyl maleate (DEM), an αβ unsaturated carbonyl (Plummer et al., 1981) with an electrophilic site, which is used as a substrate for glutathione-S-transferase (Deneke et al., 1985).

Under normal conditions, GSH scavenge and detoxify ROS through donating electrons, ensuring they are not in excess and helping to maintain good neuronal health. Formations of DEM-GSH conjugates, catalysed by glutathione-S-transferase, causes an oxidising shift in the GSH to GSSG ratio, decreasing intracellular GSH concentrations (Figure 9). Depletions of GSH means less scavenging of ROS, causing excessive levels. Thus, oxidative stress conditions are induced, a state which can cause neuronal morphological damage or even cell death.

Previous studies have demonstrated that depletion of cellular GSH leads to oxidative damage to rat brain proteins (Bizzozero et al., 2006). Applications of DEM in mature primary hippocampal rat neurons have recently been shown to cause concentration and time dependent decreases in cellular glutathione and increases in H_2O_2 secretion (Ugbode et al., 2020) causing oxidative stress, cytotoxicity and damage to neurons.

Alternatively, oxidative stress was induced using Paraquat (PQ). This compound is part of a class of redox cycling compounds which produce ROS. PQ^{2+} is enzymatically reduced to its cationic radical (Reaction 1). This can reduce molecular oxygen to a superoxide radical, also regenerating PQ^{2+} (Reaction 2). The superoxide can then be converted to H_2O_2 either spontaneously (Reaction 3) or by superoxide dismutase (Reaction 4) (Figure 10).

It has been shown that mitochondria are a major source of PQ^{2+} induced ROS generation (Castello et al., 2007), making it a somewhat mitochondrial specific induction of ROS generation and oxidative stress.

Reaction 1	$PQ^{2+} + e^- \rightarrow PQ^{+\cdot}$
Reaction 2	$PQ^{+\cdot} + O_2 \rightarrow PQ^{2+} + O_2^{-\cdot}$
Reaction 3	$PQ^{+\cdot} + O_2^{-\cdot} \rightarrow PQ^{2+} + O_2^- \rightarrow H_2O_2$
Reaction 4	$O_2^{-\cdot} + O_2^{-\cdot} \xrightarrow{H^+} O_2 + H_2O_2$

Figure 10: Proposed production of H_2O_2 by PQ^{2+}. *A series of enzymatic reactions lead to the reduction of PQ^{2+} to the $PQ^{+\cdot}$ radical (Reaction 1), which then reduces molecular O_2 to a superoxide $O_2^{-\cdot}$ radical whilst regenerating PQ^{2+} (Reaction 2). The resulting superoxide species are converted to H_2O_2 spontaneously (Reaction 3) or through superoxide dismutase (SOD) (Reaction 4).*

Some experiments were performed in transgenic *Drosophila melanogaster* expressing mammalian HDAC5. *Drosophila* have been used as a key model in neurodegenerative disease research for many years. This is partly due to high conservation between fly and human genes, their complex nervous systems and display of learning and memory behaviours (Chan & Bonini, 2000). The *Drosophila* class IIa histone deacetylase dHDAC4 and mammalian class IIa HDACs show similarities in key functional domains including regulatory phosphorylation sites. Compared to human HDAC4, *Drosophila* HDAC4 shows a 59% similarity across the whole protein and 84% similarity across the deacetylase domain containing C terminus (Fitzsimons et al., 2013). This suggests that the mechanisms regulating their subcellular localisation under conditions of oxidative stress are likely to be conserved.

These factors make *Drosophila* an advantageous tool which can allow both the study of normal functions of proteins as well as the effects of targeted genetic mutations using expressions of human mutant forms of a protein. The GAL4-UAS system has been used extensively in *Drosophila* and applied more recently to model neurodegenerative diseases through transgenic expression in subsets of neurons (Rezaval et al., 2007).

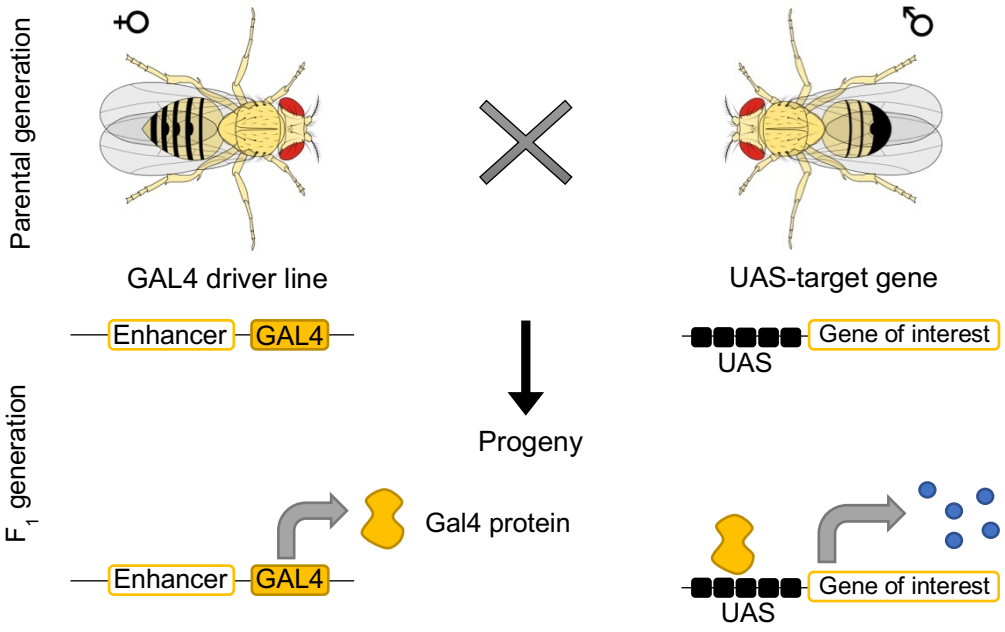

Figure 11: Schematic of the *Drosophila* GAL4/UAS system. A tissue specific enhancer drives GAL4 expression in a subset of cells which, when crossed with a UAS-target gene line, binds to the UAS sequence and drives expression of the gene of interest in the desired tissue in their progeny.

Developed in 1993, the GAL4-UAS system uses the yeast transcription activator protein GAL4, which specifically binds the upstream activating sequence (UAS) to activate gene transcription (Brand and Perrimon, 1993). Many GAL4 driver lines of *Drosophila* have been produced, under the control of a tissue specific enhancer and designed to express the GAL4 protein in a subset of tissues (Figure 11). The other necessary part of the system in *Drosophila* are reporter lines, which include the UAS region upstream of a gene of interest. This gene of interest is often tagged with an epitope or a fluorescent reporter, such as GFP, to allow visualisation of the expressed protein. The F_1 progeny produced on crossing flies from the GAL4 driver line with a line containing the UAS-target gene express the gene of interest only in the cells in which GAL4 is present. Thus, the protein of interest is produced in a specific tissue such as neuronal cells.

Throughout this thesis, four major treatments with different cellular effects are used in the study of the class IIa HDACs in neuronal antioxidant defences. For quick reference, the treatments used in this thesis and their actions are set out in Table 1 below:

Table 1. Summary of treatments and their cellular effects.

Treatment	Description	Effect
Bic/4AP	Includes bicuculline, a GABA receptor antagonist, and 4-aminopyridine, a K+ channel blocker. Known to drive cytoplasmic class IIa HDAC localisation	Increases neuronal firing/ synaptic activity and intracellular Ca^{2+}
DEM	An αβ carbonyl which conjugates to GSH, catalysed by glutathione-S-transferase	Depletes GSH levels leading to higher ROS levels. Induces oxidative stress
Paraquat	Produces ROS through a series of enzymatic reactions, where mitochondria are a major source	Increases (largely) mitochondrial specific ROS generation. Induces oxidative stress
Forskolin	Activates the enzyme adenylyl cyclase. Known to drive nuclear class IIa HDAC localisation	Increases intracellular cAMP

2. Materials and Methods

2.1 *Drosophila* genetic crosses

Genetic crosses were designed to drive neuronal expression of GFP tagged human HDAC5 in transgenic *Drosophila* with the UAS promoter upstream of either:

1. EGFP
2. Wild type, GFP tagged human HDAC5 (HDAC5-GFP)
3. GFP tagged, double phosphorylation site mutant* HDAC5 (HDAC5-DM)

*This mutation of serine 259 and 498 on human HDAC5 to alanine residues (as described in Soriano et al., 2013) renders HDAC5 constitutively nuclear. The UAS-EGFP flies were provided by Dr. Chris Elliott (University of York). The UAS-HDAC5 GFP transgenic flies were generated by microinjection of *Drosophila* embryos (Chawla and Sweeney, unpublished).

Crosses were designed using the UAS-GAL4 system, where nSyb^{115} is a neuronal driver. The crosses were set up as follows:

nSyb^{115} GAL4 x UAS-EGFP
nSyb^{115} GAL4 x UAS-HDAC5-GFP
nSyb^{115} GAL4 x UAS-HDAC5-DM

Virgin nSyb^{115} females were identified, collected and stored separately until the set-up of a new cross. Males were selected from stocks of each genotype, where straight winged males only were selected for HDAC5-GFP, and orange eyed males only for HDAC5-DM flies as these phenotypes served as markers for the presence of the UAS-HDAC5 transgene. Crosses were set up by placing 8-10 males and 6 virgin females in a vial. After 7 days the parents were removed, and larvae allowed to develop. F_1 progeny flies were collected after 10 to 12 days post set up of the cross. F_1 progeny flies were collected (both females and males) and frozen at -70 °C for future use.

Alternatively, the same crosses were set up, parents removed, and the collected F_1 progeny were then put on either ethanol (EtOH) control or 5 μM DEM (Sigma) food for 3 days or 1 week.

5 μM ethanol (EtOH) and DEM fly foods were prepared with defined media, 10% sucrose, 5% yeast and sawdust (see appendix for details of food preparation).

2.2 Protein Extraction

The collected flies produced from the genetic crosses (section 2.1) were removed from the -70°C freezer, the tubes vortexed, and the fly heads separated from the bodies using a microscope and tweezers. Around 10 heads per genotype were extracted and placed into fresh tubes. To these tubes, 50 µl 1 x RIPA was added, and they were homogenised with 20^{+} rotations using a pestle. 1 x RIPA was made using 200 µl 5 x RIPA stock (50 mM Tris, 150 mM NaCl, 1% (v/v) Triton-X-100, 0.5% (w/v) sodium deoxycholate, 0.1% (w/v) SDS, 1 mM EDTA, 1 mM NaVO43) and 800 µl de-ionised water (dH_2O), then 0.1% (v/v) β-mercaptoethanol, 0.5% (v/v) PMSF and a protease inhibitor cocktail was added to the 1 x RIPA stock. The tubes were thawed on ice and vortexed before being centrifuged for 5 minutes, at 13 k rpm speed and 4°C. The supernatant was removed and pipetted into a fresh tube. 10 µl 4 x LDS sample buffer (NuPAGE, Thermo Fisher Scientific) was added to 30 µl supernatant and the tubes stored at -20°C before use on a western blot.

35 mm dishes of cultured cortical neurons, treated as stated, were washed with 1 x PBS and lysed in 450 µl 1 x RIPA buffer using cell scrapers. The cells were scraped into tubes and incubated on ice for 10 minutes. The lysates were then centrifuged at 16.1 rcf and 4°C for 10 minutes. Around 100 µl of supernatant was collected and 33 µl 4 x LDS sample buffer (NuPAGE, Thermo Fisher Scientific) + 20 mM DTT was added. The tubes were frozen at -20 °C before use on a western blot.

2.3 Antibodies used

The following antibodies were used for western blotting and immunohistochemistry with dilutions as stated in Table 2 (primary antibodies) and Table 3 (secondary antibodies).

Table 2. Primary antibodies used for western blotting and immunohistochemistry experiments.

Name	Supplier	Dilutions
HDAC5 (D17JV) Rabbit monoclonal antibody	Cell Signalling Technology	1:1000 (western blotting), 1:200 (immunohistochemistry)
p-HDAC4 (S246)/ HDAC5(S259)/ HDAC5(S115) (D27B5) Rabbit monoclonal antibody	Cell Signalling Technology	1:1000 (western blotting), 1:200 (immunohistochemistry)
p-HDAC4 (S632)/ HDAC5(S498)/ HDAC7(S486) (3424S) Rabbit monoclonal antibody	Cell Signalling Technology	1:1000 (western blotting)
HDAC4 (D15C3) Rabbit monoclonal antibody	Cell Signalling Technology	1:100 (immunohistochemistry)
MEF2D (610775) Mouse monoclonal antibody	BD Transduction Laboratories	1:1000 (western blotting)
GFP (132 005) Guinea pig polyclonal antibody	Synaptic systems	1:1000 (western blotting)
NeuN (ABN90) Guinea Pig polyclonal antibody	Millipore	1:500 (immunohistochemistry)

Table 3. Secondary antibodies used for western blotting and immunohistochemistry experiments.

Name	Supplier	Dilutions
Goat anti Rabbit Alexa 488 (A11008)	Invitrogen	1:500 (immunohistochemistry)
Goat anti Guinea Pig Alexa 546 (A11074)	Invitrogen	1:500 (immunohistochemistry)
HRP conjugated anti-rabbit (111-035-114)	Jackson	1:10,000 (western blotting)
HRP conjugated anti-guinea pig (106-035-003)	Jackson	1:2000 (western blotting)
HRP conjugated anti-mouse (115-035-003)	Jackson	1:5000 (western blotting)

2.4 Western blotting

Western blotting techniques were used to detect levels of selected proteins in samples. See appendices for additional details of gel components and buffers.

Samples were run on 10 well, 10% SDS PAGE gels in 1 x Laemmli running buffer (0.025 M Tris, 0.192 M glycine, 0.1% SDS, pH 8.3) with a 5 µl preceding molecular weight marker (Bio-Rad Precision Plus Dual Colour Standards). This was run at 120V until the dye front reached the resolving gel, then 180V for 1 hour or until the dye ran off the edge of the gel.

The gel was then transferred overnight at 20V onto 0.45 µm PVDF membrane (Immobilon, Merck Millipore), previously wet using methanol. The membrane was checked for complete transfer using Ponceau S stain, then de-stained with 1 x PBS washes. The membrane was then blocked in either 5% milk powder in PBS or 3% BSA in PBS for 1 hour at room temperature with constant shaking.

After blocking, the membrane was incubated in the primary antibody, previously diluted to the recommended dilution in 5% BSA in 1 x TBST (20 mM Tris, 150 mM NaCl, 0.1% (w/v) Tween-20 detergent), for at least 3 hours at room temperature or overnight at 4 °C with constant shaking.

After incubation, the membrane was washed 3 x 10 mins in TBST with gentle agitation. The first wash used ~100 ml TBST and the last two washes used PBS.

After the washes, the membrane was incubated with the HRP-conjugated appropriate secondary antibody. The secondary antibody was diluted at the recommended concentration in 5% milk powder in PBS + 0.5% Tween-20. The membrane was incubated with constant shaking at room temperature for 1 hour at room temperature.

After this incubation, the membrane was again washed 3 x 10 mins as previously described. After the last wash, the membrane was incubated in 600 µl of luminol then 600 µl of peroxide ECL reagents (Thermo Fischer Scientific) and carefully agitated for 1 minute in this mixture. In the dark room, a piece of film was exposed to the blot which had been dried, sealed in cling film and taped into a film cassette. Once exposed, the film was placed into a tray with developer and agitated for 20-30 seconds, then washed and placed in a tray with fixer and again agitated. The film was finally removed, washed, and left to dry outside the dark room. The film was marked with the molecular weight markers and labelled.

Adjustments were made to the protocol, e.g. dilution of primary and secondary antibodies, length of antibody incubation and length of time film exposed to blot to optimise results and visualisation of bands.

2.5 Immunostaining

Cultured rat neurons, 14 days *in vitro,* were treated for 2 hours and fixed onto coverslips for later staining. The cells were rinsed with 1.5 ml PBS and fixed for 20 minutes with 1 ml fixative (3% paraformaldehyde, 4% sucrose in PBS) at room temperature. The cells were then washed three times in PBS, at which point the coverslips were stored in PBS in the cold room at 4 °C.

From the cold room, the coverslips were placed in a 6 well plate with 1 x PBS. The coverslips were permeabilised with 0.5% NP-40 in PBS for exactly 5 minutes, then washed in PBS. Droplets of 48-50 µl of primary antibody, diluted to the recommended dilution, were pipetted onto parafilm in a humidified chamber and coverslips placed cell side down onto the droplets. The box was sealed, and coverslips left to incubate at room temperature for at least 1 hour, or overnight at 4 °C.

After incubation, the coverslips were placed back into the 6-well plate with fresh PBS and washed for 3 x 5 minutes. The coverslips were then incubated in 500 µl of diluted secondary antibody for 1 hour at room temperature in the 6-well plate. After incubation, the coverslips were washed 2 x 5 minutes in PBS, then incubated in 500 µl Hoechst stain to stain nuclei for 5 minutes before washing twice again in PBS for 5 minutes. The coverslips were then mounted onto microscope slides with one drop of fluoromount mounting medium (Sigma) and sealed with nail varnish. The microscope slides were stored at 4 °C until imaging.

2.6 Fly brain dissections

Live flies taken from crosses in section 2.1 were anaesthetised and collected. The heads were separated from bodies, and the fly brains were dissected using tweezers under a microscope. The dissected fly brains were fixed with 4% PFA for 15 minutes before being transferred to PBS. After washing in PBS, the brains were mounted onto microscope slides with fluoromount and sealed with nail varnish before being imaged immediately. All dissections were performed by Chris Elliott.

2.7 Fluorescence microscopy

Images were taken on an inverted Zeiss microscope (880) with 20x objective using Zeiss filter sets for DAPI, Alexa 488 and 546. For each treatment (coverslip), 3 areas that included roughly 10 cells each were imaged for analysis. Consistent settings were used to image the areas at a resolution of 1072x1072 pixels. Images were imported into ImageJ for analysis (see section 3.1).

2.8 RNA isolation (neurons)

After treatment of cultured rat neurons, growth media was removed and 1 ml TRIzol reagent (Thermo Fisher Scientific) was added to the cells. Cell scrapers were used to lyse and scrape the cells into tubes, and the homogenised samples were left to sit for 5 minutes at room temperature. 200 µl of chloroform was added and the tubes were shaken vigorously by hand for 15 seconds. The samples were again incubated for 2-3 minutes at room temperature, before being centrifuged at 4 °C for 30 minutes. The aqueous phase was removed by angling the tubes at a 45 ° angle and pipetting out the upper ~50% colourless section into a new tube. 500 µl isopropanol was added to the ~500 µl extract, adjusting based on the amount extracted in a 1:1 ratio. The tubes were then vortexed and stored at -20 °C at least overnight.

The samples were removed from the freezer and centrifuged for 1 hour at 4 °C. The supernatant was removed from the tubes without disrupting the pellet and discarded. 500 µl of 75% ethanol containing DEPC water was carefully added to the tubes with pellets, and they were centrifuged for 15 minutes at 4 °C. The ethanol wash was carefully removed, leaving the pellets intact. The pellets were left to dry in the tubes with the lids open for 10 minutes at room temperature. 50 µl DEPC water was added to the pellets, which were then vortexed and frozen at -70 °C.

2.9 RNA isolation (flies)

50 µl TRIzol was added to roughly 20 frozen fly bodies or 50 frozen fly heads which were homogenised immediately with disposable plastic pestles. 750 µl TRIzol was then added to these homogenised samples which were incubated at room temperature for 5 minutes. The samples were centrifuged for 15 minutes at 12 k rcf at 4 °C to pellet the insoluble debris. The supernatant was carefully transferred to a new tube, leaving 50 µl of liquid at the bottom and not disrupting the fatty pellet. 160 µl of chloroform was added to the supernatant tubes and shaken vigorously by hand for 15 seconds, leaving them to incubate for 2-3 minutes at room temperature. The samples were centrifuged at 12 k rcf for 15 minutes at 4 °C.

The upper aqueous phase was then pipetted out and transferred to a new tube. 400 µl of isopropanol was added, and the tubes were vortexed briefly. The samples were then incubated in the fridge (4 °C) for 30 minutes before being centrifuged at 12 k rcf for 30 minutes at 4 °C. The supernatant was removed, and the pellet washed with 1 ml 75% ethanol containing DEPC water. The tubes were then centrifuged again at 12 k rcf for 5 minutes at 4 °C and the supernatant removed. The tubes were again centrifuged briefly before any remaining supernatant was removed so that no liquid remains. The pellets

were air dried for 10 minutes at room temperature before being resuspended in 50 µl RNAse free DEPC water, vortexed and frozen at -70 °C.

2.10 Reverse transcription

The RNA samples extracted from either neuronal cells (section 2.8) or flies (section 2.9) were measured for optical density (OD) to estimate the concentration of the extracted samples. The OD (wavelength 260 nm) is measured after one -70 °C freeze cycle (at least overnight). 2 µl of the RNA extracts was pipetted into 100 µl DEPC water and the diluted RNA samples were run on the spectrometer (with DEPC water alone as a reference and the OD recorded).

Once the ODs of the RNA samples were measured, the samples were DNAsed. This was done through mixing the reagents set out in Table 4.

Table 4. Reagents and amounts for DNase treatments of RNA extracts.

Amount	Reagent
10 µg (estimated using ODs)	RNA
5 µl	10 x DNAse I buffer
2 µl	RNAse free DNAse (Sigma)
1 µl	Ribolock RNAse inhibitor (Thermo Fisher Scientific)
Up to 50 µl	DEPC water

This mixture was incubated for 1 hour at 37 °C. After this, 6 µl of 25 mM EDTA was then added and the mix was incubated for 10 minutes at 65 °C.

Reverse transcription was performed to synthesise cDNA from the RNA extracts. This is done through mixing the reagents set out in Table 5.

Table 5. Reagents and amounts used for reverse transcription.

Amount	Reagent
10 pg – 5 µg	DNAsed total RNA
1 µl	50 µM oligo$(dT)_{20}$
1 µl	10 mM dNTP mix
Up to 14 µl	DEPC water

This was run on a PCR machine, which heated the mixture to 65 °C for 5 minutes. The samples were then incubated on ice for 5 minutes and the following was added as set out in Table 6.

Table 6. Reagents and amounts used for the oligo dT program.

Amount	Reagent
4 µl	5 x first strand buffer
1 µl	0.1 M DTT
0.5 µl	RNAse inhibitor
0.5 µl	SuperScript IV RT (Thermo Fisher Scientific)

The tubes were then run on a PCR machine as follows:

25 °C for 5 minutes

50 °C for 10 minutes

80 °C for 10 minutes

Stable at 4 °C after the reaction had finished.

The resulting cDNA samples were frozen at -20 °C.

2.11 qPCR

Primers for desired genes were designed using primer BLAST and selected for based on the categories of 50-60% GC content, 50-65 °C T_m and low self-complimentary. Both exon-exon junction restricted and no preference searches were made. The desalted primers were made up with de-ionised water according to the recommendations by the manufacturer for each specific primer.

Each primer was tested, and selected if multiple of one gene ordered, by running on an 1.2% agarose gel in 1 x TAE buffer to look for strong bands, tested with relevant cDNA to the experiment. The agarose gel was made with 0.6 g agarose in 500 ml 1 x TAE buffer, with 2 µl cybersafe dye. The bands were visualised using a UV light box.

For this, the following was mixed in a tube and centrifuged briefly as set out in Table 7.

Table 7. Reagents and amounts for RT-PCR reactions with primers to be tested.

Amount	Reagent
5 µl	cDNA
12.5 µl	2 x PCR mix
2 µl	5 µM forward and reverse primer mix
Up to 25 µl	Autoclaved water

The samples were then run on a PCR machine as follows:

94 °C for 2 minutes for denaturing DNA and activating the polymerase
25-35 cycles of 94 °C for 30 seconds
60 °C for 30 seconds
72 °C for 1 minute per Kb,
72 °C for 10 minutes for final extension
4 °C after the reaction has finished.
Samples were stored at - 20 °C until use.

For the qPCRs, 96 well plates were pipetted as indicated.
Each sample (well) contained the following reagents as set out in Table 8.

Table 8: Reagents and amounts in each well of the qPCR plate.

Amount	Reagent
10 µl	Fast SYBR Green master mix (ThermoFisher)
2 µl	Forward and reverse primer mix
3 µl	dH_2O
+	
5 µl	cDNA

The qPCR reactions were run in duplicate on a StepOne™ Real-Time PCR System (Applied Biosystems). Relative expressions were determined by the 2-ΔΔCT method. A control well was selected for normalisation (Gapdh for neurons, Rpl1 for flies).

Duplicate cDNA samples of each treatment including control (untreated) were pipetted when running the qPCRs with different primers. Normalisation to the house keeping gene Gapdh/Rpl1 was conducted for individual wells within the duplicates. Data from individual wells was excluded if a high standard error (SD) was displayed between duplicate wells with the same primer and treatment. Primers were previously checked for specificity of a single product using agarose gels (see above, page 35) to confirm that the primers tested generated a single band in a PCR reaction. Melt curves were additionally used to confirm that each primer generated a single peak during running of the qPCR.

The qPCR data was analysed through taking the relative expression (RQ) values for each well (treatment) and dividing the values against the control well of that gene for normalisation. This normalised relative expression value was averaged across the stated number of experiments, the mean plotted, and SEM displayed as error bars. Statistical analysis was performed for the mean RQs for each treatment against the control RQ (value = 1) using one-way ANOVAs and post-hoc tests as stated.

The primers used were as follows (Table 9).

Table 9. Primers used for qPCR reactions.

Name	Sequence
rHDAC4mRNAFex	GCAAGTGTGAGTGCATCCG
rHDAC4mRNARex	CGAGCTGTCCAGTTTCTGTCT
rHDAC5mRNAFex	ATTTGCCATCATCCGACCCC
rHDAC5mRNARex	GGTGAATGTCCCAGTCCACG
rHDAC9mRNAFnp	GTTACCCCAAGGAGCTTCCAA
rHDAC9mRNARnp	GGAGGTCAGATGCTGGGTTT
rSpp1mRNAFex	CCAGCCAAGGACCAACTACA
rSpp1mRNARex	AGTGTTTGCTGTAATGCGCC
rTpm2mRNAFex	CAGGCTCTCAAGTCGCTGAT
rTpm2mRNARex	GCACTAGCCAAAGTCTCTTCCA
rTxnipmRNAFex	AGCTGATCGAGAGCAAGGAAG
rTxnipmRNARex	TGGCAGTCATCCACGTCTAC
dMoeFex	GGAGAAGAATGCCAAACAGC
dMoeRex	GATCCTCGTACTCCTGCTGC
dUsfFnp	CTGGTCCACAGTTCCTTTGC
dUsfRnp	CACCTTGGCTATTCATCAGCG
dGadd45F	CATCAACGTGCTCTCCAAGTC
dGadd45R	GTAGATGTCGTTCTCGTAGC

2.12 Culture of neurons

Cortical neurons were cultured as described in Ugbode *et al*., 2020. Cultures were treated with cytosine arabinoside (AraC) at 1 day *in vitro* to inhibit any contaminating astrocytes in the neuronal cultures.

All treatments were performed in the absence of serum and growth factors in a defined medium called Transfection medium (TM), which is made up of 10% Minimal essential medium (Invitrogen) and 90% Salt-Glucose-Glycine (SGG) medium (SGG composition: 114 mM NaCl, 0.219% $NaHCO_3$, 5.929 mM KCl, 1 mM $MgCl_2$, 2 mM $CaCl_2$, 10 mM HEPES, 1 mM Glycine, 30 mM Glucose, 0.5 mM sodium pyruvate, 0.1% Phenol Red).

The TM was supplemented with insulin/transferrin/selenium (4140045, Thermo Scientific), penicillin (50 U/ml) and streptomycin (50 µg/ml). Neurons were in TM for 24 hours prior to treatments with DEM, bicuculline/4-aminopyridine, paraquat, TTX or forskolin at concentrations and durations as stated.

The culturing of neurons for this project was performed by Chris Ugbode.

3. Localisation and post-translational modifications of class IIa HDACs

It is well established that increases in synaptic activity in neurons can cause a cytoplasmic translocation of class IIa HDACs through Ca^{2+} signalling and subsequent activation of kinases (Chawla et al., 2003). In contrast, an increase in cellular cAMP in neurons by bath application of forskolin is known to induce a nuclear translocation (Belfield et al., 2006). Nevertheless, little is known about the localisation of these class IIa HDACs in the brain under conditions of oxidative stress. This chapter aims to investigate the effect of imposed oxidative stress on the subcellular localisation of HDAC4 and HDAC5 in primary cultured rat cortical neurons.

This chapter includes the findings that overall oxidative stress conditions, induced by DEM treatments, drive a nuclear translocation of both endogenous HDAC4 and HDAC5 in rat neuronal cells. Investigations into HDAC5 phosphorylation levels revealed some evidence of HDAC5 dephosphorylation after treatments with DEM, supporting the findings of its nuclear accumulation in the same conditions. Oxidative stress induced by paraquat, on the other hand, causes a primarily cytoplasmic and often punctate localisation of HDAC4. Inducing synaptic activity through treatments with Bic/4AP drives a largely cytoplasmic distribution of HDAC4 and HDAC5, as expected. Interestingly, combining DEM and Bic/4AP treatments led to even stronger cytoplasmic localisations of these HDACs. The nuclear shuttling of HDAC4 and 5 under oxidative stress is a novel finding and worthy of further investigations, as the mechanism underlying their ROS-induced nuclear translocation has relevance to neurodegenerative disease. This is especially relevant given the reported nuclear localisation of HDAC4 in Alzheimer's disease (Shen et al., 2016).

3.1. Oxidative stress causes a nuclear translocation of class IIa HDACs

To investigate whether oxidative stress alters the localisation of HDAC4/5 in neurons, immunostaining for endogenous HDAC4 and HDAC5 was performed in rat cortical neurons at 14 days *in vitro*. Localisation of HDAC4 and 5 was compared in neurons treated with bicuculline and 4-AP to increase synaptic activity; forskolin to increase cAMP levels; DEM and paraquat to increase ROS. Figure 12 shows representative confocal images of neurons fixed 2 hours after 100 μM DEM treatment and probed using an antibody to HDAC5 (Fig 12A) or HDAC4 (Fig 12B). Neurons were distinguished from astroglia by co-staining with an antibody to the neuronal marker protein NeuN.

In the untreated or control condition (- DEM), HDAC5 is localised in both the cytoplasm and the nucleus of neurons. In DEM treated neurons, HDAC5 immunoreactivity is strongly nuclear, suggesting that DEM induces a nuclear translocation of HDAC5 (Figure 12A). A similar localisation change was also observed for HDAC4 under the same DEM treatment (Figure 12B), but with a less marked change.

In contrast to DEM, treatments with 100 μM paraquat caused opposite reactions in HDAC4 and 5. Whilst HDAC5 translocated to the nucleus as it did with DEM treatment (Figure 13A), HDAC4 was observed as being more cytoplasmic after strong doses of paraquat treatment (Figure 13B).

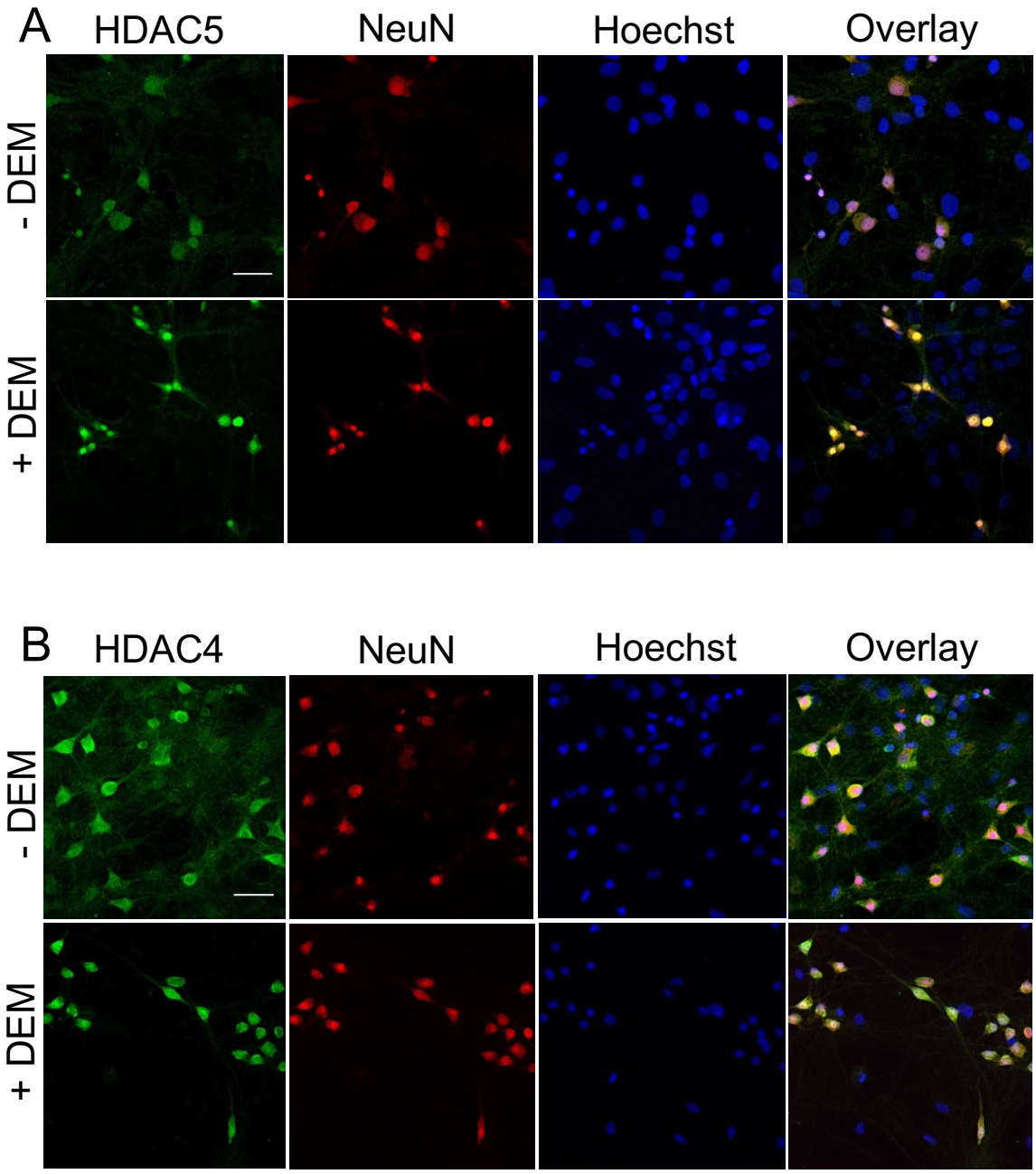

Figure 12: HDAC4 and 5 localise to the nucleus in neurons following DEM treatment. Representative confocal images displaying examples of cells showing localisation of (A) HDAC5 and (B) HDAC4 in immunostained cortical rat neurons. Neurons were left untreated (- DEM) or treated for 2h with 100 µM DEM (+ DEM). Green fluorescence signal represents HDAC4/5 immunoreactivity. Neurons were co-stained with NeuN, a neuronal marker, showing in red the whole of the neuronal cell. Nuclei were stained with Hoechst stain, showing in blue the location of the nucleus compared to the rest of the cell. The overlay displays the localisation of the green fluorescence HDAC4/5 immunoreactive signal in the context of the neuronal cells. Images taken at x20 objective. Scale bar = 35 µm.

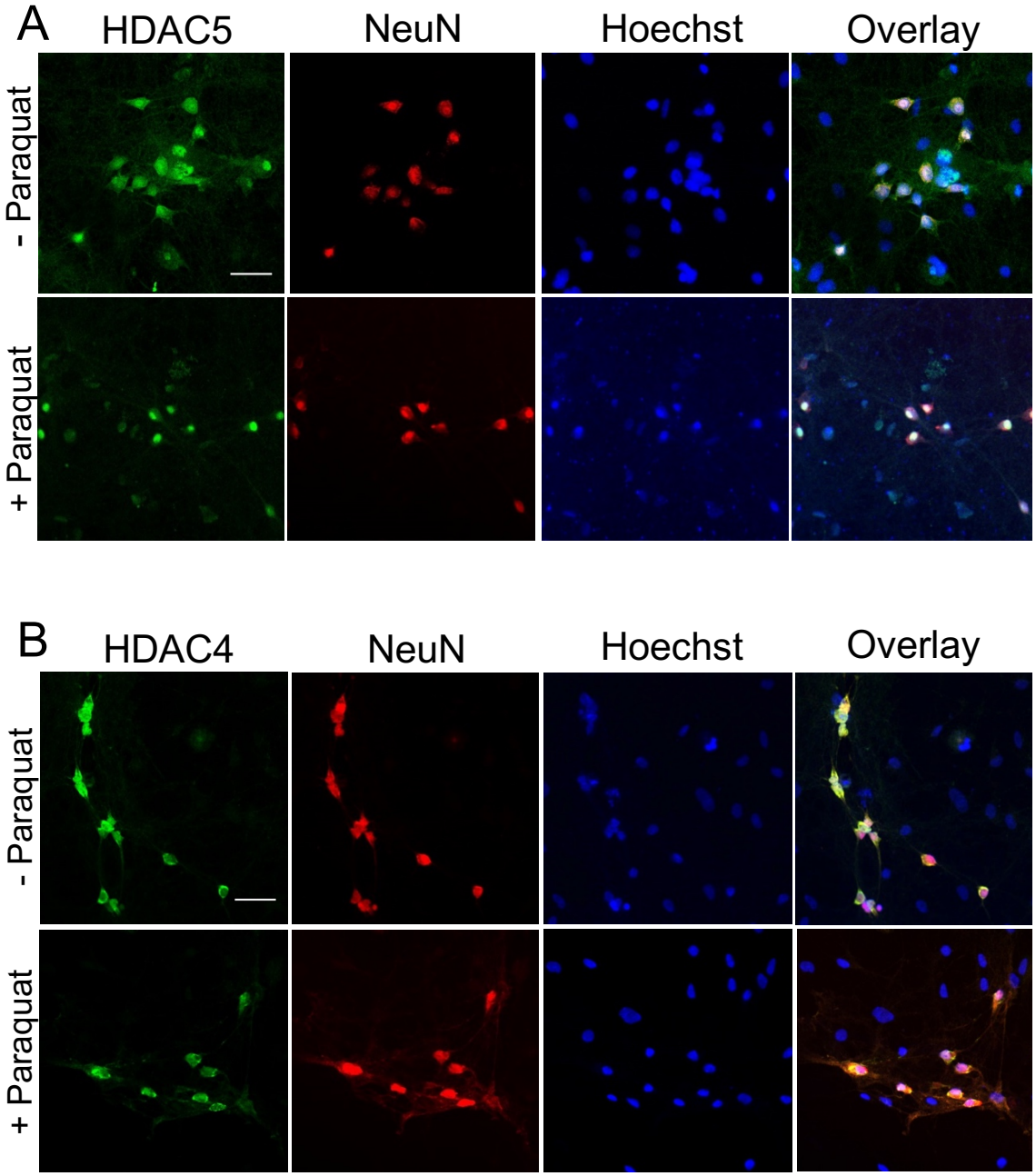

Figure 13: HDAC4 and 5 translocate in different directions in neurons following paraquat treatment. Representative confocal images displaying examples of cells showing localisation of (A) HDAC5 and (B) HDAC4 in immunostained cortical rat neurons. Neurons were left untreated (- Paraquat) or treated for 2h with 100 µM paraquat (+ Paraquat). Green fluorescence signal represents HDAC4/5 immunoreactivity. Neurons were co-stained with NeuN, a neuronal marker, showing in red the whole of the neuronal cell. Nuclei were stained with Hoechst stain, showing in blue the location of the nucleus compared to the rest of the cell. The overlay displays the localisation of the green fluorescence HDAC4/5 immunoreactive signal in the context of the neuronal cells. Images taken at x20 objective. Scale bar = 35 µm.

A quantitative analysis of these confocal images was performed: for each treatment, the percentage of cells showing HDAC4 and 5 immunoreactivity in the cytoplasm, nucleus, or both were determined. Images were analysed with ImageJ. Within ImageJ, a line was selected over the individual cell and the immunofluorescence signal was plotted across the distance of the cell (Figure 14). Comparing these plots with the images of the selected cells, it was possible to classify the fluorescent signal as either cytoplasmic, nuclear or both. A peak in the middle of the cell (Figure 14C) was classified as nuclear, a trough in the middle (Figure 14A) classified as cytoplasmic and a constant signal across the whole cell (Figure 14B) was classified as both. Bic/4AP treatment was used to increase synaptic activity and forskolin treatment to increase cAMP levels with these conditions providing positive controls for cytoplasmic and nuclear localisation of HDAC4/5 respectively.

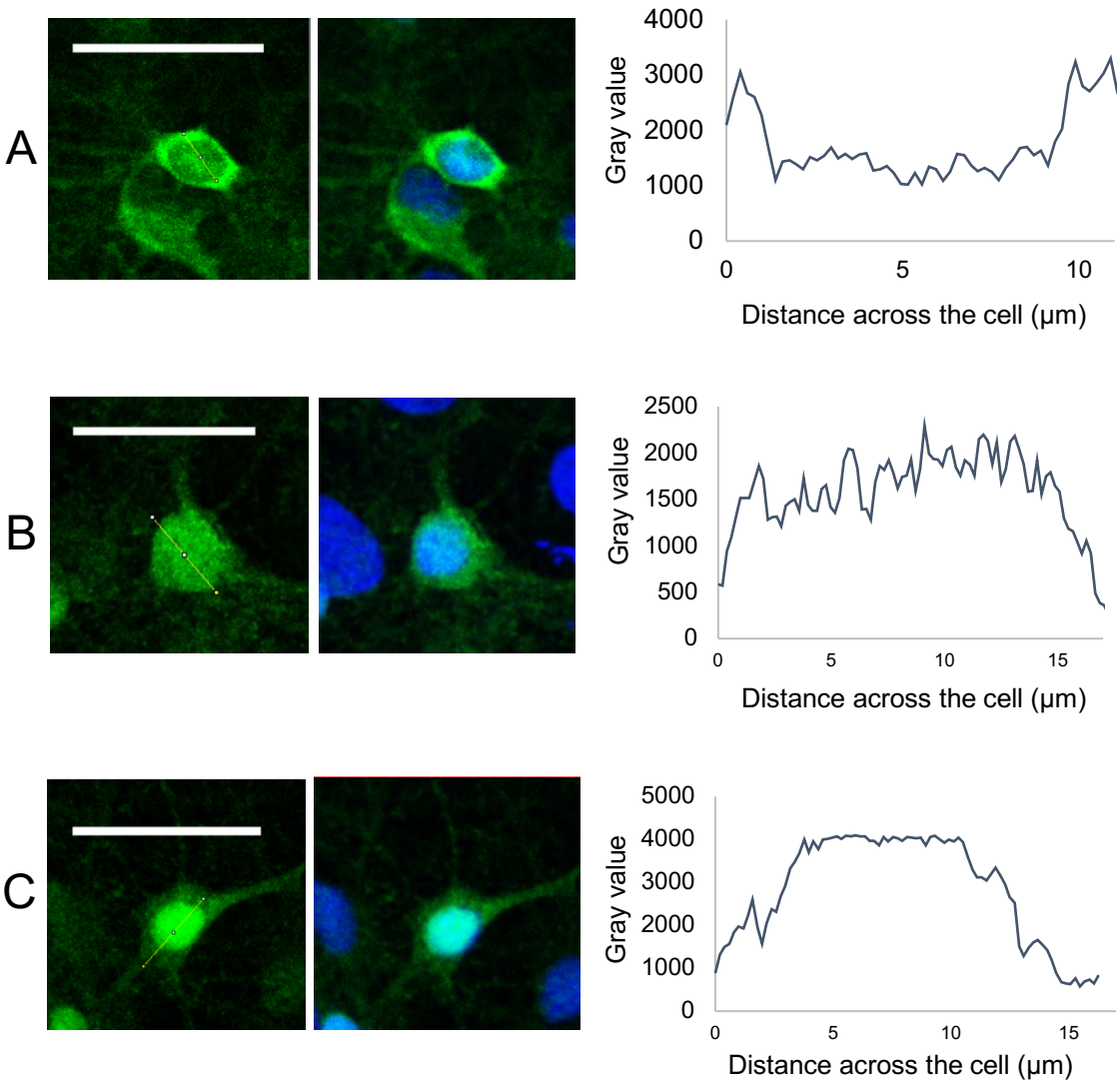

Figure 14: Representative examples of neuronal cells classed as cytoplasmic, nuclear or both HDAC4/5 immunoreactivity. Representation of how individual neuronal immunostained cells were analysed using ImageJ and classified as either (A) cytoplasmic, (B) both or (C) nuclear. In ImageJ, a line was selected across each cell (left panels) to measure the fluorescent green signal across the distance of the cell. The blue Hoechst stain show the location of the nuclei of the cells. Cells were classified based on representative images and the rough shape of the plots (right panels) as either having a trough in the middle of the cell (where the nucleus is) and being cytoplasmic, a peak in the middle and nuclear, or roughly the same signal across the distance of the cell and classified as both. Scale bar = 35 µm.

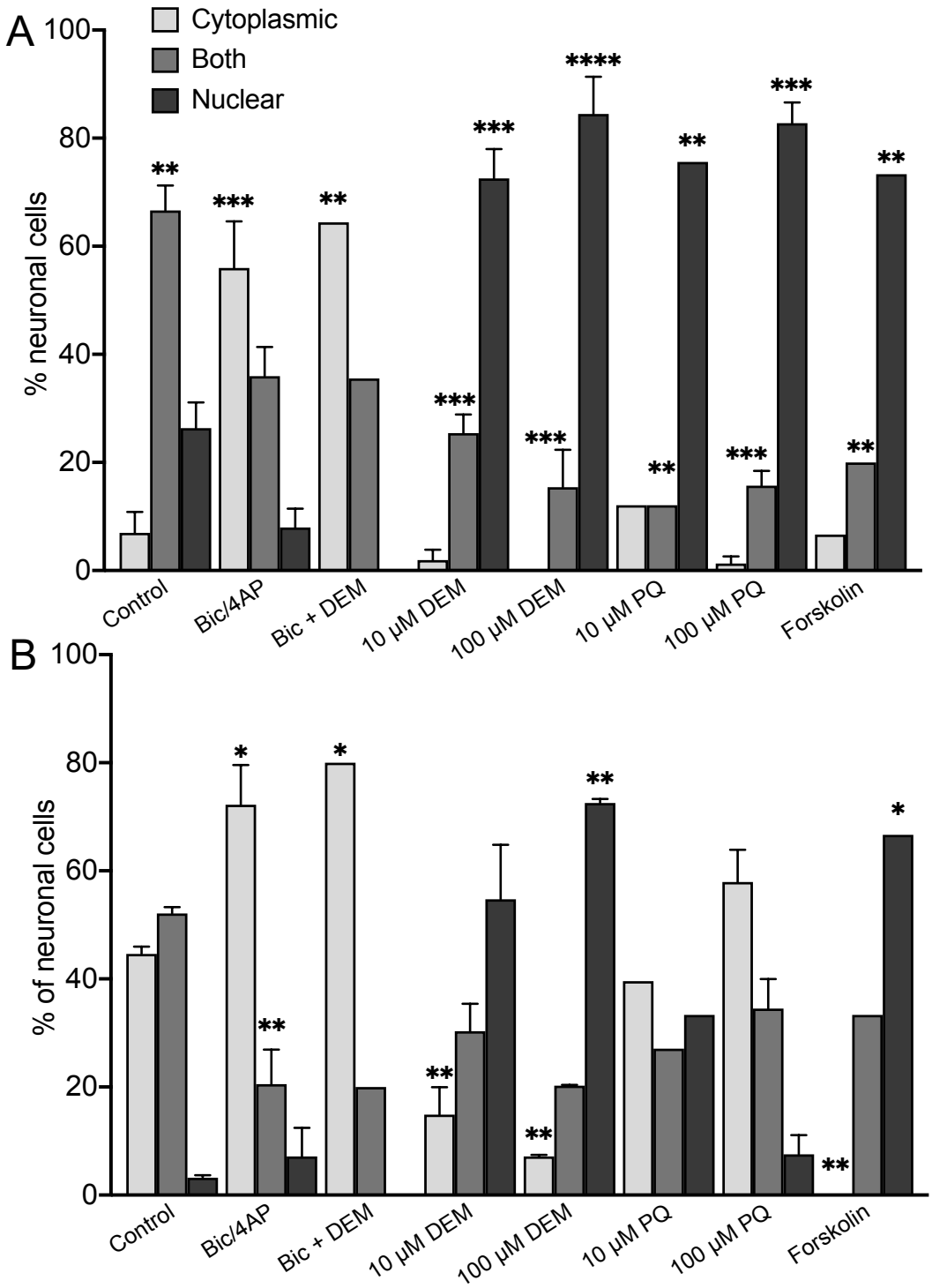

Figure 15: Synaptic activity and oxidative stress generate distinct subcellular distributions of HDAC5 and HDAC4 in neurons. Neurons were treated for 2 hours with the indicated treatments or left untreated (control) and stained for HDAC4 or HDAC5. Neurons in each treatment group were classified as showing cytoplasmic (light grey), both (dark grey) or nuclear (black) localisation and the percentage of cells in each category was plotted for HDAC5 (A) and HDAC4 (B). The mean percentages from 3 independent experiments are shown. Error bars indicate ± SEM. Localisation was assessed in roughly 150 cells per independent culture. (*P<0.05 One way ANOVA followed by Dunnett's post-hoc test*P<0.05 **P<0.005 ***P<0.0005 ****P<0.0001 n = 3 independent

cultures). The asterisks indicate statistically significant differences between control and treated neurons in the indicated localisation category.

As observed in the confocal images of the cells, quantitative analysis shows that HDAC5 in neurons is both cytoplasmic and nuclear in control conditions, with a very low proportion of cells (6.99 ± 3.86%) showing exclusively cytoplasmic localisation and 26.34 ± 4.77% of cells showing exclusively nuclear HDAC5 immunoreactivity (Figure 15A). HDAC4, on the other hand, is cytoplasmic in much higher proportion of cells (44.61 ± 1.36%) under control conditions with very few neurons display exclusively nuclear immunoreactivity (3.22 ± 0.81%) (Figure 15B).

Increased synaptic activity induced by Bic/4AP treatments show a cytoplasmic shuttling of both HDAC4 and 5, as expected in accordance with previous studies (Chawla et al., 2003). Forskolin treatments show a movement of both HDAC4 and HDAC5 towards the nucleus, also as expected, with HDAC5 being strongly nuclear in this condition. Whilst HDAC4 has movement towards a nuclear localisation, a substantial proportion (33.33%) of the classified cells are still categorised as both cytoplasmic and nuclear with forskolin treatment (Figure 15B).

The data in Figure 15 confirms the nuclear translocation of both HDAC4 and 5 in response to DEM-induced oxidative stress conditions. Both HDAC4 and 5 show a nuclear shuttling in response to DEM in a dose-dependent manner, with higher concentrations of DEM (100 μM) causing a more marked change (a nuclear distribution increase of 3.22% to 72.54% for HDAC4 and 26.34% to 84.46% for HDAC5) compared with lower concentrations (10 μM) (an increase of 3.22% to 54.75% for HDAC4 and 26.34% to 72.55% for HDAC5). For HDAC5, 10 μM DEM treatments show very similar localisation to forskolin treatment, with over 70% of cells analysed displaying nuclear immunoreactivity. HDAC4 also shuttles to the nucleus following DEM treatment, but based on the data in both Figure 12 and Figure 15, the DEM-induced HDAC4 nuclear translocation (72.54 ± 1.06% nuclear following 100 μM DEM treatment) is less pronounced than for HDAC5 (84.46 ± 11.97% nuclear following 100 μM DEM).

Oxidative stress conditions induced by paraquat treatments had similar effects on HDAC5 localisation as DEM, but markedly different effects on HDAC4 localisation. Similar to DEM, paraquat treated neurons showed a dose-dependent nuclear translocation of HDAC5 in Figure 15A. HDAC4 on the other hand, displayed a predominantly cytoplasmic localisation in response to both low (10 μM) and high concentrations (100 μM) of paraquat treatments (Figure 15B) with 57.94 ± 5.94% of cells showing cytoplasmic HDAC4 in 100 μM paraquat compared to 44.61 ± 1.36% of cells showing cytoplasmic HDAC4 in control conditions.

When looking at the proportion of HDAC5 stained cells stained showing a cytoplasmic localisation, the DEM, paraquat and forskolin treatments show no difference compared to the control treatment, whilst bath application of bicuculline and 4-aminopyridine causes an increase from 6.99% to 55.97% of cells displaying cytoplasmic HDAC5 distributions. When comparing the percentage of cells showing a nuclear HDAC5 localisation, Bic/4AP treatments cause a decrease in nuclear HDAC5 from 26.34% to 7.97% whilst DEM, paraquat and forskolin cause highly significant increases in cells with a nuclear HDAC5 distribution (Figure 15A). The 10 μM DEM, paraquat and forskolin treatments show very similar nuclear localisations in cells stained for HDAC5, indicating they are driving a similar HDAC5 translocation mechanism at these concentrations.

On the other hand, when comparing the proportion of nuclear HDAC4, Bic/4AP and 100 μM paraquat treatments show little difference in comparison to control, whilst 10 μM DEM and forskolin cause increases from 3.22% to 54.75% and 66.67% respectively. For cytoplasmic HDAC4 distributions, 100 μM DEM shows a decrease from 44.61% in the control condition to 7.14%. Meanwhile, 100 μM paraquat induces an increase of cytoplasmic HDAC4 to 57.94%, indicating an opposing localisation pattern to that found after high concentration DEM treatment.

Given that synaptic activity and DEM had opposing effects on HDAC4/5 localisation, the effect of combined treatment with both Bic/4AP and 10 μM DEM was also investigated. The combination of these treatments was used to help elucidate the mechanism by which DEM drives a HDAC4/5 nuclear translocation. It was hypothesised that DEM either inhibits the normal processes involving class IIa HDAC nuclear export or activates independent mechanism for their nuclear import.

Under these conditions, both HDAC4 and 5 showed predominantly cytoplasmic localisations (Figure 15) and interestingly, this cytoplasmic translocation with the combined treatment was more marked than with just Bic/4AP treatment alone.

3.2. High concentrations of paraquat causes HDAC4/5 accumulation in distinct immunoreactive puncta

During imaging of both HDAC4 and HDAC5 immunostained cells, occurrences of immunoreactive puncta were observed in the 100 μM paraquat treated neurons (Figure 16). The appearance of puncta was observed in the perinuclear region of the cytoplasm for HDAC4 (Figure 16A) and HDAC5. However, puncta were also observed in the nucleus for HDAC5 as shown in Figure 16B. This discrete pattern of immunoreactivity was not observed in NeuN stained images and therefore is unlikely that paraquat is causing a general accumulation of all cellular proteins.

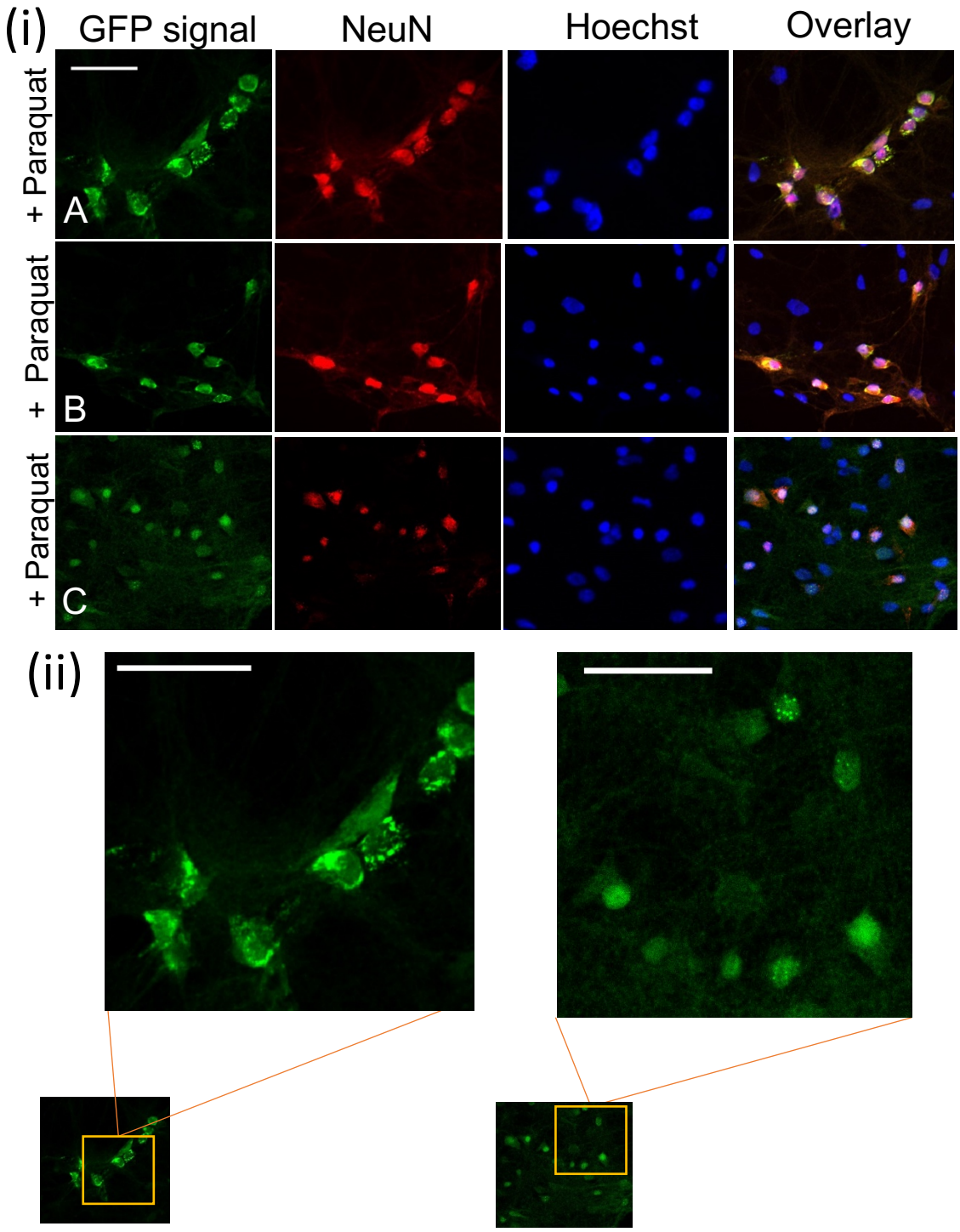

Figure 16: HDAC4 and 5 immunoreactive puncta are observed in neurons following high concentrations of paraquat treatment. (i) Representative images of examples of HDAC4 and HDAC5 immunoreactive puncta in neurons following 100 µM paraquat treatments. Examples of 100 µM paraquat treated neurons are shown with (A-B) HDAC4 and (C) HDAC5 immunoreactivity. (ii) A closer look at examples of punctuative fluorescent signal images from (A) and (C). Green fluorescence signal represents HDAC4/5 immunoreactivity. Neurons co-stained with NeuN, a neuronal marker. Nuclei were stained with Hoechst stain. Scale bar = 35 µm.

3.3. Oxidative stress causes a dephosphorylation of HDAC5

The data thus far show a marked change in HDAC4/5 localisation from mainly cytoplasmic in control conditions to mainly nuclear in DEM treated neurons. Since the cytoplasmic localisation of HDAC4/5 requires the phosphorylation of conserved serine residues, the phosphorylation status of HDAC5 was investigated by western blotting. This was performed using a phospho-specific antibody that detects phosphorylated serine 259 on HDAC5 (and p-246 on HDAC4) (see section 2.3). Cortical neurons, 14 days *in vitro*, were treated for 3 hours with either 50 μM Bic/4AP, 10 μM DEM, 100 μM DEM or left untreated (control).

After treatment, the cells were lysed in 1 x RIPA buffer (see section 2.2) and a western blot protocol (see section 2.4) was performed with primary antibodies against HDAC5 and phospho-HDAC5 (p-259). The bands from this western blot are shown in Figure 17A where the bands were analysed using the gel analyser tool in ImageJ, and relative densities plotted. The phospho-HDAC5 relative densities plotted are normalised to their respective inputs of total HDAC5 in the same treatment.

Compared to the control, all treatments appear to have very similar band densities for total HDAC5 indicating that the inputs were all the same (Figure 17A). The p-HDAC5 band after Bic/4AP treatment shows a stronger signal compared with the control band. However, the plotted relative densities show a dose-dependent decrease in the p-259 band signal, indicating a dephosphorylation, whilst re-probing of the blot with an antibody for MEF2D confirmed equal sample loading.

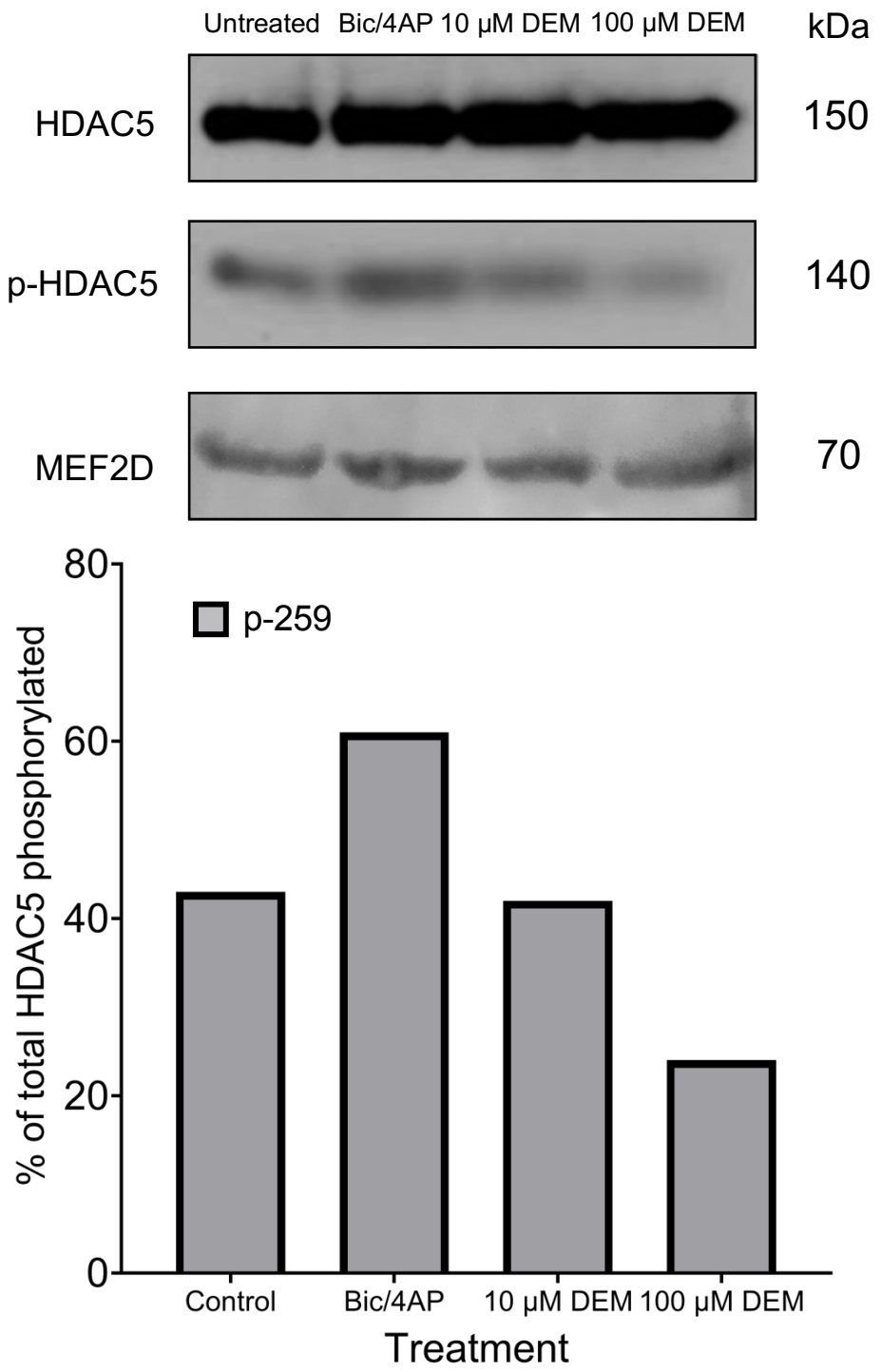

Figure 17: HDAC5 is dephosphorylated in neurons following DEM treatments. (A) Representative western blots of lysates derived from neurons treated as indicated or left untreated (control). All treatments were for 1 hour. Blots were probed with antibodies against total HDAC5 (top), p-HDAC5 (259) (middle) and MEF2D (bottom). (B) Relative densities from analysed phosphorylated HDAC5 (p-259) western blot bands are plotted as percentage of total HDAC5 phosphorylated. Total HDAC5 bands were normalised to MEF2D bands (shown in A to be unchanged) which was used as a loading control.

To test if the observed dephosphorylation is a result of changing HDAC5 gene expression, a qPCR (see section 2.11) was performed using primers for HDAC4, 5 and 9. The cDNA was synthesised (see section 2.10) from RNA extracted from rat cortical neurons at 14 days *in vitro*. Relative expressions were compared with neurons treated with 50 µM bicuculine and 4-AP or DEM for 1 or 4 hours.

Figure 18 shows the plotted relative expressions of HDAC4, HDAC5 and HDAC9 under these treatments, which show no significant expression changes with 1 hour Bic/4AP and DEM treatments. HDAC4 and 9 show no change with 4-hour Bic/4AP treatments. However, HDAC5 does have a slight, but not significant, increase in expression (1.68 ± 0.40-fold change) during these long-term bath applications of Bic/4AP and resulting increased synaptic activity, but we cannot confidently conclude whether HDAC5 levels are changing in this condition.

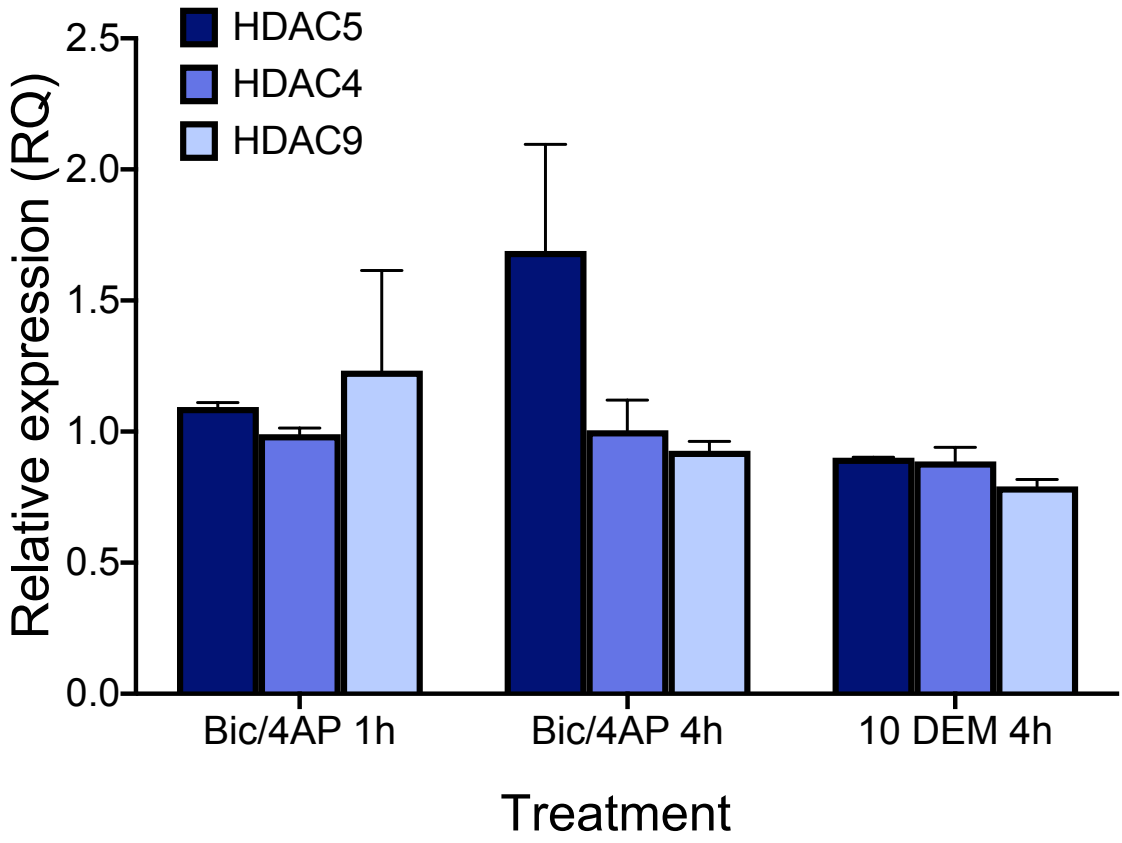

Figure 18: HDAC4, 5 and 9 gene expressions are unchanged in neurons following DEM treatments. Representation of relative expressions (RQ) of HDAC4, 5 and 9 from real time quantitative PCR experiments. Neurons were treated for 1 hour or 4 hours with the indicated treatments. The mean relative expressions from 3 independent experiments are shown. Error bars indicate ± SEM. ($P>0.05$ (ns), one way ANOVA, n = 3 independent cultures).

3.4. Discussion

The subcellular localisation of class IIa HDACs is highly dynamic and signal regulated. The data in this chapter show that overall oxidative stress conditions cause a nuclear accumulation of HDAC4 and HDAC5, suggesting that ROS induce a nuclear translocation of class IIa HDACs. There were, however, some notable differences between HDAC4 and HDAC5 depending on the mode of ROS induction. HDAC5 shows very similar levels of nuclear translocations in both 10 μM DEM and 10 μM paraquat oxidative stress conditions. HDAC4, on the other hand, was nuclear in neurons treated with DEM but cytoplasmic in those treated with paraquat. Moreover, HDAC4 showed a punctate localisation in many neurons. Further experiments could explore visualising GFP-tagged HDAC4/5 nucleocytoplasmic shuttling in live cells over time with DEM and paraquat treatments. This could identify how long after treatment these HDACs start to shuttle to the nucleus, helping to elucidate a timeline for the mechanism.

HDAC4 has previously been shown to be largely, but not exclusively, cytoplasmic during basal conditions in mouse brains (Mielcarek et al., 2013; Bolger & Yao, 2005). This is consistent with our findings of HDAC4 being localised to both the cytoplasm and nuclei under control conditions, where the percentage of neuronal cells with HDAC4 cytoplasmic localisation is high. Previous work has shown that a cytoplasmic localisation of HDAC4 in untreated neurons is due to spontaneous electrical activity (Chawla et al., 2003). Increasing synaptic activity further with Bic/4AP is therefore expected to amplify the cytoplasmic shuttling of HDAC4. In our findings, Bic/4AP makes HDAC4 adopt an even more cytoplasmic distribution, especially when compared with HDAC5 under the same conditions. This cytoplasmic distribution bias also explains the less marked nuclear translocation change of HDAC4 with DEM treatments.

The largely cytoplasmic localisation of HDAC4 in neurons under normal conditions could be due to a basal phosphorylation level, where the calcium dependent kinases may have a low threshold for activation. Findings suggest that the CamKII kinases specifically phosphorylate HDAC4 but not HDAC5 (Backs et al., 2006). Moreover, the nuclear export of HDAC4, but not HDAC5, is shown to be triggered by spontaneous electrical activity (Chawla et al., 2003). Therefore, it could be postulated that these kinases could be activated by spontaneous electrical activity alone. Treatment with Bic/4AP, which increases neuronal firing, may additionally activate other kinases including CamKIV which acts on both HDAC4 and HDAC5. Alternatively, differences in HDAC4 and 5 structural domains and phosphorylation sites may mean that HDAC4 acts as a less optimal substrate for the action of phosphatases which induce their nuclear import.

Interestingly, both HDAC4 and 5 show a slight increase in cytoplasmic localisations with treatments of Bic/4AP and 10 μM DEM combined compared with Bic/4AP alone where these stimuli usually cause opposing translocations. This indicates that the DEM oxidative stress condition does not inhibit HDAC nuclear export, but activates an independent pathway to drive their nuclear import. It can be postulated that the neuroprotective effects of Bic/4AP signals, and subsequent cytoplasmic distributions of the HDACs, may be enough to combat conditions of low oxidative stress. Furthermore, this low DEM dose seems to accentuate the shuttling towards the cytoplasm for both HDAC4 and HDAC5.

With respect to paraquat-induced oxidative stress, HDAC4 and 5 do not share the same pattern of translocation as with DEM. HDAC5 has a very similar nuclear shuttling in response to paraquat and DEM, suggesting that the oxidative stress-induced mechanism causing its nuclear translocation is active under both these treatments. In contrast, HDAC4 shows a dose-dependent shuttling into the cytoplasm with paraquat treatment, although not to the same level as the Bic/4AP positive control. It is likely HDAC4 nuclear shuttling under DEM conditions is regulated by the same mechanism that controls HDAC5 nuclear shuttling, but this raises questions about paraquat's mode of action and cellular effects. Recent, unpublished data from the Chawla lab indicates that paraquat treatments can cause low amplitude oscillatory calcium bursts in cultured neurons. These low amplitude oscillations might be sufficient to activate a HDAC4 kinase such as CamKII, but not HDAC5 kinases. The mechanism by which paraquat causes Ca^{2+} release could be related to its previously reported effects on calmodulin stimulated plasma membrane Ca^{2+}-ATPase (PMCA) (Zaidi et al., 2009).

Resulting increases in intracellular calcium levels in neuronal cells is a known signal for the nuclear export of HDAC4 (see section 1.4), where this signal appears to work more strongly than the opposing mechanism driving its nuclear import during DEM treatments. As discussed previously, cytoplasmic HDAC4 is neuroprotective (Majdzadeh et al., 2008), and therefore it could be interesting for this calcium burst signal to be exploited from a therapeutic point of view. This could drive neuroprotective cytoplasmic HDAC4 movements, even when neuronal cells are under conditions of elevated ROS levels and oxidative stress so common in disease.

Under high concentrations of paraquat, punctate immunoreactive signals were seen for both HDAC4 and HDAC5. This could be due to the neuronal cells being apoptotic in such extreme oxidative stress conditions. If this is the case, TUNEL staining could be performed to identify if the cells are undergoing apoptosis in these conditions. However, the NeuN stain do not appear to have these same puncta, suggesting this change is HDAC4/5 protein specific. Moreover, there is no apparent nuclear shrinking or blubbing

of the stained nuclei which is indicative of cells undergoing apoptosis. Alternatively, this could be due to the HDACs moving into other functional compartments (Takase et al., 2013). Previous studies observed distinct dot-like structures of GFP tagged HDAC4 in HeLa cells (Miska et al., 1999), thought to co-localise with MEF2A, and YFP tagged mouse HDAC5 in CV-1 cells, thought to co-localise with mouse HDAC7 in subnuclear compartments (Kao et al., 2000). In 2010, Darcy *et al*. found that HDAC4 immunoreactivity is punctate in the cytoplasm of neuronal cells across the whole of the mouse brain. In addition, some of these observed puncta were seen around the cytoplasmic surface of the nuclei, where some were present in dendritic spines (Darcy et al., 2010). This was similarly seen in the presented images (Figure 16) where HDAC4 immunoreactive puncta was perinuclear. Whilst it is unclear what specifically these puncta represent, their presence may suggest that the class IIa HDACs may move into these functional compartments and co-localise with other proteins.

It has previously been shown that, in response to high ROS levels, class IIa HDACs are subject to different post-translational modifications. Recently, evidence has emerged that specific cysteine residues, Cys 667 and Cys 669 on HDAC4 (Figure 4), are oxidised in response to oxidative stress in cardiomyocytes, where these redox sensitive cysteines are conserved in all class IIa HDACs (Ago et al., 2008). Whilst the irreversible oxidation of proteins via ROS can lead to their dysfunctionality, the reversible oxidation of cysteine residues on proteins can contribute to the regulation of enzymatic activity, interactions, localisation and signalling cascades (Van der Reest et al., 2018). This indicates that the class IIa HDACs may undergo a number of post-translational modifications during oxidative stress conditions that may contribute to their mechanism of shuttling and action.

As of yet there has been no specific evidence or research on these class IIa HDAC cysteine oxidations when neuronal ROS levels are excessive. Pull down experiments were attempted under normal and DEM-induced oxidative stress conditions using biotinylated-iodoacetamide, an agent that binds free thiol levels. These experiments aimed to detect free thiol levels and therefore oxidation modifications (where free thiol levels went down) in HDAC5 under these conditions. Whilst attempts were not successful in yielding a reliable result, this would be an interesting future approach. This would help in the understanding of how the class IIa HDACs are modified under oxidative stress conditions in the brain, and how their modifications may contribute to or affect their mechanisms of action.

Two phospho-HDAC5 antibodies (p-259 and p-498 phosphorylation sites) were used for immunostaining sets of treated cortical neurons in the same way as HDAC4 and HDAC5. However, it was deemed that these antibodies were not specific enough in the context

of visualising the fluorescent signals by confocal microscopy as they appear to represent the location of HDAC5 rather than actual phosphorylated HDAC5.

From these images, it was also not possible to deduce if a dephosphorylation was occurring. Thus, western blots were used instead for these investigations, which displayed a likely dephosphorylation of HDAC5 under DEM conditions, supporting our previous findings of a HDAC5 nuclear translocation. As discussed in section 1.4, the dephosphorylation of the class IIa HDACs by phosphatases (such as PP2A) is a key part in their nuclear import. This result was corroborated by qPCR data which showed no significant changes in HDAC5 gene expression with DEM treatments, in line with the observed similar band densities for total HDAC5. Together, these findings indicate that the decrease in phospho-HDAC5 levels detected in the western blot was not due to decreases in overall HDAC5 gene expression. However, the HDAC5 dephosphorylation data was from one experiment and would therefore require repetition.

In addition, a slight upregulation of HDAC5 after long (4-hour) treatments with Bic/4AP was observed. The statistics revealed no significance in the change in HDAC5 levels in this condition, however if HDAC5 expression is increasing, this could help to explain the slight increase in total HDAC5 and phospho-HDAC5 levels in Figure 17. An important role for HDAC5 in the detoxifying antioxidant mechanisms is therefore suggested, triggered by increases in neuronal firing. Further experiments could be performed to investigate why HDAC5 might be transcriptionally upregulated after these long periods of high synaptic activity, and what it might be interacting with in the cytosol. The HDAC5 localisation changes were seen after 2-hour treatments with Bic/4AP in this study, and previous studies demonstrated the same increase in cytoplasmic HDAC5 after 1 hour. Therefore, it would be appropriate to repeat the experiment with a 4-hour Bic/4AP treatment to determine if HDAC5 is still retained in the cytoplasm at this point.

Nucleocytoplasmic fractionations were attempted during the project with neurons treated similarly to the neurons used for the localisation data, and the samples ran on a western blot. The western blot approach was not sensitive enough to pick up the lower levels in each fraction compared to whole cell lysates. However, additional experiments could re-attempt this to support the findings of HDAC4 and 5 shuttling under DEM treatments.

In addition, this fractionation technique could be used to confirm the observation of a slight increase in HDAC5 expression after Bic/4AP treatment. This may be attempted using buffers of different stringencies (e.g. soft lysis and RIPA buffers) to fractionate out nuclear and cytoplasmic samples. Immunoprecipitation (IP) techniques could then be used on these fractionated samples to explore interactions of HDAC5 in the cytoplasm during bouts of increased neuronal activity. If these techniques are not sensitive enough to pick up the interactions, proteomics screens may prove beneficial.

4. Interactions of class IIa HDACs in the nucleus

This chapter aims to investigate the impact of the oxidative stress-induced nuclear import of HDAC4/5 on gene regulation by assessing mRNA levels of putative HDAC4/5 target genes. This chapter includes the findings that the genes Spp1 and Tpm2, both with links to CNS related disease, are likely upregulated specifically in neuronal cells following treatments with low doses of DEM. This correlates well with the nuclear imports of HDAC4/5 under the same conditions, and was found to be most significant with short, 1-hour treatments. Treatments of the same neuronal cells with TTX, an agent which blocks synaptic activity, also showed a possible induction of the Tpm2 gene, whilst Bic/4AP, which increases synaptic activity, saw a likely Tpm2 repression. Together, these findings suggest that the Spp1 and Tpm2 genes may be induced under oxidative stress conditions through nuclear HDAC4/5 activation of FOXO transcription factors. Additionally, the Gadd45 gene, implicated in DNA damage repair and protective pathways in the brain, was found to possibly be induced in wildtype flies and flies expressing mammalian GFP tagged HDAC5 raised on DEM food. Images from brain dissections of the same flies expressing GFP-HDAC5 show a possible nuclear translocation of the expressed HDAC5 under oxidative stress conditions. This, together with sequence alignments of the Gadd45 gene promoter in flies, rats and humans suggest a conserved mechanism of Gadd45 regulation by HDAC4/5. Therefore, these findings could translate into the human brain.

4.1. A group of genes is induced under oxidative stress conditions in neurons

Following on from the observation of the oxidative stress-induced nuclear import of HDAC4 and 5, it was important to explore their subsequent impact on gene regulation to help identify mechanisms which may be occurring under these conditions.

In 2012, Sando *et al*. investigated differentially expressed genes in the mouse forebrain with a constitutively nuclear HDAC4 mutant (3SA) compared to wildtype HDAC4. This mutant substituted alanine residues for key serine phosphorylation sites. This ensured the chaperone protein 14-3-3 could no longer bind and sequester the HDAC4 mutant in the cytoplasm (Sando et al., 2012). Within their DNA microarray data, the nuclear 3SA mutant was shown to repress a large array of genes, as well as induce a small gene group compared to the wildtype. As class IIa HDACs have been shown to activate FOXO transcription factors (Mihaylova et al., 2011) it is possible that the 3SA mutant in Sando *et al*. is acting via FOXO. Experiments reported in the previous chapter show that DEM caused a nuclear localisation of HDAC4/5. This chapter therefore investigated whether DEM increases transcription of the genes that are upregulated by a constitutively nuclear HDAC4 mutant.

Table 10 displays some of the genes that were induced with the greatest fold change in the 3SA mutant over wildtype (Sando et al., 2012). This, therefore, identified them as genes of particular interest in this study.

Table 10. List of genes induced with the 3SA HDAC4 mutant compared with wildtype and their relative fold changes (Sando et al., 2012).

Gene	Fold change (3SA/WT)
Spp1	4.7
Tpm2	2.4
Gadd45a	1.8
Msn	1.8
Usf1	1.5

Among these genes is secreted phosphoprotein 1 (Spp1), which encodes the protein osteopontin (OPN) and is a constituent of the extracellular matrix of the central nervous system (CNS). Spp1 has been found to be upregulated in microglia (Yu et al., 2017), and is hypothesised to have a role in the pathogenesis of neurodegenerative diseases such as Alzheimer's (Wung et al., 2007).

Tropomyosin 2 (Tpm2) encodes beta-tropomyosin, an actin-filament binding protein which is mainly functional in skeletal muscles. Despite this, actin dynamics are beginning to be identified as playing key roles in neural development (Kumar et al., 2016). Whilst the precise role of actin binding proteins in nervous system development remains unknown, recent studies demonstrated that knockdown of Tpm2 expression leads to impaired spatial learning and memory performance in the rat hippocampus (Hsu et al., 2017).

Like Tpm2, moesin (Msn) is an actin binding protein and has been found to restrain synaptic growth in flies (Seabrooke & Stewart, 2008) and is elevated in the visual cortex of sensory deprived mice (Tropea et al., 2006).

Growth arrest DNA damage-inducible protein (Gadd45) is involved in DNA damage repair and is a known FOXO target gene. The Gadd45 gene has been shown to be induced in cases of Alzheimer's disease (Torp et al., 1998) and implicated in apoptosis and protective pathways against stress in the brain (Moskalev et al., 2012).

The upstream transcription factor 1 (Usf1) gene encodes for a ubiquitously expressed transcription factor known to regulate diverse functions (Yamanaka et al., 2016) including stress responses (Corre & Galibert, 2005). However, their role in the brain remains unclear. As described in section 1.5, Txnip is a FOXO target gene and an oxidative stress sensor part of the protective redox control system in the brain.

In this study, these genes were investigated in both rat cortical neurons and transgenic *Drosophila* to evaluate conserved mechanisms involving the class IIa HDACs under oxidative stress conditions between fly and rat brains.

In order to examine whether these genes had altered gene expression under conditions of oxidative stress, quantitative PCRs were performed. Cortical neurons in culture at 14 days *in vitro* were left untreated (control) or treated for 1 or 4 hours with either Bic/4AP, which causes cytoplasmic translocation of HDAC4/5, or 10 μM DEM, which induces HDAC4/5 nuclear import. Tetrodotoxin (TTX) treatment was included for comparison as silencing of neuronal activity with TTX also results in a nuclear localisation of both HDACs (Chawla et al., 2003).

RNA was extracted from these treated neurons (see section 2.8), subjected to cDNA synthesis (see section 2.10) and qPCRs (as in the protocol in section 2.11) were performed with the primers as set out in Table 9.

All samples were normalised to Gapdh untreated (control) samples.

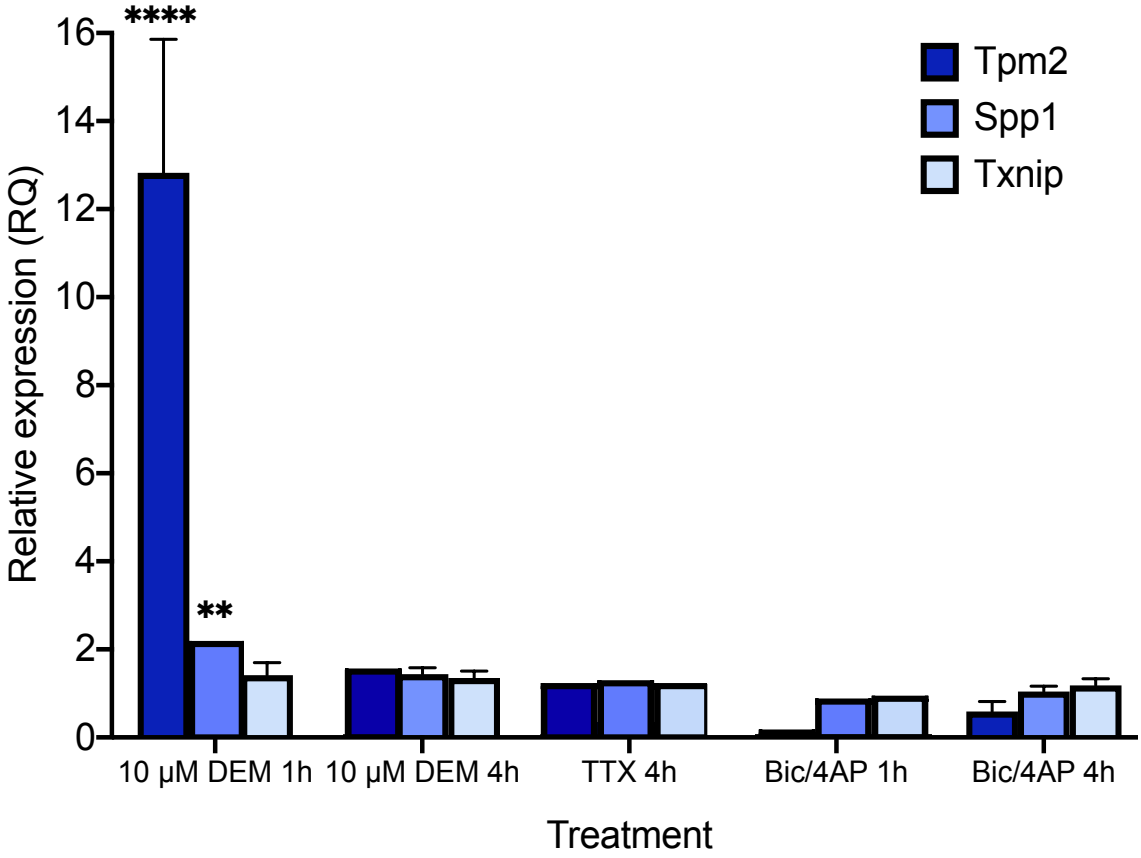

Figure 19: Oxidative stress conditions upregulate Tpm2 and Spp1 gene expression in neurons. Neurons were treated for 1 hour or 4 hours with the indicated treatments. Representations of relative gene expressions (RQ) are plotted for Tpm2 (dark blue), Spp1 (light blue) and Txnip (pale blue). Gapdh was used as the housekeeping gene. The mean relative expressions from 2-4 independent experiments are shown. Error bars indicate ± SEM where n = 3 or more. ($P<0.001$ One way ANOVA followed by Dunnett's post-hoc test *$P<0.005$ ****$P<0.0001$).

As shown in Figure 19, the Tpm2 gene in neurons showed both induction and repression of expression under different treatments. A highly significant ($p<0.0001$) induction of Tpm2 expression (12.8 ± 3.0-fold change) was observed following 10 µM DEM treatment, where this change was much stronger after 1 hour compared to a slight, but not significant, induction after 4 hours (1.5 ± 0.30-fold change). Conversely, a repression of Tpm2 was observed following Bic/4AP treatment, with a more marked change seen within 1 hour (0.16 ± 0.06-fold change) compared to 4 hours (0.59 ± 0.22-fold change) (Figure 19). Treatment with TTX showed a slight induction of Tpm2 expression (1.2 ± 0.18-fold change).

Results indicated no significant changes in Spp1 relative expression after 4-hour treatments with 10 µM DEM, TTX or any Bic/4AP treatments. However, 1-hour treatments with 10 µM DEM did show an induction of the Spp1 gene in cultured rat neurons (2.16 ± 0.09-fold change) (Figure 19). Whilst no significant changes were found,

the Spp1 relative expressions seemed to follow similar patterns to Tpm2, where after 4 hours 10 μM DEM treatments, Spp1 showed a smaller possible induction (1.44 ± 0.14-fold change) than 1 hour, and TTX showed an even smaller possible induction (1.28 ± 0.09-fold change). Finally, Spp1 may cause a very small (and therefore not significant) repression after 1 hour Bic/4AP treatment (0.86 ± 0.54-fold change) as found with Tpm2.

Results for the Txnip gene show insignificant changes across all treatments of 1-hour 10 μM DEM, Bic/4AP and TTX treatments. Interestingly, Txnip also followed the same pattern as Tpm2 and Spp1, with the biggest induction following 10 μM DEM treatments (1.41 ± 0.49-fold change), a smaller change with 4 hours 10 μM DEM (1.35 ± 0.26-fold change), and even less so with 4-hour TTX treatments (1.21 ± 0.09-fold change). However, Bic/4AP bath application does not appear to show any repressive activity on Txnip in neurons (0.925 ± 0.43-fold change, 1.185 ± 0.30-fold change for 1- and 4-hour treatments respectively).

Overall, the most marked changes in relative expressions were observed in the relative order of Tpm2, Spp1 and Txnip. All three genes followed similar patterns over time and treatments and notably all three genes are induced by 10 μM DEM treatments and could be targets of nuclear HDAC4/5.

4.2. Tpm2 is likely regulated by FOXO transcription factors

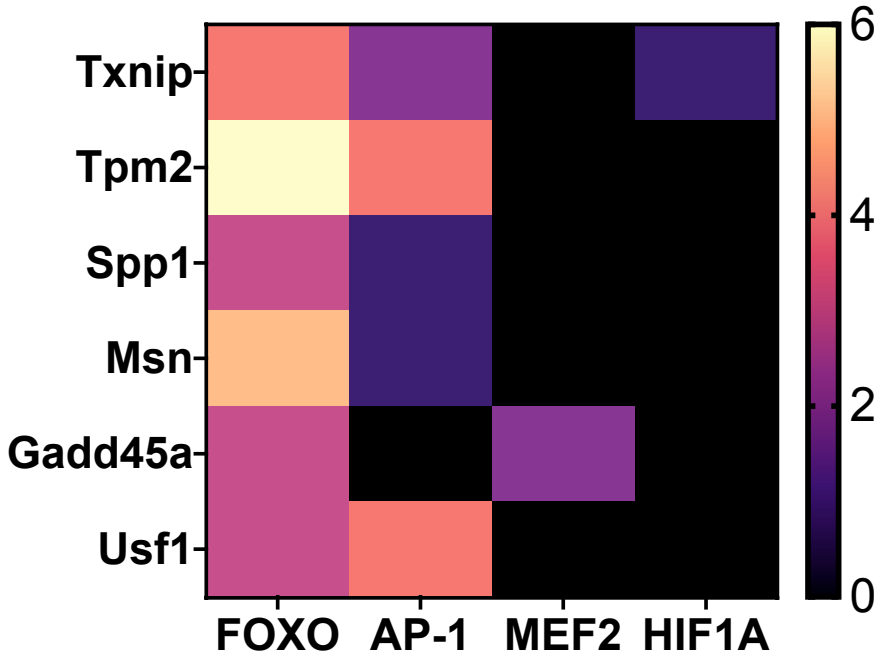

Figure 20: A heatmap of putative transcription factor binding site hits for selected genes of interest. FOXO1, 3 and 4, AP-1, MEF2 and HIF1A transcription factors were searched with Txnip, Tpm2, Spp1, Msn, Gadd45a and Usf1 genes on the LASAGNA 2.0 search tool for transcription factor binding sites. Hits with $p<0.005$ were considered putative, where FOXO1, 3 and 4 were combined into a general FOXO family group. The putative hits were compiled and plotted as a heatmap for each gene and the number of hits for a specific transcription factor family. Scale bar ranges from least number of hits in black up to the greatest number of hits in light yellow.

The LASAGNA 2.0 search tool identifies and visualises transcription factor binding sites (Lee & Huang, 2013) through inputting a list of selected transcription factors and target genes. A heatmap of the putative hits for each transcription factor family among a group of genes of interest was plotted in Figure 20, where putative hits were defined as those with p values <0.005. The number of hits within that threshold were counted and plotted for the individual genes. Activator protein 1 (AP-1) is a transcription factor that controls many processes including cell proliferation, differentiation, survival and apoptosis (Shaulain & Karin, 2001). The AP-1 transcription factors have been implicated specifically in oxidative stress where they are induced in response to hydrogen peroxide (Jawed et al., 2000). Hypoxia inducible factor 1 alpha (HIF1A) is a stress inducible transcription factor which is thought of as a master regulator in adaptive cellular responses to hypoxia (Semenza, 1998). This heatmap reveals that this gene group have more putative hits for FOXO factors, and are more likely regulated by these transcription factors compared to AP-1, MEF2 or HIF1A factors.

4.3. Gadd45 is upregulated in *Drosophila* under oxidative stress conditions

At present, no primary antibodies for *Drosophila* HDAC4 are available for use in immunohistochemistry techniques to directly compare with HDAC4/5 in cortical neurons. Instead, transgenic flies expressing mammalian HDAC5 fused to GFP were used. Figure 21 shows sequence alignments of *Drosophila* HDAC4, human HDAC4 and HDAC5 protein sequences for key domains and residues including serine residues required for 14-3-3 binding. This demonstrates high protein conservation between the *Drosophila* HDAC4 and human HDAC4 and 5, and thus it would be logical for this conservation to also apply to signalling mechanisms.

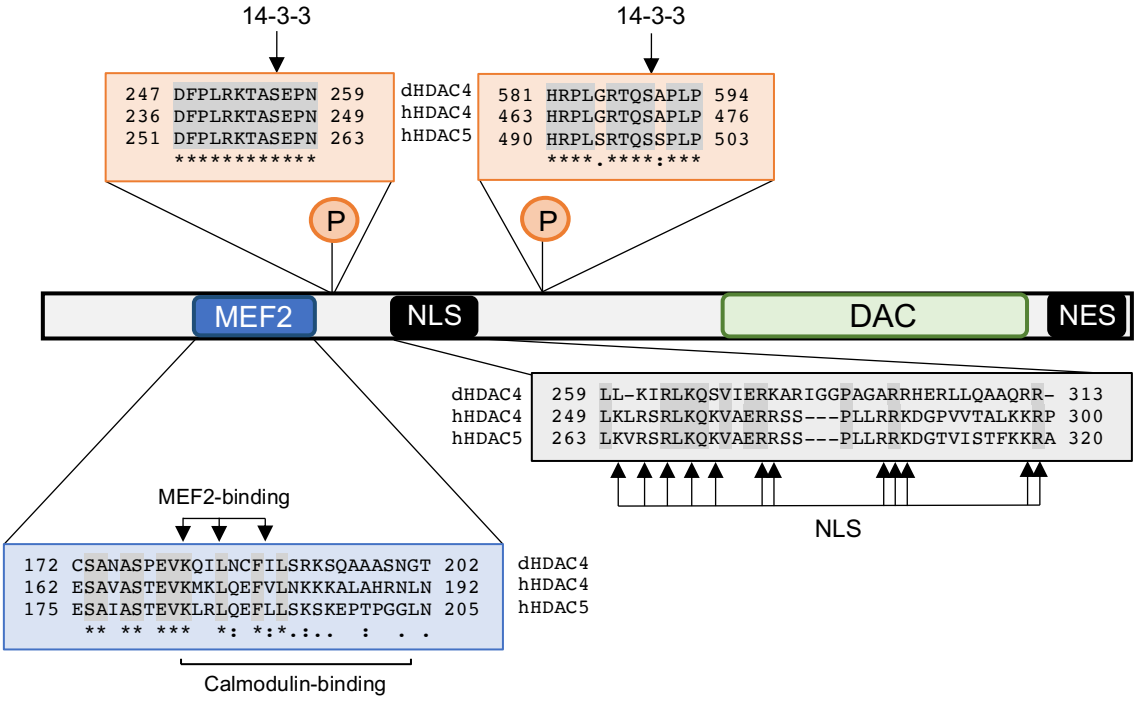

Figure 21: Sequence alignment of protein sequences for *Drosophila* HDAC4, human HDAC4 and human HDAC5. Shaded in grey are sequences of identical, highly conserved residues. Arrows indicate important residues for MEF2, calmodulin and phosphorylation sites for 14-3-3 binding as well as key sites in the nuclear localisation signal (NLS). "*" indicates residues in that column are identical between all three species. ":" indicates that conserved substitutions are observed and "." Indicate that semi-conserved substitutions are observed. Where conserved is described as the residue being substituted with one that has similar characteristics. Sequence alignments were performed using the Clustal W tool (Larkin et al., 2007).

Experiments were designed to test from the same group of genes (Table 10), where a fly orthologue was known, and investigate any changes in their gene expressions under oxidative stress conditions. Thus, we can directly compare the class IIa HDAC mechanism seen in neurons with that in flies. The *Drosophila* genetic crosses designed to express GFP tagged mammalian (human) HDAC5 in neurons only were set up (as

described in section 2.1) and given a diet of food containing either ethanol (EtOH) or DEM for a period of either 3 days or 1 week.

RNA was extracted from the frozen whole flies with the protocol as set out in section 2.9, and cDNA was synthesised as described in section 2.10.

qPCRs were performed with primers designed for the *Drosophila* orthologs of USF1 (dUsf), Msn (dMoe) and Gadd45 (dGadd45) as set out in Table 9.

All samples were normalised to Rpl1 gene EGFP EtOH control samples.

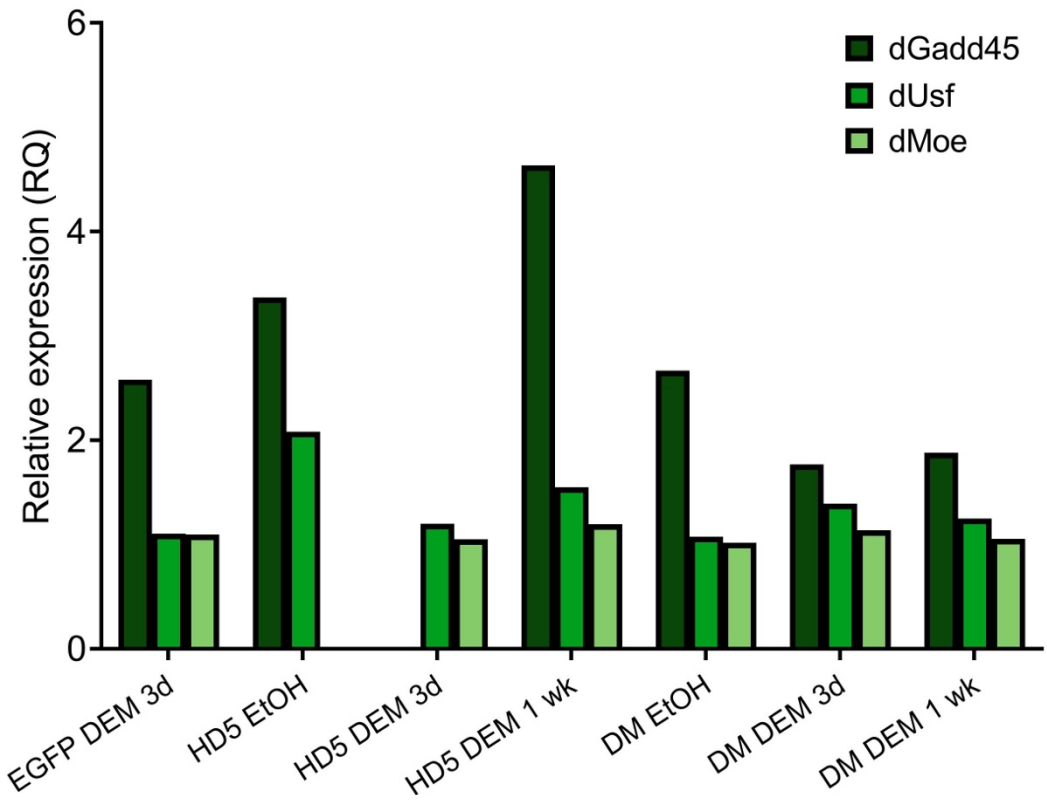

Figure 22: The *Drosophila* Gadd45 gene is likely induced in flies raised on DEM food and in flies expressing a constitutively nuclear HDAC5 transgene. Flies expressing GFP alone (EGFP), GFP tagged human HDAC5 (HD5) or a GFP tagged nuclear mutant human HDAC5 (DM) were raised and maintained on food containing ethanol or DEM for 3 days to 1 week as indicated. Representation of relative expressions plotted for the *Drosophila* Gadd45, Usf and Moe genes. Rpl1 was used as a housekeeping gene and expression is relative to gene expressions of the genes in control EGFP flies raised on EtOH containing food. RNA was extracted from 10 to 20 whole flies in each condition. n = 1 for all conditions except HD5 DEM 1 wk, which is n = 2.

As shown in Figure 22, the Gadd45 gene in *Drosophila* appears to be induced across all the fly genotypes and foods compared to control. The most significant induction for the HDAC5-GFP flies was seen after 1 week on DEM food (4.63 ± 3.5-fold change), where these flies already showed dGadd45 induction on ethanol food (3.37-fold change). The mutant HDAC5-DM flies saw a marked increase in Gadd45 expression on all treated foods, with the most significant change seen after 1 week on ethanol food (2.6-fold change) compared to DEM foods (1.76- and 1.87-fold changes respectively).

The Usf gene in *Drosophila* showed no significant changes in relative expression, except in the HDAC5-GFP flies left on ethanol (2.07-fold change) and DEM food (1.54-fold change) for 1 week. The same HDAC5-GFP flies on DEM food for 3 days did not show any significant induction (1.19-fold change) of the dUsf gene (Figure 22).

The Moe (moesin) gene in *Drosophila* showed no significant changes in relative expression in any of the fly genotypes or treatments (Figure 22).

4.4. Dissection of *Drosophila* brains expressing GFP tagged HDAC5 show a possible conserved nuclear translocation

Given the conservation of phosphorylation sites that regulate HDAC4/5 localisation (as shown in Figure 21), it is expected that the signalling mechanisms are also conserved. The localisation of human HDAC5-GFP in response to DEM treatment was therefore investigated in transgenic flies.

After setting up the genetic crosses, as set out in section 2.1, to drive neuronal expression of mammalian GFP tagged HDAC5 in transgenic *Drosophila,* the F_1 generation progeny were tested for GFP expression. After collection, the progeny were frozen, the heads removed and lysed in either 1 x RIPA buffer or 2 x SDS sample buffer as stated in section 2.2. These samples were run on a western blot (see section 2.4) with an antibody against GFP (see section 2.3 for antibody details). Figure 23 shows the resulting western blot confirming GFP expression within all the *Drosophila* cross genotypes. However, the mutant DM flies appear to display much lower GFP expression compared to wildtype HDAC5-GFP flies (Figure 23).

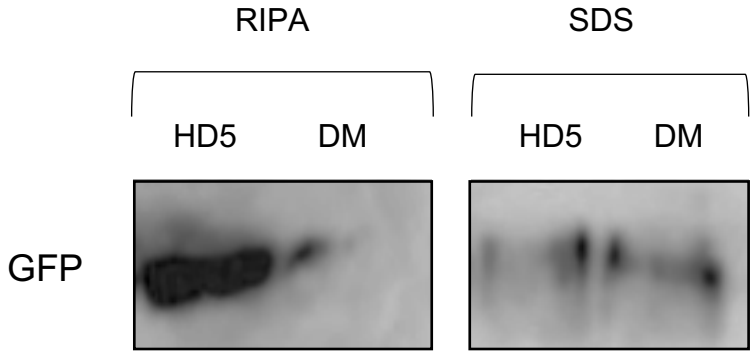

Figure 23: Western blot scans confirming GFP expression in brains of transgenic *Drosophila.* Lysates from *Drosophila* heads expressing either GFP tagged wildtype HDAC5 (HD5) or GFP tagged double mutant HDAC5 (DM) were ran on a western blot with a polyclonal antibody against GFP. 10 fly heads per genotype were lysed in either 1 x RIPA or 2 x SDS buffer and samples ran on a 10% SDS PAGE gel.

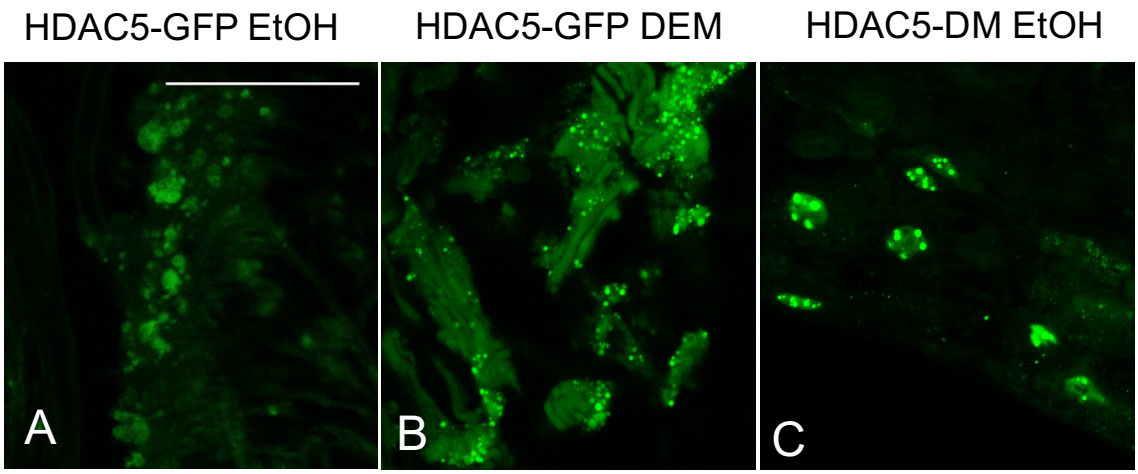

Figure 24: A possible nuclear translocation of expressed GFP tagged human HDAC5 is observed in the brains of transgenic *Drosophila* raised on DEM food. Flies expressing GFP tagged human HDAC5 or a GFP tagged nuclear mutant HDAC5-DM were raised and maintained on food containing ethanol or DEM for 1 week as indicated. Representative confocal images of GFP fluorescent signals from (A) HDAC5-GFP flies on ethanol food, (B) HDAC5-GFP flies on DEM food and (C) HDAC5-DM mutant flies on ethanol food. Images taken at x64 objective. Scale bar = 35 µm.

Figure 24 shows representative confocal images of GFP fluorescent signal taken from dissected fly brains expressing HDAC5-GFP and HDAC5-GFP-DM nuclear mutant flies raised on EtOH or DEM food for 1 week. As described in section 2.1, an nSyb[115] neuronal driver was used to drive neuronal specific expression of the GFP tagged wildtype and mutant forms of HDAC5 in *Drosophila*. Neuronal synaptobrevin (nSyb) is thought to be expressed in all neurons (but not other cell types) (Davis et al., 2020) and its promoter region has been used to generate a pan-neuronal driver for *Drosophila*. This genetic driver has been shown to be specific for neurons (Zhao et al., 2020) and it therefore was assumed that there was no expression outside of neuronal cells.

The HDAC5-GFP signal is quite dispersed and generally localised to the neuronal cells in the dissected *Drosophila* brains on EtOH control food (Figure 24A). With the same flies, the HDAC5-GFP signal appears to be more localised after 1 week on DEM food (Figure 24B). The HDAC5-GFP-DM mutant flies, which are constitutively nuclear, also show this localised fluorescent signal (Figure 24C). This acts as a positive control for the nuclear accumulation of the expressed human HDAC5 in the *Drosophila* neuronal cells. Despite this, there was no staining for the neuronal cells performed, as done in section 3.1 in cultured rat neurons. This therefore would be an important step to add if this experiment was repeated in order to confirm the movement of HDAC5-GFP and that the images display neuronal cells.

4.5. The Gadd45 gene is largely conserved among species

To further investigate whether Gadd45 could be regulated by HDAC4/5 and FOXO, an *in silico* approach was used to look for FOXO putative binding sites in the Gadd45 gene promoter. The LASAGNA web tool (Lee & Huang, 2013) was used to find FOXO binding sites in the Gadd45 gene from different species. Sequence alignments of the Gadd45 gene promoter in different species is shown in Figure 25. This displays a forkhead binding element (FBHE) coloured in red in the *Drosophila* Gadd45 gene which is shown to be largely conserved amongst the Gadd45a genes in other species, including those in human, rat and mouse.

```
dGadd45   1198 CAGAACCATACATAAATATAGCCAATTT--GTTTC-------------TGT 1234
hGadd45a  1691 CAGGGCAG--ATTAGATAAAGCCAAATGAATT-CCTGGCTCACCCCTCATT 1739
rGadd45a   931 CAGAACAG--ATTAGATAAAGCCACATTAAGTTCCCGGTTCACCCTTCGTT 980
mGadd45a   939 CAGAACAG--ATTAGATAAAGCCAAATA-AATTCCCGGTTTACCCTTCGTT 987
                 ***  *      ** *** *****  *    *  *              *
```

***Figure 25*: Sequence alignments of the Gadd45 gene promoter in different species.** *Drosophila* Gadd45 and human, rat and mouse Gadd45a promoter genomic sequences are aligned. Highly conserved sequences are highlighted in grey. Coloured in red is a forkhead (FOXO) binding element shown to be largely conserved. Positions indicated are in relation to the transcriptional start sites and beginning of the promoters. "*" indicates residues in that column are identical between all three species. Sequence alignments were performed using the Clustal W tool (Larkin et al., 2007).

4.6. Discussion

No study of the role of class IIa HDACs under neuronal oxidative stress could be complete without investigation of their epigenetic influence. OPN (encoded by Spp1) has been found to be upregulated in human AD brains, where it was shown to localise to neurons already vulnerable to death (Wung et al., 2007). It was postulated that OPN plays a role in the prevention of apoptosis and the promotion of cell proliferation as a response to neurodegeneration in these cases. Studies in rats also found increased OPN expression in neurons after brain trauma (Shin et al., 2005) and it appears to have a protective role against nitric oxide (NO)-induced oxidative damage in the aging human brain (Wung et al., 2007). As previously discussed, a novel role for Tpm2 has recently been suggested in learning and memory formation in the rat hippocampus (Hsu et al., 2017) which may be indicative of further roles for Tpm2 in the brain.

The results from qPCRs with cDNA from treated neuronal cells show an induction of Spp1 and Tpm2 after 10 μM DEM treatments, which correlates well with the observed nuclear import of HDAC4 and 5 under the same conditions. Tpm2 and Spp1 both showed significant inductions with short, 1-hour treatments of 10 μM DEM compared to 4-hour treatments, suggesting that this mechanism happens in a relatively short time frame.

Inductions of their gene expressions were still seen after 4 hours of DEM treatment, albeit not to the same extent, suggesting that this mechanism is most active up to 1 hour and gradually dissipates over time. These changes were observed in cultured cortical neurons with 1-day *in vitro* cytosine arabinoside (AraC) treatment, which inhibits non-neuronal cells. Experiments with the same treatments in the neurons after 4-days *in vitro* AraC treatment (indicative of more astrocytes) did not show the same significant changes (data not shown). This therefore suggests that these changes are neuronal specific and do not occur in astrocytes or microglia.

4-hour TTX treatments (designed to block synaptic activity) also showed some induction of the Tpm2 gene, however this was below the change seen with 4-hour 10 μM DEM treatments. On the other hand, Bic/4AP (which increases synaptic activity) caused repression of Tpm2 where a stronger change was seen within 1-hour compared to 4-hour treatments, suggesting the mechanism of its repression also happens on a similar short time scale.

As DEM and TTX treatments are shown to cause a nuclear translocation of the class IIa HDACs in rat cortical neurons, it can be hypothesised that Spp1, Tpm2 and, to an extent, Txnip genes are induced after the movement of these HDACs into the nucleus. Their subsequent activity, perhaps through binding to and activation of FOXO transcription factors, could therefore lead to these genes being upregulated. Supporting this, NMDAR

blockades are shown to upregulate Txnip expression in rat neurons (Papadia et al., 2008). These genes are indicated as having the same or even more putative hits compared to the known FOXO targets Txnip and Gadd45 when interrogated for transcription factor binding sites (Figure 20). Therefore, they are likely to be similarly regulated by these FOXO factors.

Alternatively, signals such as Bic/4AP treatments (which cause class IIa HDAC cytoplasmic movements) may cause repressions of Tpm2 as they are no longer able to bind and regulate FOXOs in the nucleus. The changes seen are neuronal specific and most significantly occur with short treatments of low DEM doses, suggesting this mechanism is working quickly to combat the oxidative stress state. This supports previous findings where the Spp1 encoded protein OPN is upregulated in human and rat brains where neurodegeneration is present, and the postulations that it has a protective role against oxidative stress.

The Gadd45 gene is well known to be implicated in protective mechanisms, and specifically D-GADD45 overexpression has been found to increase stress resistance in (Moskalev et al., 2012) and lifespan of *Drosophila melanogaster*. In the same study, D-GADD45 expression was also increased in wildtype flies exposed to different stress factors, demonstrating its protective role in flies. Oxidative stress was also shown to increase Gadd45a mRNA in a mouse model, indicating a similar role in mammals (Furukawa-Hibi et al., 2002).

As seen in Figure 22, the Gadd45 gene in *Drosophila* is shown likely to be induced in the EGFP control flies by DEM as well as being likely upregulated in the HDAC5-GFP and HDAC5-DM mutant flies on both EtOH and DEM foods. Expression of mammalian HDAC5 in the flies seems to somewhat increase the dGadd45 gene expression even in the absence of oxidative stress conditions. The possible inductions seen under DEM conditions appear to be even more marked, suggesting that the dGadd45 gene may be induced due to the shuttling of the expressed HDAC5 into the nucleus in fly neurons, similar to investigations in the rat brain.

The observation of a larger possible induction of Gadd45 seen in EGFP control flies raised on DEM suggests this shuttling is also happening for *Drosophila* HDAC4, where a conserved mechanism between rat and fly class IIa HDACs may be occurring under the oxidative stress state. The likely upregulation also supports previous findings of its protective role and upregulation during stress stimuli in flies. Interestingly, the constitutively nuclear DM mutant flies showed the highest increase when raised on ethanol control food and a similarly lower induction of the dGadd45 gene after both 3 days and 1 week on DEM food. This could indicate that this gene is possibly induced on a short timescale with the presence of nuclear HDAC5. With further applications of DEM

and prolonged nuclear HDAC5, the upregulation of dGadd45 gene expression could be reduced, with the nuclear cells perhaps becoming apoptotic. However, this data is from a single experiment and needs to be repeated.

In the same experiment, the *Drosophila* USF1 ortholog (dUsf) showed similar changes in mRNA levels. The qPCR results indicated that the *Drosophila* dUsf gene was likely upregulated in the HDAC5-GFP flies, where this change after 3 days on DEM food was smaller compared to EtOH food. Therefore, this suggests that the transgenic expression of HDAC5 may upregulate dUsf, especially in the absence of stress stimuli. This could further suggest a possible physiological role for USF1 in rat and human brains under normal conditions, where any upregulation is prevented during oxidative stress.

Western blots of the F1 progeny lysates from the *Drosophila* crosses (as described in section 2.1) confirmed GFP expression in all the genotypes, although it was observed that lysates of HDAC5-DM mutant flies showed less GFP signal than the HDAC5-GFP fly lysates (Figure 23). Brains dissected from the F1 progenies revealed a possible nuclear translocation of transgenic expressed HDAC5, where the GFP signal seems more concentrated in HDAC5-GFP flies on DEM food and all HDAC5-DM mutant flies. This suggests that the mechanism of the class IIa HDACs shuttling to the nucleus under oxidative stress conditions may be conserved between species. However, future experiments would be needed with a stain for the nuclei and general neuronal markers (as done with rat neurons in section 3.1) to confirm this translocation and observe the HDAC5-GFP signal in the context of the *Drosophila* neuronal cells.

Sequence alignments of the Gadd45 gene promoter regions in flies, humans, rat and mouse indicate a largely conserved FOXO binding site on the gene further supporting a conserved mechanism between the species. Whilst many of the key motifs for *Drosophila* HDAC4 are similar to human HDAC4 and 5 (Figure 21), the conservation of transcription factor binding sites helps to identify if the regulation of genes such as Gadd45 are occurring in the same manner under oxidative stress conditions. Key future experiments would include using a Gadd45a primer in qPCR experiments using treated cultured rat cortical neurons to explore whether this gene is also induced in the rat brain under the same DEM conditions.

After confirmation of GFP signals by western blotting, pull down experiments were attempted to screen for conserved interactors between *Drosophila* HDAC4 and human HDAC5, however this yielded no solid results. Future work could include repetition of these GFP pull downs with tweaking of the protocol where necessary. Separation of male and female flies in these experiments may also reveal differences in the mechanisms, gene expressions or interactions between genders in *Drosophila* brains.

Whilst qPCRs with the *Drosophila* crosses provided some promising results, this would require more repeats to be confirmed and to establish any significant inductions of gene expressions in the chosen genes. However, some of the flies raised on DEM food died before collection after 1 week, and as such the concentration of DEM in the food may need to be reduced to collect large enough sample sizes for these experiments.

Future experiments would also include a proteomics screen for protein-protein interactions with the same *Drosophila* crosses and genotypes to identify differences in their interactions between control, HDAC5 expressing and HDAC5-DM constitutively nuclear mutant flies. This would reveal any interactions which are conserved between *Drosophila* HDAC4 and mammalian HDAC5, and specifically what the HDAC5-DM mutant is interacting with in the nucleus of fly neuronal cells.

5. Concluding Remarks

In this study, it was found that the class IIa HDACs 4 and 5 both translocate to the nucleus of rat cultured cortical neurons under oxidative stress conditions induced by glutathione depletion. HDAC5 was found to likely be dephosphorylated under the same conditions, shown previously to be a key step in HDAC5 nuclear import (Greco et al., 2011) and supporting the finding of its nuclear accumulation. During fasting in the liver, these class IIa HDACs are known to shuttle to the nucleus after dephosphorylation to activate FOXO transcription factors and boost their target genes (Klotz et al., 2015). In addition, a ROS-induced nuclear import of FOXO factors has been established (Van der Horst & Burgering, 2007).

Moreover, the Spp1 and Tpm2 genes showed neuronal specific increases in gene expressions after DEM applications, most significantly with short, low dose treatments. Tetrodotoxin (TTX) treatments, designed to block synaptic activity through blocking voltage gated sodium channels (Geffeney & Ruben, 2006), also led to the induction of these genes. Bic/4AP on the other hand, designed to increase synaptic activity, saw repressions in a similar time-dependent manner. Observations were made of a possible nuclear translocation of GFP tagged human HDAC5 expressed in transgenic *Drosophila* brains. Additionally, the DNA damage repair Gadd45 gene, shown to be part of a stress protective mechanism in *Drosophila* (Moskalev et al., 2012) was found to be likely upregulated in flies raised on DEM food. Moreover, *in silico* techniques revealed a conserved FOXO binding site in the promoter regions of Gadd45 between species.

Therefore, the following conserved mechanism is proposed. An increase in ROS species, induced by glutathione depletion (Ugbode et al., 2020), causes both HDAC4 and 5 to become dephosphorylated by serine/threonine phosphatases. Subsequently, they shuttle to the nucleus along with FOXO transcription factors (Figure 26). Once in the nucleus, the HDACs bind and deacetylate the FOXOs in association with HDAC3-NCoR co-repressor complexes. This allows the FOXO transcription factors to transactivate genes including Spp1, Tpm2, Txnip and Gadd45. Conversely, increases in synaptic activity, induced by bath applications of Bic/4AP, leads to HDAC4/5 cytoplasmic translocation and retention. There they are prevented from activating these genes via FOXO binding in the nucleus. It is further proposed that this protective mechanism is most active up to 1 hour post treatment and may then dissipate over time.

The mechanisms that lead to the nuclear translocation of the class IIa HDACs under oxidative stress conditions remains unknown. However, it is hypothesised that either: (i) ROS may inhibit the protein kinases (e.g. CamKII and CamKIV) that phosphorylate the HDACs and allow their nuclear export and retention in the cytoplasm (Figure 26) or (ii)

ROS may activate the serine/threonine phosphatases (e.g. PP2A), thus dephosphorylating the HDACs and causing their nuclear import. It is also possible the ROS species may oxidise the class IIa HDACs leading to their inactivation, but this is not supported by recent mouse cardiomyocytes studies in which oxidation of HDAC4 after oxidative stress induced its nuclear export (Matsushima et al., 2013). However, this may be different in the brain and further investigations are warranted.

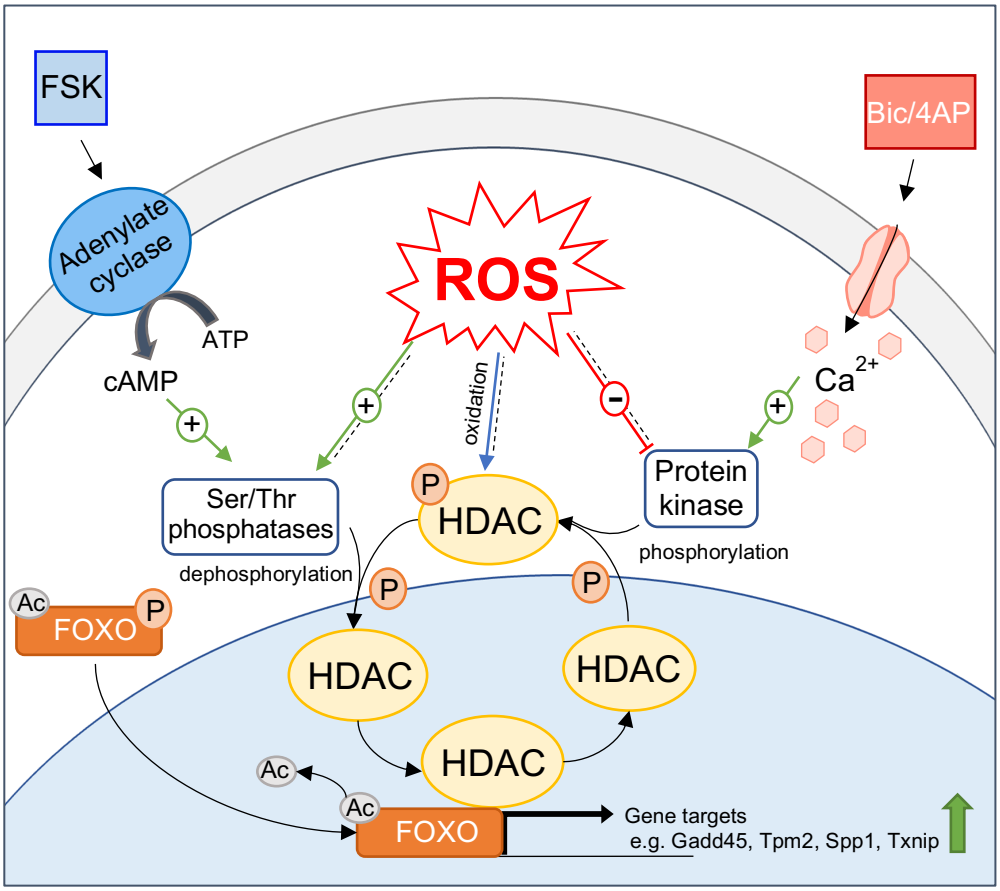

Figure 26: **Proposed mechanism of HDAC4/5 nuclear import during oxidative stress.** Increased synaptic activity induced by Bic/4AP bath application causes a Ca^{2+} influx which activates kinases to phosphorylate the HDACs and incites their nuclear exit. Forskolin activates the adenylate cyclase enzyme, responsible for the production of cAMP, which in turn activates serine/threonine phosphatases which are responsible for the HDACs dephosphorylation and nuclear import. Proposed pathways are indicated with dotted lines and include the ROS inhibiting the HDAC kinases, activating the phosphatases or oxidising the HDACs to drive their nuclear translocation during oxidative stress.

It is further proposed that, as a protective mechanism, under low conditions of oxidative stress and just over the cytotoxic tipping point of the ROS to antioxidant balance, HDAC4 and 5 move towards the nucleus within one hour to induce Tpm2, Spp1, Txnip and Gadd45 through FOXO binding and deacetylation. However, during high levels of

oxidative stress, the neuronal cells become overwhelmed and become apoptotic. Nuclear HDAC4 has been implicated in the repression of genes essential for synapse health and function (Sando et al., 2012) and in the progression of disease in the brain (Fitzsimons, 2015). In addition, the nuclear exclusion of HDAC5 has also been found to promote neuronal survival (Linseman et al., 2003). This might suggest that after the initial protective mechanism proposed above, the continued nuclear accumulation of the class IIa HDACs becomes neurotoxic.

A link between *Drosophila* HDAC4 and Alzheimer's disease has already been found (Cao et al., 2008) and therefore, the proposition of a conserved mechanism is of importance. *Drosophila* are shown to be excellent models for neurodegenerative disorders (Bolus et al., 2020), where functional sites in *Drosophila* HDAC4 is highly conserved with human HDAC4 and HDAC5 (Figure 21). Concurrent investigations using *Drosophila* and *Rattus norvegicus* models would be invaluable in any future work based on these findings. Eventual thorough understanding of the mechanisms, modifications and interactions of the class IIa HDACs in the brain during oxidative stress conditions could be translated well to the human brain and used as a foundation for therapeutic intervention.

Previous work indicates that overexpression of the sulfiredoxin (SRXN-1) antioxidant gene can rescue morphological neuronal damage due to an ROS burden (Ugbode et al., 2020). Synaptic activity is also shown to increase SRXN-1 expression (Bell & Hardingham, 2011) and in this study increasing synaptic activity led to a protective cytoplasmic accumulation of the class IIa HDACs. Therefore, exploiting Ca^{2+} influx signals to induce this neuroprotection during conditions of low oxidative stress may prove a promising therapeutic approach in a diseased brain.

Findings in this thesis, along with findings in the literature (Chawla et al., 2003), show that the induction of synaptic activity was enough to cause nuclear exports of the class IIa HDACs, even under oxidative stress conditions. Histone deacetylase inhibitors, while unspecific, have recently been shown to be neuroprotective in the context of ischemia (Pickell et al., 2020) through promoting prosurvival pathways in injured cells. In a similar concept, approaches which prevent class IIa HDAC nuclear import may prove beneficial in a diseased brain struggling to counteract excessive ROS levels and resulting morphological neuronal damages. However, this must be carefully considered given the complicated crosstalk between Ca^{2+} signalling and ROS release (Hempel & Trebak, 2017) and thus this approach would need to be careful to not accentuate the ROS burden instead of aiding in its detoxification.

Further work is needed to understand the role and regulation of the class IIa HDACs under oxidative stress in the brain. Firstly, it would be appropriate to explore specifically how increased ROS levels may drive a nuclear import of the class IIa HDACs. Treatments with CaMK inhibitors are shown to induce the nuclear transport of HDAC4 and 5 in cerebellar granule neurons (Linseman et al., 2003). Therefore, future approaches could include *in vivo* activation of the CaMKIV kinase in rat neuronal cells or the use of serine/threonine phosphatase inhibitors under control, DEM and paraquat conditions. This would reveal any changes in class IIa HDACs localisations with those seen in Figure 12 and 13.

The use of a HDAC4 mutant with the oxidisable cysteines mutated (such that they could no longer be oxidised) may also prove useful in this investigation. Immunohistochemistry to identify the location of this HDAC4 mutant within the neuronal cell under physiological and oxidative stress states would reveal how oxidation modifications, if any, affect class IIa HDAC localisation. It may also be interesting to produce HDAC4/5 mutants with both the phosphorylation site serines, such as the 3SA HDAC4 mutant produced in Sando *et al.*, 2012, along with oxidation site cysteines mutated together for use in these experiments. Evidence of FOXO1 interactions with both HDAC4, along with HDAC3, and HDAC5 have been found in different cell types (Cho et al., 2018). Once shuttled into the nucleus, it should be considered if the presence of the ROS species may be promoting HDAC4/5 binding to FOXO transcription factors as part of their mechanism within the oxidative stress state in the brain. Therefore, testing FOXO-HDAC4/5 binding using biochemical techniques such as co-immunoprecipitation would indicate any increase in their binding following DEM treatments.

Finally, investigations into a calcium influx into neuronal cells in the absence of increased synaptic firing could be performed. HDAC5 nuclear export has been shown to be induced in hippocampal neurons following stimulation of calcium flux through L-type calcium channels (Chawla et al., 2003). Thus, comparing low DEM treatments (and therefore low oxidative stress conditions) with and without Ca^{2+} influxes could reveal if morphological damages to neurons could be rescued due to the cytoplasmic accumulation of the class IIa HDACs. If this proves successful in being neuroprotective, it may provide an exciting outlook for the treatment of neurodegenerative diseases in which neuronal damage is so commonly found.

Word count excluding figure legends: 15,644 words

6. References

Accili, D., & Arden, K. C. (2004). FoxOs at the crossroads of cellular metabolism, differentiation, and transformation. *Cell, 117*(4), 421-426.

Ago, T., Liu, T., Zhai, P., Chen, W., Li, H., Molkentin, J. D., Vatner, S. F., & Sadoshima, J. (2008). A redox-dependent pathway for regulating class II HDACs and cardiac hypertrophy. *Cell, 133*(6), 978-993.

Ahn, J.-H., McAvoy, T., Rakhilin, S. V., Nishi, A., Greengard, P., & Nairn, A. C. (2007). Protein kinase A activates protein phosphatase 2A by phosphorylation of the B56δ subunit. *Proceedings of the National Academy of Sciences (PNAS), 104*(8), 2969-2984.

Aoyama, K., & Nakaki, T. (2015). Glutathione in cellular redox homeostasis: Association with the excitatory amino acid carrier 1 (EAAC1). *Molecules, 20*(5), 8742-8758.

Backs, J., Song, K., Bezprozvannaya, S., Chang, S., & Olson, E. N. (2006). CaM kinase II selectively signals to histone deacetylase 4 during cardiomyocyte hypertrophy. *The Journal of Clinical Investigation , 116*(7), 1853-1864.

Bassi, S., Tripathi, T., Monziani, A., Di Leva, F., & Biagioli, M. (2017). Epigenetics of Huntington's disease. *Advances in Experimental Medicine and Biology, 978*, 277-299.

Baxter, P. S., & Hardingham, G. E. (2016). Adaptive regulation of the brain's antioxidant defences by neurons and astrocytes. *Free Radical Biology and Medicine, 100*, 147-152.

Baxter, P. S., Bell, K. F., Hasel, P., Kaindl, A. M., Fricker, M., Thomson, D., Cregan, S. P., Gillingwater, T. H., & Hardingham, G. E. (2015). Synaptic NMDA receptor activity is coupled to the transcriptional control of the glutathione system. *Nature communications, 6*, 6761.

Belfield, J. L., Whittaker, C., Cader, M. Z., & Chawla, S. (2006). Differential effects of Ca^{2+} and cAMP on transcription mediated by MEF2D and cAMP-response element-binding protein in hippocampal neurons. *Journal of Biological Chemistry, 281*(38), 27724-27732.

Bell, K. F., & Hardingham, G. E. (2011). The influence of synaptic activity on neuronal health. *Current Opinion in Neurobiology, 21*(2), 299-305.

Birben, E., Sahiner, U. M., Sackesen, C., & Erzurum, S., & Kalayci, O. (2012). Oxidative stress and antioxidant defense. *World Allergy Organisation Journal, 5*(1), 9-19.

Bizzozero, O. A., Ziegler, J. L., De Jesus, G., Bolognani, F. (2006). Acute depletion of reduced glutathione causes extensive carbonylation of rat brain proteins. *Journal of Neuroscience Research, 83*(4), 656-667.

Blander, G., & Guarente, L. (2004). The Sir2 Family of Protein Deacetylases. *Annual Review of Biochemistry, 73*, 417-435.

Bolger, T. A., & Yao, T.-P. (2005). Intracellular Trafficking of Histone Deacetylase 4 Regulates Neuronal Cell Death. *Journal of Neuroscience , 25*(41), 9544-9553.

Bolus, H., Crocker, K., Boekhoff-Falk, G., Chtarbanova, S. (2020). Modeling neurodegenerative disorders in *Drosophila melanogaster. International Journal of Molecular Sciences, 21*(9), 3055.

Bottomley, M. J., Lo Surdo, P., Di Giovine, P., Cirillo, A., Scarpelli, R., Ferrigno, F., Jones, P., Neddermann, P., De Francesco, R., Steinkühler, C., Gallinari, P., & Carfi, A. (2008). Structural and functional analysis of the human HDAC4 catalytic domain reveals a regulatory structural zinc-binding domain. *Journal of Biological Chemistry, 283*(39), 26694-26704.

Bradner, J. E., West, N., Grachan, M. L., Greenberg, E. F., Haggarty, S. J., Warnow, T., & Mazitschek, R. (2010). Chemical phylogenetics of histone deacetylases. *Nature Chemical Biology, 6*(3), 238-243.

Brand, A. H. & Perrimon, N. (1993). Targeted gene expression as a means of altering cell fates and generating dominant phenotypes. *Development, 118*(2), 401-415.

Brunet, A., Sweeney, L. B., Sturgill, J. F., Chua, K. F., Greer, P. L., Lin, Y., Tran, H., Ross, S. E., Mostoslavsky, R., Cohen, H. Y., Hu, L. S., Cheng, H. L., Jedrychowski, M. P., Gygi, S. P., Sinclair, D. A., Alt, F., & Greenberg, M. E. (2004). Stress-dependent regulation of FOXO transcription factors by the SIRT1 deacetylase. *Science, 5666*(303), 2011-2015.

Burnside, S. W., & Hardingham, G. E. (2017). Transcriptional regulators of redox balance and other homeostatic processes with the potential to alter neurodegenerative disease trajectory. *Biochemical Society Transactions, 45*(6), 1295-1303.

Candas, D., & Li, J. (2014). MnSOD in oxidative stress response-potential regulation via mitochondrial protein influx. *Antioxidants & Redox Signaling, 20*(10), 1599-1617.

Cao, W., Song, H.-J., Gangi, T., Kelkar, A., Antani, I., Garza, D., & Konsolaki, M. (2008). Identification of novel genes that modify phenotypes induced by Alzheimer's β-amyloid overexpression in *Drosophila*. *Genetics, 178*(3), 1457-1471.

Castello, P. R., Drechsel, D. A., & Patel, M. (2007). Mitochondria are a major source of paraquat-induced reactive oxygen species production in the brain. *Journal of Biological Chemistry, 282*(19), 14186-14193.

Chan, H., & Bonini, N. (2000). *Drosophila* models of human neurodegenerative disease. *Cell Death & Differentiation, 7*, 1075-1080.

Chawla, S., Vanhoutte, P., Arnold, F. J., Huang, C. L.-H., & Bading, H. (2003). Neuronal activity-dependent nucleocytoplasmic shuttling of HDAC4 and HDAC5. *Journal of Neurochemistry, 85*(1), 151-159.

Cho, H. M., Seok, Y. M., Lee, H. A., Song, M., Kim, I. (2018). Repression of transcriptional activity of forkhead box O1 by histone deacetylase inhibitors ameliorates hyperglycemia in type 2 diabetic rats. *International Journal of Molecular Sciences, 19*(11), 3539.

Choi, B. (1993). Oxygen, antioxidants and brain dysfunction. *Yonsei Medical Journal, 34*(1), 1-10.

Collins, C. A., Wairkar, Y. P., Johnson, S. L., DiAntonio, A. (2006). Highwire restrains synaptic growth by attenuating a MAP kinase signal. *Neuron, 1*(51), 57-69.

Corre, S., & Galibert, M.-D. (2005). Upstream stimulating factors: highly versatile stress-responsive transcription factors. *Pigment Cell Research, 18*(5), 337-348.

Darcy, M. J., Calvin, K., Cavnar, K., & Ouimet, C. C. (2010). Regional and subcellular distribution of HDAC4 in mouse brain. *The Journal of Comparative Neurology, 518*(5), 722-740.

Davis, F. P., Nern, A., Picard, S., Reiser, M. B., Rubin, G. M., Eddy, S. R., Henry, G. L. (2020). A genetic, genomic, and computational resource for exploring neural circuit function. *eLife, 9,* e50901.

Delcuve, G. P., Khan, D. H., & Davie, J. R. (2012). Roles of histone deacetylases in epigenetic regulation: emerging paradigms from studies with inhibitors. *Clinical Epigenetics ,4*, 5.

Deneke, S. M., Lynch, B. A., Fanburg, B. L. (1985). Transient depletion of lung glutathione by diethyl maleate enhances oxygen toxicity. *Journal of Applied Physiology, 58*(2), 571-574.

De Ruijter, A. J. M., Van Gennip, A. H., Caron, H. N., Kemp, S., Van Kuilenburg, A. B. P. (2003). Histone deacetylases (HDACs): characterisation of the classical HDAC family. *Biochemical Journal, 370*(3), 737-749.

Dringen, R. (1999). Metabolism and functions of glutathione in brain. *Progress in Neurobiology, 62*(6), 649-671.

Fischle, W., Dequiedt, F., Hendzel, M. J., Guenther, M. G., Lazar, M., Voelter, W., & Verdin, E. (2002). Enzymatic activity associated with class II HDACs is dependent on a multiprotein complex containing HDAC3 and SMRT/N-CoR. *Molecular Cell, 9*(1), 45-57.

Fitzsimons, H. L., Schwartz, S., Given, F. M., Scott, M. J. (2013). The histone deacetylase HDAC4 regulates long-term memory in *Drosophila*. *PLoS One, 8*(12), e83903.

Fitzsimons, H. L. (2015). The Class IIa histone deacetylase HDAC4 and neuronal function: Nuclear nuisance and cytoplasmic stalwart? *Neurobiology of learning and memory, 123*, 149-158.

Flavell, S. W., Cowan, C. W., Kim, T.-K., Greer, P. L., Lin , Y., Paradis, S., Griffith, E. C., Hu, L. S., Chen, C., & Greenberg, M. E. (2006). Activity-dependent regulation of MEF2 transcription factors suppresses excitatory syanpse number. *Science, 311*(5763), 1008-1012.

Furukawa-Hibi, Y., Yoshida-Araki, K., Ohta, T., Ikeda, K., & Motoyama, N. (2002). FOXO forkhead transcription factors induce G(2)-M checkpoint in response to oxidative stress. *Journal of Biological Chemistry, 277*(30), 26729-26732.

Gallinari, P., Di Marco, S., Jones, P., Pallaoro, M., & Steinkühler, C. (2007). HDACs, histone deacetylation and gene transcription: from molecular biology to cancer therapeutics. *Cell Research, 17*, 195-211.

Gandhi, S., & Abramov, A. Y. (2012). Mechanism of oxidative stress in neurodegeneration. *Oxidative Medicine and Cellular Longevity, 2012*, 1-11.

Geffeney, S.-L., Ruben, P.-C. (2006). The structural basis and functional consequences of interactions between tetrodotoxin and voltage-gated sodium channels. *Marine Drugs, 4*(3), 143-156.

Greco, T. M., Yu, F., Guise, A. J., Cristea, I. M. (2011). Nuclear import of histone deacetylase 5 by requisite nuclear localisation signal phosphorylation. *Molecular and Cellular Proteomics, 10*(2), M110.004317.

Gu, F., Chauhan, V., & Chauhan, A. (2015). Glutathione redox imbalance in brain disorders. *Current Opinion in Clinical Nutrition and Metabolic Care, 18*(1), 89-95.

Haberland, M., Montgomery, R. L., & Olson, E. N. (2009). The many roles of histone deacetylases in development and physiology: Implications for disease and therapy. *Nature Review Genetics, 10*(1), 32-42.

Hempel, N., & Trebak, M. (2017). Crosstalk between calcium and reactive oxygen species signaling in cancer. *63*, 70-96.

Hertz, L., Dringen, R., Schousboe, A., & Robinson, S. R. (1999). Astrocytes: Glutamate producers for neurons. *Journal of Neuroscience research, 57*(4), 417-428.

Hsu, W. L., Ma, Y. L., Liu, Y. C., & Lee, E. H. (2017). Smad4 SUMOylation is essential for memory formation through upregulation of the skeletal myopathy gene TPM2. *BMC Biology, 15*, 112.

Hubbert, C., Guardiola, A., Shao, R., Kawaguchi, Y., Ito, A., Nixon, A., Yoshida, M., Wang, X.-F., Yao, T.-P. (2002). HDAC6 is a microtubule-associated deacetylase. *Nature, 417*(6887), 455-458.

Jawed, S., Edmonds, S., Gilston, V., & Blake, D. (2000). Hypoxia, oxidative stress and exercise in rheumatoid arthritis. In *Handbook of Oxidants and Antioxidants in Exercise* (pp. 1147-1188).

Jayathilaka, N., Han, A., Gaffney, K. J., Dey, R., Jarusiewicz, J. A., Noridomi, K., Philips, M. A., Lei, X., He, J., Ye, J., Gao, T., Petasis, N. A., & Chen, L. (2012). Inhibition of the function of class IIa HDACs by blocking their interaction with MEF2. *Nucleic Acids Research, 40*(12), 5378-5388.

Kao, H. -Y., Downes, M., Ordentlich, P., & Evans, R. M. (2000). Isolation of a novel histone deacetylase reveals that class I and class II deacetylases promote SMRT-mediated repression. *Genes & Development, 14*(1), 55-66.

Kim, G., Kim, J. E., Rhie, S. J., & Yoon, S. (2015). The role of oxidative stress in neurodegenerative diseases. *Experimental Neurobiology, 24*(4), 325-340.

Kim, M.-S., Akhtar, M. W., Adachi, M., Mahgoub, M., Bassel-Duby, R., Kavalali, E. T., Olson, E. N., & Monteggia, L. M. (2012). An essential role for histone deacetylase 4 in synaptic plasticity and memory formation. *The Journal of Neuroscience, 32*(32), 10879-10886.

Klotz, L.- O., Sanchez-Ramos, C., Prieto-Arroyo, I., Urbanek, P., Steinbrenner, H., Monsalve, M. (2015). Redox regulation of FoxO transcription factors. *Redox Biology, 6,* 51-72.

Konsoula, Z., & Barile, F. A. (2012). Epigenetic histone acetylation and deacetylation mechanisms in experimental models of neurodegenerative disorders. *Journal of Pharmacological and Toxicological Methods, 66*(3), 215-220.

Kumar , A., Paeger, L., Kosmas, K., Kloppenburg, P., Noegel, A. A., & Peche, V. S. (2016). Neuronal actin dynamics, spine density and neuronal dendritic complexity are regulated by CAP2. *Frontiers in cellular neuroscience, 10*, 180.

Larkin, M., Blackshields, G., Brown, N., Chenna, R., McGettigan, P., McWilliam , H., Valentin, F., Wallace, I. M., Wilm, A., Lopez, R., Thompson, J., Gibson, T., & Higgins, D. (2007). Clustal W and Clustal X version 2.0. *Bioninformatics, 23*(21), 2947-2948.

Lee, C., & Huang, C.-H. (2013). LASAGNA-Search: an integrated web tool for transcription factor binding site search and visualisation. *Biotechniques, 54*(3), 141-53.

Lee, J., Kim, Y., Liu, T., Hwang, Y. J., Hyeon, S. J., Im, H., Lee, K., Alvarez, V. E., McKee, A. C., Um, S.-J., Hur, M., Mook-Jung, I., Kowall, N.W., & Ryu, H. (2018). SIRT3 deregulation is linked to mitochondrial dysfunction in Alzheimer's disease. *Aging Cell, 17*(1), e12679.

Lee, K. H., Cha, M., & Lee, B. H. (2020). Neuroprotective effect of antioxidants in the brain. *International Journal of Molecular Sciences, 21*(19), 7152.

Li, J., Chen, J., Ricupero, C. L., Hart, R. P., Schwartz, M. S., Kusnecov, A., & Herrup, K. (2012). Nuclear accumulation of HDAC4 in ATM deficiency promotes neurodegeneration in ataxia-telangiectasia. *Nature Medicine, 18*(5), 783-790.

Lincoln, D. T., Ali Emadi, E. M., Tonissen, K. F., & Clarke, F. M. (2003). The thioredoxin-thioredoxin reductase system: over-expression in human cancer. *Anticancer Research, 23*(3B), 2425-2433.

Linseman, D. A., Bartley, C. M., Le, S. S., Laessig, T. A., Bouchard, R. J., Meintzer, M. K., Li, M., & Heidenreich, K. A. (2003). Inactivation of the myocyte enhancer factor-2 repressor histone deacetylase-5 by endogenous Ca(2+)//calmodulin-dependent kinase II promotes depolarisation-mediated cerebellar granule neuron survival. *The Journal of Biological Chemistry, 278*(42), 41472-81.

Liu, Y., Hernandez-Ochoa, E. O., Randall, W. R., & Schneider, M. F. (2012). NOX2-dependent ROS is required for HDAC5 nuclear efflux and contributes to HDAC4 nuclear efflux during intense repetitive activity of fast skeletal muscle fibers. *American Journal of Physiology - Cell Physiology, 303*(3), C334-C347.

Liu, Z., Ren, Z., Zhang, J., Chuang, C.-C., Kandaswamy, E., Zhou, T., & Zuo, L. (2018). Role of ROS and nutritional antioxidants in human diseases. *Frontiers in Physiology, 9*, 477.

Magistretti, P. J., & Allaman, I. (2015). A cellular perspective on brain energy metabolism and functional Imaging. *Neuron, 86*(4), 883-901.

Majdzadeh, N., Wang, L., Morrison, B. E., Bassel-Duby, R., Olson, E. N., & D'Mello, S. R. (2008). HDAC4 inhibits cell-cycle progression and protects neurons from cell death. *Developmental Neurobiology, 68*(8), 1076-1092.

Mandal, P. K., Saharan, S., Tripathi, M., & Murari, G. (2015). Brain glutathione levels -- a novel biomarker for mild cognitive impairment and Alzheimer's disease. *Biological Psychiatry, 78*(10), 702-710.

Martin, M., Kettmann, R., & Dequiedt, F. (2007). Class IIa histone deacetylases: regulating the regulators. *Oncogene, 26*, 5450-5467.

Matsukawa, J., Matsuzawa, A., Takeda, K., Ichijo, H. (2004). The ASK1-MAP kinase cascades in mammalian stress response. *The Journal of Biochemistry, 136*(3), 261-265.

Matsushima, S., Kuroda, J., Ago, T., Zhai, P.Y., Park, J., Xie, L.-H., Tian, B., & Sadoshima, J. (2013). Increased oxidative stress in the nucleus caused by Nox4 mediates oxidation of HDAC4 and cardiac hypertrophy. *Circulation research, 112*(4), 651-63.

Mennerick, S., & Zorumski , C. F. (2000). Neural activity and survival in the developing nervous system. *Molecular Neurobiology, 22*, 41-54.

Mielcarek, M., Seredenina, T., Stokes, M. P., Osborne, G. F., Landles, C., Inuabasi, L., Franklin, S. A., Silva, J. C., Luthi-Carter, R., Beaumont, V., & Bates, G. P. (2013). HDAC4 does not act as a protein deacetylase in the postnatal murine brain *in vivo*. *PLOS One, 8*(11), e80849.

Mielcarek, M., Zielonka, D., Carnemolla, A., Marcinkowski, J. T., & Guidez, F. (2015). HDAC4 as a potential therapeutic target in neurodegenerative diseases: a summary of recent achievements. *Frontiers in Cellular Neuroscience, 9*, 42.

Mihaylova, M. M., Vasquez, D. S., Ravnskjaer, K., Denechaud, P.-D., Yu, R. T., Alvarez, J. G., Downes, M., Evans, R. M., Montminy, M., & Shaw, R. J. (2011). Class IIa histone deacetylases are hormone-activated regulators of FOXO and mammalian glucose homeostasis. *Cell, 145*(4), 607-621.

Miska, E. A., Karlsson, C., Langley, E., Nielsen, S. J., Pines, J., & Kouzarides, T. (1999). HDAC4 deacetylase associates with and represses the MEF2 transcription factor. *EMBO Journal, 18*(18), 5099-5107.

Moskalev, A., Plyusnina, E., Shaposhnikov, M., Shilova, L., Kazachenok, A., & Zhavoronkov, A. (2012). The role of D-GADD45 in oxidative, thermal and genotoxic stress resistance. *Cell cycle, 11*(22), 4222-4241.

Nandi, A., Yan, L.-J., Jana, C., & Das, N. (2019). Role of catalase in oxidative stress- and age-associated degenerative diseases. *Oxidative Medicine and Cellular Longevity, 2019*, 1-19.

Oka, S.-i., Ago, T., Kitazono, T., Zablocki, D., & Sadoshima, J. (2009). The role of redox modulation of class II histone deacetylases in mediating pathological cardiac hypertrophy. *Journal of Molecular Medicine, 87*, 785-791.

Oswald, M. C., Brooks, P. S., Zwart , M. F., Mukherjee, A., West, R. J., Giachello, C. N., Morarach, K., Baines, R. A., Sweeney, S. T., & Landgraf, M. (2018). Reactive oxygen species regulate activity-dependent neuronal plasticity in *Drosophila*. *eLife, 7*, e39393.

Papadia, S., Soriano, F. X., Léveillé, F., Martel, M. -A., Dakin, K. A., Hansen, H. H., Kaindl, A., Sifringer, M., Fowler, J., Stefovska, V., Mckenzie, G., Craigon, M., Corriveau, R., Ghazal, P., Horsburgh, K., Yankner, B. A., Wyllie, D. J. A., Ikonomidou, C., & Hardingham, G. E. (2008). Synaptic NMDA receptor activity boosts intrinsic antioxidant defenses. *Nature Neuroscience, 11*, 476-487.

Parra, M. (2014). Class IIa HDACs – new insights into their functions in physiology and pathology. *The FEBS Journal, 282*(9), 1736-1744.

Park, S.-Y. & Kim, J.-S. (2020). A short guide to histone deacetylases including recent progress on class II enzymes. *Experimental and Molecular Medicine, 52,* 204-212.

Paroni, G., Cernotta, N., Dello Russo, C., Gallinari, P., Pallaoro, M., Foti, C., Talamo, F., Orsatti, L., Steinkühler, C., & Brancolini, C. (2008). PP2A regulates HDAC4 nuclear import. *Molecular Biology of the cell, 19*(2), 655-667.

Pickell, Z., Williams, A. M., Alam, H. B., Hsu, C. H. (2020). Histone deacetylase inhibitors: A novel strategy for neuroprotection and cardioprotection following ischemia/reperfusion injury. Journal of the American Heart Association, 9(11), e016349.

Plummer, J. L., Smith, B. R., Sies, H., Bend, J. R. (1981). Chemical depletion of glutathione *in vivo*. *Methods in Enzymology, 77,* 50-59.

Poon, H., Calabrese, V., Scapagnini, G., & Butterfield, D. (2004). Free radicals: key to brain aging and heme oxygenase as a cellular response to oxidative stress. *The Journals of Gerontology. Series A, Biological Sciences and Medical Sciences, 59*(5), 478-493.

Popa-Wagner, A., Mitran, S., Sivanesan, S., Chang, E., & Buga, A.-M. (2013). ROS and brain diseases: the good, the bad and the ugly. *Oxidative Medicine and Cellular Longevity, 2013*, 963520.

Potthoff, M. J., & Olson, E. N. (2007). MEF2: a central regulator of diverse developmental programs. *Development, 134*, 4131-4140.

Qiu, J., Dando, O., Febery, J. A., Fowler, J. H., Chandran, S., & Hardingham, G. E. (2020). Neuronal activity and its role in controlling antioxidant genes. *International Journal of Molecular Sciences, 21*(6), 1933.

Reddy, D. S., Wu, X., Golub, V. M., Dashwood, W. M., & Dashwood, R. H. (2018). Measuring histone deacetylase inhibition in the brain. *Current Protocols in Pharmacology, 81*(1), e41.

Redza-Dutordoir, M. & Averill-Bates, D. A. (2016). Activation of apoptosis signalling pathways by reactive oxygen species. *Biochemicia et Biophysica Acta (BBA) – Molecular Cell Research, 1863*(12), 2977-2992.

Resende, R., Moreira, P. I., Proenca, T., Deshpande, A., Busciglio, J., Pereira, C., & Oliveira, C. R. (2008). Brain oxidative stress in a triple-transgenic mouse model of Alzheimer's disease. *Free Radical Biology and Medicine, 44*(12), 2051-2057.

Rezaval, C., Werbajh, S., Ceriani, M. F. (2007). Neuronal death in *Drosophila* triggered by GAL4 accumulation. *European Journal of Neuroscience, 25*(3), 683-694.

Sando, R., 3rd, Gounko, N., Pieraut, S., Liao, L., Yates, J., 3rd, & Maximov, A. (2012). HDAC4 governs a transcriptional program essential for synaptic plasticity and memory. *Cell, 151*(4), 821-834.

Seabrooke, S., & Stewart, B. A. (2008). Moesin helps to restrain synaptic growth at the *Drosophila* neuromuscular junction. *Developmental Neurobiology, 68*(3), 379-391.

Semenza, G. L. (1998). Hypoxia-inducible factor 1: master regulator of O_2 homeostasis. *Current Opinion in Genetics & Development, 8*(5), 588-594.

Seto, E. & Yoshida, M. (2014). Erasers of histone acetylation: the histone deacetylase enzymes. *Cold Spring Harbor Perspectives in Biology, 6*(4), a018713.

Shaulain, E., & Karin, M. (2001). AP-1 in cell proliferation and survival. *Oncogene, 20*(19), 2390-400.

Shen, X., Chen, J., Li, J., Kofler, J., Herrup, K. (2016). Neurons in vulnerable regions of the Alzheimer's disease brain display reduced ATM signaling. *eNeuro, 3*(1), e0124-15.2016 1-18.

Shin, T., Ahn, M., Kim, H., Moon, C., Kang, T.-Y., Lee, J.-M., Sim, K. B., & Hyun, J.-W. (2005). Temporal expresion of osteopontin and CD44 in rat brains with experimental cryolesions. *Brain Research, 1041*(1), 95-101.

Soriano, F. X., Chawla, S., Skehel, P., & Hardingham, G. E. (2013). SMRT-Mediated co-shuttling enables export of class IIa HDACs indepdenent of their CaM kinase phosphorylation sites. *Journal of Neurochemistry, 124*(1), 26-35.

Takase, K., Oda, S., Kuroda, M., & Funato, H. (2013). Monoaminergic and neuropeptidergic neurons have distinct expression profiles of histone deacetylases. *PLOS One, 8*(3), e58473.

Thomas, E. A., & D'Mello, S. R. (2018). Complex neuroprotective and neurotoxic effects of histone deacetylases. *Journal of Neurochemistry, 145*(2), 96-110.

Torp, R., Su, J. H., Deng, G., & Cotman, C. W. (1998). GADD45 is induced in Alzheimer's disease, and protects against Apoptosis *in vitro*. *Neurobiology of Disease, 5*(4), 245-252.

Tropea, D., Kreiman, G., Lyckman, A., Mukherjee, S., Yu, H., Horng, S., & Sur, M. (2006). Gene expression changes and molecular pathways mediating activity-dependent plasticity in visual cortex . *Nature neuroscience , 9*(5), 660-668.

Turpaev, K. T. (2002). Reactive oxygen species and regulation of gene expression. *Biochemistry (Moscow), 67,* 281-292.

Ugbode, C., Garnham, N., Fort-Anzar, L., Evans, G. J., Chawla, S., & Sweeney, S. T. (2020). JNK signalling regulates antioxidant responses in neurons. *Redox Biology, 37*, 101712.

Usui, S., Komeima, K., Lee, S. Y., Jo, Y.-J., Ueno, S., Rogers, B. S., Wu, Z., Shen, J., Lu, L., Oveson, B. C., Rabinovitch, P. S., & Campochiaro, P. A. (2009). Increased expression of catalase and superoxide dismutase 2 reduces cone cell death in retinitis pigmentosa. *Molecular Therapy, 17*(5), 778-786.

Van der Horst, A., & Burgering, B. M. (2007). Stressing the role of FoxO proteins in lifespan and disease. *Nature Reviews Molecular Cell Biology, 8*(6), 440-450.

Van der Reest, J., Lilla, S., Zheng, L., Zanivan, S., & Gottlieb, E. (2018). Proteome-wide analysis of cysteine oxidation reveals metabolic sensitivity to redox stress. *Nature communications, 9*, 1581.

Wang, A. H., & Yang, X.- J. (2001). Histone deacetylase 4 possesses intrinsic nuclear import and export signals. *Molecular and Cellular Biology*, *21*(17), 5992-6005.

Wang, B., Moya, N., Niessen, S., Hoover, H., Mihaylova, M. M., Shaw, R. J., Yates, J., 3rd, Fischer, W. H., Thomas, J. B., & Montminy, M. (2011). A hormone-dependent module regulating energy balance. *Cell, 145*(4), 596-606.

Wiseman, H., & Halliwell, B. (1996). Damage to DNA by reactive oxygen and nitrogen species: role in inflammatory disease and progression to cancer. *Biochemical Journal, 313*(1), 17-29.

Wung, J. K., Perry, G., Kowalski, A., Harris, P. L., Bishop, G. M., Trivedi, M. A., Johnson, S. C., Smith, M. A., Denhardt, D. T., & Atwood, C. S. (2007). Increased expression of the remodeling- and tumorigenic- associated factor osteopontin in pyramidal neurons of the Alzheimers disease brain. *Current Alzheimer Research, 4*(1), 67-72.

Yamanaka, T., Tosaki, A., Kurosawa, M., Shimogori, T., Hattori, N., & Nukina, N. (2016). Genome-wide analyses in neuronal cells reveal that upstream transcription factors regulate lysosomal gene expression. *FEBS Journal, 283*(6), 1077-1087.

Yu, H., Liu, X., & Zhong, Y. (2017). The effect of osteopontin on microglia. *BioMed Research International, 2017*, 1879437.

Zaidi, A., Fernandes, D., Bean, J. L., & Michaelis, M. L. (2009). Effects of paraquat-induced oxidative stress on the neuronal plasma membrane Ca^{2+}-ATPase. *Free Radical Biology and Medicine, 47*(10), 1507-1514.

Zhang, J., Wang, X., Vikash, V., Ye, Q., Wu, D., Liu, Y., Dong, W. (2016). ROS and ROS-mediated cellular signaling. *Oxidative Medicine and Cellular Longevity, 2016,* 1-18.

Zhao, R.-Z., Jiang, S., Zhang, L., & Yu, Z.-B. (2019). Mitochondrial electron transport chain, ROS generation and uncoupling (Review). *International Journal of Molecular Medicine, 44*(1), 3-15.

Zhao, Z., Tian, D., McBride, C. S. (2020). Development of a pan-neuronal genetic driver in *Aedes aegypti* mosquitoes. *bioRxiv – Neuroscience*.

Zorov, D. B., Juhaszova, M., & Sollott, S. J. (2014). Mitochondrial reactive oxygen species (ROS) and ROS-induced ROS release. *Physiological Reviews , 94*(3), 909-950.

7. Appendices

7.1. Buffers and Solutions

Table 11. Gel and buffer components used for western blotting.

Buffer	Components
10% SDS PAGE (Resolving gel)	4.2 ml dH_2O, 2.5 ml resolving gel buffer, 3.3 ml acrylamide, 50 µl APS solution, 12-15 µl TEMED
Resolving gel buffer	375 mM Tris-HCl, 0.1% SDS; pH 8.8
10% SDS PAGE (Stacking gel)	3.1 ml dH_2O, 1.25 ml stacking gel buffer, 0.65 ml acrylamide, 25 µl APS solution, 5-7 µl TEMED
Stacking gel buffer	125 mM Tris-HCl, 0.1% SDS; pH 6.8
1 x PBS	137 mM NaCl, 2.7 mM KCl, 10 mM Na_2HPO_4, 1.8 mM KH_2PO_4
1 x Transfer buffer	25 mM Tris, 192 mM Glycine, 20% (v/v) methanol, pH ~8.3

7.2. Fly food preparation

50 g sucrose and 25 g dried yeast were added to a clean 500 ml bottle and a small amount of boiled water was added and swirled in the bottle. The bottle was microwaved for 2-3 minutes (in 30 second intervals) and hot water was used to top up the bottle to 500 ml which was then autoclaved. 200 ml sucrose solution was measured out and 162 µl of either vehicle (ethanol) or DEM was pipetted in to make 5 µM treated foods. The solution was swirled to mix and 40 g sawdust was added and mixed until thick. A pipette was used to aliquot around 1 inch of the food mix into tubes and the tubes tapped on the workbench to remove bubbles until smooth. A cotton wool bud was pushed down into the tube until almost touching the wet food. The tubes were left to dry overnight at room temperature before being stored at 4 °C until use.

7.3. Abbreviations

Table 12. List of abbreviations and full terms.

Abbreviation	Full name
SDS	Sodium dodecyl sulfate
TBST	Tris buffered saline, 0.1% Tween-20
PBS	Phosphate buffered saline
APS	Ammonium persulfate
TEMED	Tetramethylethylenediamine
BSA	Bovine Serum Albumin
EDTA	Ethylenediamine tetraacetic acid
SGG	CO_2 dependent salt glucose glycine
MEM	Minimal essential medium
HEPES	N-2-hydroxyethylpiperazine-N-ethanesulfonic acid
DTT	Dithiothreitol
PMSF	Phenylmethylsulfonyl fluoride
LDS	Lithium dodecyl sulfate
PVDF	Polyvinylidene fluoride
ECL	Enhanced chemiluminescence
NP-40	Nonyl phenoxypolyethoxylethanol
PFA	Paraformaldehyde
DEPC	Diethylpyrocarbonate
TAE	Tris acetate EDTA
TM	Transfection medium